The University *of* Western Ontario
BIOLOGICAL AGENTS REGISTRY FORM
Approved Biohazards Subcommittee: October 14, 2011
Biosafety Website: www.uwo.ca/humanresources/biosafety/

This form must be completed by each Principal Investigator holding a grant administered by the University of Western Ontario (UWO) or in charge of a laboratory/facility where the use of Level 1, 2 or 3 biological agents is described in the laboratory or animal work proposed. The form must also be completed if any work is proposed involving animals carrying zoonotic agents infectious to humans or involving plants, fungi, or insects that require Public Health Agency of Canada (PHAC) or Canadian Food Inspection Agency (CFIA) permits.

This form must be updated at least every 3 years or when there are changes to the biological agents being used.

Containment Levels will be established in accordance with Laboratory Biosafety Guidelines, 3rd edition, 2004, Public Health Agency of Canada (PHAC) or Containment Standards for Veterinary Facilities, 1st edition 1996, Canadian Food Inspection Agency (CFIA).

Electronically completed forms are to be submitted to Occupational Health and Safety, (OHS), (Support Services Building, Room 4190 or to jstanle2@uwo.ca) for distribution to the Biohazards Subcommittee. For questions regarding this form, please contact the Biosafety Officer at extension 81135 or biosafety@uwo.ca. If there are changes to the information on this form (excluding grant title and funding agencies), contact Occupational Health and Safety for a modification form. See website: www.uwo.ca/humanresources/biosafety.

Please ensure that all questions are fully and clearly answered. Failure to do so will lead to the form being returned, which will cause delays in your approval and frustration for you and your colleagues on the Committee.

If you are re-submitting this form as requested by the Biohazards Subcommittee, please make modifications to the form in bold print, highlighted in yellow. Please re-submit forms electronically.

PRINCIPAL INVESTIGATOR:	**Vania F. Prado**
DEPARTMENT:	**Anatomy and Cell Biology/ Physiology and Pharmacol**
ADDRESS:	**Robarts REsearch Institute- 3rd floor, room 3286.**
PHONE NUMBER:	**519-9315777 ext 24889**
EMERGENCY PHONE NUMBER(S):	**519-6705109**
EMAIL:	**vprado@uwo.ca**

Location of experimental work to be carried out :

Building :	**Robarts Research Institute**	Room(s):	**3286**
Building :	**Robarts Research Institute**	Room(s):	**3290**
Building :		Room(s):	

***For work being performed at Institutions affiliated with the University of Western Ontario, the Safety Officer for the Institution where experiments will take place must sign the form prior to its being sent to the University of Western Ontario Biosafety Officer (See Section 15.0, Approvals).**

FUNDING AGENCY/AGENCIES: **CIHR; HSFO; PrioNet Canada; Alzheimer's Association- USA**

GRANT TITLE(S): **- The role of basal forebrain cholinergic neurons in synaptic plasticity and cognition (CIHR);**
- Decreased cholinergic tone and heart dysfunction (HSFO);
- The Prion Protein as a therapeutic target in Alzheimer's disease (PrioNet).

UNDERGRADUATE COURSE NAME(IF APPLICABLE):

List all personnel working under Principal Investigators supervision in this location:

Name	UWO E-mail Address	Date of Biosafety Training
1- Ashbeel Ro	**aroy44@uwo.ca**	**Dec 17/09**
2- Amro Atari	**amoham59@uwo.ca**	**May 10/10**
3- William Fields	**wfields@uwo.ca**	**Jan11/11**

4- Ana Cristina Guimaraes	amagalh@uwo.ca	Feb 02/12
5- Amanda Martyns	amarty@uwo.ca	Mar25/11
6- Flavio Paiva	beraldo@yahoo.com	Apr27/09
7- Valeriy Ostapchenko	vostapc@uwo.ca	Jan 17/11
8- Monica Guzman	monicasofia@gmail.com	Dec09/09
9- Iaci Nunes Soares	iacins@gmail.com	Jan11/12
10- Anu Alice Thomas	athoma57@uwo.ca	Feb15/10
11- Jue Fan	jfan27@uwo.ca	Oct28/11
12- Sanda Raulic	sraulic4@uwo.ca	May10/09
13- Weiyan Wen	wwen@uwo.ca	Jan18/08
14- Daniela Goncalves	fontesgd@yahoo.com.br	Apr26/11

Please explain how the biological agents are used in your project and how they are stored and disposed of. The BARF without this description will not be reviewed.

See attached

Please include a ONE page research summary or teaching protocol in lay terms.
Forms with summaries more than one page will not be reviewed.

One of the objectives of my research is to understand physiological roles of distinct neurons that secrete acetylcholine in the brain and in the peripheral nervous system. The neurotransmitter acetylcholine is decreased in several neurological conditions such as Alzheimer's disease, Huntington´s disease, myasthenia and altered transmitter can change autonomic function. I generate genetically modified mice that model cholinergic dysfunction in different areas of the brain. My goal is to gain novel insights into the mechanisms underlying control by acetylcholine of cognitive functions, such as learning, memory, attention, control of motor balance and how this relates to symptoms and treatment for Alzheimer's disease, Huntington´s disease, cardiac function and congenital myasthenia.

I also work on the development of novel drugs based on peptide toxins. We have cloned, expressed and characterized different toxins isolated from the venom of the South American spider Phoneutria nigriventer. We have found that many of these small peptides are active on ion channels, such as calcium, sodium and potassium channels. We are now testing for their potential use as therapeutic drugs (for instance in the treatment of chronic pain or cardiac arrhythmias).

1.0 Microorganisms

1.1 Does your work involve the use of biological agents? ☒ YES ☐ NO
(non-pathogenic and pathogenic biological agents including but not limited to bacteria and other microorganisms, viruses, prions, parasites or pathogens of plant or animal origin)? If no, please proceed to Section 2.0

Do you use microorganisms that require a permit from the CFIA? ☐ YES ☒ NO
If YES, please give the name of the species ______________________
What is the origin of the microorganism(s)? ______________________

Please describe the risk (if any) of escape and how this will be mitigated:

Please attach the CFIA permit.

Please describe any CFIA permit conditions:

1.2 Please complete the table below:

Full Scientific Name of Biological Agent(s)* (Be specific)	Is it known to be a human pathogen? YES/NO	Is it known to be an animal pathogen? YES/NO	Is it known to be a zoonotic agent? YES/NO	Maximum quantity to be cultured at one time? (in Litres)	Source/ Supplier	PHAC or CFIA Containment Level
E.coli ***-DH5alpha*** ***- Top10*** ***-BL21*** ***-ORIGAMI*** -	☐ Yes ☒ No	☐ Yes ☒ No KM71H – C182-00	☐ Yes ☒ No	**1 liter**	**GE/ NEB**	☒ 1 ☐ 2 ☐ 2+ ☐ 3
S. cerevisiae (Invitrogen) X-33 = pC180-00 G5115 = pC181-00	☐ Yes ☒ No	☐ Yes ☒ No	☐ Yes ☒ No	**1 liter**	**Invitrogen/ Clontech**	☒ 1 ☐ 2 ☐ 2+ ☐ 3
Adeno Associated Virus (AAV)	☐ Yes ☒ No	☐ Yes ☒ No	☐ Yes ☒ No	**it will not be cultured.**	**Vector Biolabs**	☐ 1 ☒ 2 ☐ 2+ ☐ 3
	☐ Yes ☐ No	☐ Yes ☐ No	☐ Yes ☐ No			☐ 1 ☐ 2 ☐ 2+ ☐ 3
	☐ Yes ☐ No	☐ Yes ☐ No	☐ Yes ☐ No			☐ 1 ☐ 2 ☐ 2+ ☐ 3
	☐ Yes ☐ No	☐ Yes ☐ No	☐ Yes ☐ No			☐ 1 ☐ 2 ☐ 2+ ☐ 3
	☐ Yes ☐ No	☐ Yes ☐ No	☐ Yes ☐ No			☐ 1 ☐ 2 ☐ 2+ ☐ 3
	☐ Yes ☐ No	☐ Yes ☐ No	☐ Yes ☐ No			☐ 1 ☐ 2 ☐ 2+ ☐ 3

****Please attach a Material Safety Data Sheet or equivalent from the supplier if the bacterium used is not on this link:***
http://www.uwo.ca/humanresources/docandform/docs/ohs/CFIA_Ecoli_list.pdf

Additional Comments: ______________________

2.0 Cell Culture

2.1 Does your work involve the use of cell cultures? ☒ YES ☐ NO
(If NO, please proceed to Section 3.0)

2.2 Please indicate the type of primary cells (i.e. derived from fresh tissue) that will be grown in culture:

Cell Type	Is this cell type used in your work?	Source of Primary Cell Culture Tissue	AUS Protocol Number
Human	☐ Yes ☒ No		Not applicable
Rodent	☒ Yes ☐ No	**brain, heart**	**2008-127**
Non-human primate	☐ Yes ☐ No		
Other (specify)	☐ Yes ☐ No		

2.3 Please indicate the type of established cells that will be grown in culture in:

Cell Type	Is this cell type used in your work?	Specific cell line(s)*	Containment Level of each cell line	Supplier / Source of cell line(s)
Human	☒ Yes ☐ No	**HEK-293**	**Level 2**	**ATCC**
Rodent	☒ Yes ☐ No	**CF10; SN56** (Mouse septum) Mouse embryos	**Level 1**	~~Vilma~~ Sue Priola ~~Martins~~/Bruce Wainer
Non-human primate	☐ Yes ☒ No			
Other (specify)	☐ Yes ☒ No			

**Please attach a Material Safety Data Sheet or equivalent from the supplier. (For more information, see www.atcc.org)*

2.4 For above named cell types(s) indicate PHAC or CFIA containment level required ☐ 1 ☒ 2 ☐ 2+ ☐ 3

Additional Comments: _____

3.0 Use of Human Source Materials

3.1 Does your work involve the use of human source materials? ☐ YES ☒ NO
If no, please proceed to Section 4.0

3.2 Indicate in the table below the Human Source Material to be used.

Human Source Material	**Source/Supplier /Company Name**	**Is Human Source Material Infected With An Infectious Agent? YES/UNKNOWN**	**Name of Infectious Agent (If applicable)**	**PHAC or CFIA Containment Level (Select one)**
Human Blood (whole) or other Body Fluid		☐ Yes ☐ Unknown		☐1 ☐2 ☐2+ ☐3
Human Blood (fraction) or other Body Fluid		☐ Yes ☐ Unknown		☐1 ☐2 ☐2+ ☐3
Human Organs or Tissues (unpreserved)	BRAIN/ Brain Bank	☐ Yes ☒ Unknown		☐1 ☒2 ☐2+ ☐3
Human Organs or Tissues (preserved)		Not Applicable		Not Applicable

Additional Comments: _____

4.0 Genetically Modified Organisms and Cell lines

4.1 Will genetic modifications be made to the microorganisms, biological agents, or cells described in Sections 1.0 and 2.0? ☒ YES ☐ NO If **NO**, please proceed to Section 5.0

4.2 Will genetic modification(s) involving plasmids be done? ☐ YES, complete table below ☐ NO

Bacteria Used for Cloning *	Plasmid(s) **	Source of Plasmid	Gene Transformed or Transfected	Will there be a change due to transformation of the bacteria?	Will there be a change in the pathogenicity of the bacteria after the genetic modification?	What are the consequences due to the transformation of the bacteria?
E. Coli	**several**	**several**	**several**	**no**	**no**	

** Please attach a Material Safety Data Sheet or equivalent if available.*
*** Please attach a plasmid map.*
****No Material Safety Data Sheet is required for the following strains of E. coli:*
http://www.uwo.ca/humanresources/docandform/docs/ohs/CFIA_Ecoli_list.pdf

4.3 Will genetic modification(s) of bacteria and/or cells involving viral vectors be made?
☒ YES, complete table below ☐ NO

Virus Used for Vector Construction	Vector(s) *	Source of Vector	Gene(s) Transduced	Describe the change that results from transduction
Adeno Associated Vector	**AAV1-cre-GFP** **AAV1-GFP** **AAV2-cre-GFP** **AAV2-GFP** **AAV5-cre-GFP** **AAV5-GFP**	**Vector Biolabs**	**cre-recombinase** **GFP**	**deletion of floxed allele** **fluorescent protein**

** Please attach a Material Safety Data Sheet or equivalent.*

4.3.1 Will virus be replication defective? ☒ YES ☐ NO

4.3.2 Will virus be infectious to humans or animals? ☒ YES ☐ NO

4.3.3 Will this be expected to increase the containment level required? ☐ YES ☒ NO

5.0 Will genetic sequences from the following be involved?

- HIV ☒ NO ☐ YES, specify
- HTLV 1 or 2 or genes from any Level 1 or Level 2 pathogens ☒ NO ☐ YES, specify
- SV 40 Large T antigen ☒ NO ☐ YES
- E1A oncogene ☐ NO ☒ YES
- Known oncogenes ☒ NO ☐ YES, specify
- Other human or animal pathogen and or their toxins ☐ NO ☒ YES, specify **Ca+ and K+ channel toxins**

5.1 Is any work being conducted with prions or prion sequences? ☒ NO ☐ YES

Additional Comments: **We work with the PrPc (the cellular prion protein, which is NOT infectious)**

6.0 Human Gene Therapy Trials

6.1 Will human clinical trials be conducted involving a biological agent? ☐ YES ☒ NO
(including but not limited to microorganisms, viruses, prions, parasites or pathogens of plant or animal origin)
If no, please proceed to Section 7.0

6.2 If YES, please specify which biological agent will be used:
Please attach a full description of the biological agent.

6.3 Will the biological agent be able to replicate in the host? ☐ YES ☐ NO

6.4 How will the biological agent be administered?

6.5 Please give the Health Care Facility where the clinical trial will be conducted:

6.6 Has human ethics approval been obtained? ☐ YES, number: ☐ NO ☐ PENDING

7.0 Animal Experiments

7.1 Will live animals be used? ☒ YES ☐ NO If **NO**, please proceed to section 8.0

7.2 Name of animal species to be used **Mice (Mus musculus)**

7.3 AUS protocol **# 2008-127**

7.4 List the location(s) for the animal experimentation and housing. **ACVS-conventional; ACVS-barrier; WV Barrier;**

7.5 Will any of the agents listed in section 4.0 be used in live animals
☐ NO ☒ YES, specify: **AAV-vectors**

7.6 Will the agent(s) be shed by the animal:
☒ YES ☐ NO, please justify:

8.0 Use of Animal species with Zoonotic Hazards

8.1 Will any animals with zoonotic hazards or their organs, tissues, lavages or other body fluids including blood be used (see list below)? ☐ YES ☒ NO - If **NO**, please proceed to section 9.0

8.2 Will live animals be used? ☐ YES ☐ NO

8.3 If **YES**, please specify the animal(s) used:

♦ Pound source dogs	☐ YES	☒ NO
♦ Pound source cats	☐ YES	☒ NO
♦ Cattle, sheep or goats	☐ YES, species	☒ NO
♦ Non-human primates	☐ YES, species	☒ NO
♦ Wild caught animals	☐ YES, species & colony #	☒ NO
♦ Birds	☐ YES, species	☒ NO
♦ Others (wild or domestic)	☐ YES, specify	☒ NO

8.4 If no live animals are used, please specify the source of the specimens:

9.0 Biological Toxins and Hormones

9.1 Will toxins or hormones of biological origin be used? ☒ YES ☐ NO If **NO**, please proceed to Section 10.0

9.2 If YES, please name the toxin(s) or hormones(s) **spider venom toxins (Phoneutria nigriventer)**
Please attach information, such as a Material Safety Data Sheet, for the toxin(s) used.

9.3 What is the LD_{50} (specify species) of the toxin or hormone **137ug/Kg mouse**

9.4 How much of the toxin or hormone is handled at one time*? **200ug**

9.5 How much of the toxin or hormone is stored*? **2mg (divide in aliquots of 200ug)**

9.6 Will any biological toxins or hormones be used in live animals? ☐ YES ☒ NO
If **YES**, Please provide details:

*For information on biosecurity requirements, please see:
http://www.uwo.ca/humanresources/docandform/docs/healthandsafety/biosafety/Biosecurity_Requirements.pdf

Additional Comments: _____

10.0 Insects

10.1 Do you use insects? ☐ YES ☒ NO - If **NO**, please proceed to Section 11.0

10.2 If YES, please give the name of the species.

10.3 What is the origin of the insect?

10.4 What is the life stage of the insect?

10.5 What is your intention? ☐ Initiate and maintain colony, give location:
☐ "One-time" use, give location:

10.6 Please describe the risk (if any) of escape and how this will be mitigated:

10.7 Do you use insects that require a permit from the CFIA permit? ☐ YES ☐ NO
If **YES**, Please attach the CFIA permit & describe any CFIA permit conditions:

11.0 Plants

11.1 Do you use plants? ☐ YES ☒ NO - If **NO**, please proceed to Section 12.0

11.2 If YES, please give the name of the species.

11.3 What is the origin of the plant?

11.4 What is the form of the plant (seed, seedling, plant, tree...)?

11.5 What is your intention? ☐ Grow and maintain a crop ☐ "One-time" use

11.6 Do you do any modifications to the plant? ☐ YES ☐ NO
If yes, please describe:

11.7 Please describe the risk (if any) of loss of the material from the lab and how this will be mitigated:

11.8 Is the CFIA permit attached? ☐ YES ☐ NO
If **YES**, Please attach the CFIA permit & describe any CFIA permit conditions:

12.0 Import Requirements

12.1 Will any of the above agents be imported? ☒ YES, country of origin **USA (HEK-293cells)** ☐ NO
If **NO**, please proceed to Section 13.0

12.2 Has an Import Permit been obtained from HC for human pathogens? ☒ YES ☒ NO

12.3 Has an import permit been obtained from CFIA for animal or plant pathogens? ☐ YES ☒ NO

12.4 Has the import permit been sent to OHS? ☐ YES, please provide permit # ☒ NO

13.0 Training Requirements for Personnel Named on Form

All personnel named on the above form who will be using any of the above named agents are required to attend the following training courses given by OHS:

- Biosafety
- Laboratory and Environmental/Waste Management Safety
- WHMIS (Western or equivalent)
- Employee Health and Safety Orientation

As the Principal Investigator, I have ensured that all of the personnel named on the form who will be using any of the biological agents in Sections 1.0 to 9.0 have been trained.

An X in the check box indicates you agree with the above statement... ☒
Enter Your Name Vania Prado ***Date:*** Feb 01, 2012

Vania Prado

14.0 Containment Levels

14.1 For the work described in sections 1.0 to 9.0, please indicate the highest HC or CFIA Containment Level required. ☐ 1 ☒ 2 ☐ 2+ ☐ 3

14.2 Has the facility been certified by OHS for this level of containment?
☒ YES, location and date of most recent biosafety inspection: Feb. 22, 2011
☐ NO, please certify
☐ NOT REQUIRED for Level 1 containment

14.3 Please indicate permit number (not applicable for first time applicants): **BIO-RRI-0053**

15.0 Procedures to be Followed

15.1 Are additional risk reduction measures necessary beyond containment level 1, 2, 2+ or 3 measures that are unique to these agents? ☐ YES ☒ NO
If **YES** please describe:

15.2 Please outline what will be done if there is an exposure to the biological agents listed such as a needlestick injury or an accidental splash:
Spills: decontamination and clean-up procedures will be performed. If spill is large or of a nature that cannot be handled by laboratory personnel, will call University Police at 911. Needlestic injury: Wash the would (water+soap). Refer affected worker to the nearest hospital emergency with appropriate information on the infectious agent (toxin dose used not lethal). Report incident to Hum Res

15.3 As the Principal Investigator, I will ensure that this project will follow the Western Biosafety Guidelines and Procedures Manual for Containment Level 1 & 2 Laboratories (and the Level 3 Facilities Manual for Level 3 projects). I will ensure that UWO faculty, staff and students working in my laboratory have an up-to-date Hazard Communication Form, found at http://www.shs.uwo.ca/workplace/workplacehealth.html

An X in the check box indicates you agree with the above statement. ☒
Enter Your Name Vania Prado ***Date:*** Feb 01, 2012 Vania Prado

15.4 Additional Comments: _____

16.0 Approvals

1) UWO Biohazards Subcommittee:
SIGNATURE: _____
Date: _____

2) Safety Officer for the University of Western Ontario
SIGNATURE: _____
Date: _____

3) Safety Officer for Institution where experiments will take place (~~if not~~ UWO):
SIGNATURE: Ronald Worsley
Date: Feb. 08, 2012

Approval Number: _____ Expiry Date (3 years from Approval): _____

Special Conditions of Approval:

BRIEF DESCRIPTION THAT EXPLAINS BIOHAZARDS USED AND HOW THEY WILL BE USED

We have used genetic recombination to generate novel mouse models of dementia by targeting the vesicular acetylcholine transporter (VAChT). This protein is responsible for the accumulation of ACh into synaptic vesicles and is thought to mediate the rate-limiting step for ACh release. For this proposal, we have generated floxed VAChT mice (Flanked by loxP), to use the Cre/LoxP strategy to create mouse lines with brain region specific deletion of the VAChT gene. The enzyme Cre mediates a recombination event that removes loxP intervening sequences and therefore can remove the floxed VAChT gene. This gene targeting strategy allows temporal and spatial control of gene inactivation.

We will use the approach of infusing an adenovirus vector to drive the expression of Cre in the Nucleus basalis or medial septum of $VAChT^{flox/flox}$ mice to generate animals with ablation of VAChT from neurons that project either to the cortex or hippocampus respectively. We will also use the adenovirus vector to generate animals with ablation of VAChT from neurons that project to the heart and other tissues.

Using adenovirus vector expressing Cre to generate brain region specific VAChT KO. We will also rely on injecting the $VAChT^{flox/flox}$ mice with AAV-Cre construct that leads to Cre expression in neurons when injected stereotaxically in the brain [62].The advantage of using such vectors is that the recombinant virus cannot replicate and therefore expression of Cre should be limited to the site of injection. We will infuse the virus to either the nucleus basalis or to the medial septum to knockout the VAChT gene in cholinergic neurons that project to the cortex or the hippocampus.

Pre-surgery handling of viral vectors: Hamilton syringes or glass micropipettes used for surgeries are filled in laminar flow-hood and transported to the surgery facility in a closed container.

Surgery:
The surgery space is subjected to BL2 regulations: Personnel is required to wear appropriate protective gear, consisting of cap, gown, mask, goggles, and gloves.
Mice will be anaesthetized and placed into a stereotaxic apparatus (Kopf). A single scalp incision is made. A burr hole (approximately 3 mm in diameter) is made in the skull and a glass micro pipette filled with 1 microliter of AAV-Cre is going to be stereotaxically microinjected into a specific brain area (into either the medial septum (0.98 AP, 0 LL and 3.25 DV) or into the nucleus basalis (-0.94 AP, 1.5 LL and 3.25 DV)). Only one area of the brain will be injected in each animal. To minimize tissue injury,these injections are going to be performed using glass pipettes with a 10- to 20-micrometer diameter tip, and AAV-Cre is going to be slowly injected over 1 hr using a pressure-injection system. After an additional period of 5 minutes, the micropipette is removed and the scalp incision is closed with wound clips. Sham surgeries will be performed the same way, except that the pipette will be filled with vehicle, and no

injection will be made. Animals are kept on heat pads or under heat lamps to maintain body temperature throughout the procedures. During recovery, animals are kept in the surgery room to allow frequent monitoring of breathing and general activity (according to SOP330-03 POST-OPERATIVE/POST ANAESTHETIC CARE RODENTS) before being transported back to the holding room. The procedure is going to be performed once in each animal and we will use adult mice (8-20 wks).

Disposal of viral vectors and micropipettes: Instruments and needles are soaked in bleach solution prior to disposal. Cages should also be soaked in bleach solution and autoclaved after use. Animal carcasses do not need special treatment.

Post-operative care: SOP procedures for rodent surgeries will be followed. Mice are going to be kept in microisolators on level 2 containment efor 10-14 days

Mechanisms involved in the cellular trafficking of the high affinity choline transporter (CHT1) , the vesicular acetylcholine transporter (VAChT) and Cellular prion protein (PrPc).

We have been studying trafficking of the high affinity choline transporter (CHT1), the vesicular acetylcholine transporter (VAChT) and the cellular prion protein (PrPc) in culture cells (HEK-293, SN56, CF-10). To do that we transfect cells with fluorescent proteins (CHT1-WT tagged with HA, CHT1 mutants tagged with HA, EGFP-VAChT, EGFP-VAChT mutants, VAChT-HA, VAChT-HA mutants, GFP-PrPc, GFP-PrPc mutants) and follow the trafficking of the recombinant protein in live cells using confocal microscopy. Mutants that interfere with different trafficking pathways (mutants of rab5, rab7, rab11, AP180, dynamin-1) are also used in these studies.

HEK-293 Cell Cultures:

HEK-293 cell cultures are handled as a potentially biohazardous material under Biosafety Level 2 containment.

In case of any accident with these cells the following procedures are going to be followed:
Dermal exposure: Immediately wash skin with copious amounts of water followed by washing with soap and copious amounts of water. Remove all contaminated clothing.
Eye exposures: Flush eyes with copious amounts of water for at least 15 minutes with eyelids separated and call a physician.

Refer affected worker to the nearest hospital emergency with appropriate information on the infectious agent (toxin dose used not lethal). Report incident to Hum Resources.

Human Brain samples:

Brain tissue samples were provided by Dr. Margaret Fahnestock (McMaster University)

approx weight - 110-130mg/subject

Original source: Rusty Oshita & Vivian Castelo -
Institute for Brain Aging & Dementia Tissue Repository
University California Irvine

These samples are from parietal cortex of patients with Alzheimer's disease and age matching control donors.
Samples are going to be used for western-blots and qPCRs.

Human brain samples are handled as a potentially biohazardous material under Biosafety Level 2 containment.

In case of any accident with these samples the following procedures are going to be followed:
Dermal exposure: Immediately wash skin with copious amounts of water followed by washing with soap and copious amounts of water. Remove all contaminated clothing.
Eye exposures: Flush eyes with copious amounts of water for at least 15 minutes with eyelids separated and call a physician.

Refer affected worker to the nearest hospital emergency with appropriate information on the infectious agent. Report incident to Hum Resources.

Disposal of used material: Instruments, needles and micropipettes are soaked in bleach solution prior to disposal.

Developing novel drugs based on spider toxins.
We have cloned, expressed and characterized different toxins isolated from the venom of the spider *Phoneutria nigriventer*. These peptides are known to interfere with the function of different ion channels and therefore are important tools to help in the understanding of basic functions of these channels. Furthermore, they can be potentially used as drugs with important medical applications. We are currently developing approaches to use these recombinant peptides as painkillers and anti-arrhythmic drugs.

HANDLING AND STORAGE of spider toxins
Storage: Keep aliquots of 200ug in tightly closed containers.
storage temperature: -20 °C (general use) -80°C (longer than 6 month storage).

PERSONAL PROTECTION during work

Respiratory protection is not required. Handle with gloves to avoid skin contact with this product. Dispose of contaminated gloves after use in biohazard containers. Wash and dry hands. Wear goggles for eye protection.

In case of accidents:
skin contact (needlestick injury): Wash off with soap and plenty of water.
eye contact: Flush eyes with water as a precaution.
Refer affected worker to the nearest hospital emergency with appropriate information on the infectious agent (toxin dose used not lethal). Report incident to Hum Res

invitrogen™

Material Safety Data Sheet

Revision Date: 17-Oct-2007

1. IDENTIFICATION OF THE SUBSTANCE/PREPARATION AND THE COMPANY/UNDERTAKING

Product code 500090
Product name X-33 Stab yeast

Company/Undertaking Identification

INVITROGEN CORPORATON
1600 FARADAY AVENUE
PO BOX 6482
CARLSBAD, CA 92008
760-603-7200

INVITROGEN CORPORATION
2270 INDUSTRIAL STREET
BURLINGTON, ONT
CANADA L7P 1A1
800-263-6236

GIBCO PRODUCTS
INVITROGEN CORPORATION
3175 STALEY ROAD P.O. BOX 68
GRAND ISLAND, NY 14072
716-774-6700

2. COMPOSITION/INFORMATION ON INGREDIENTS

Hazardous/Non-hazardous Components
The product contains no substances which at their given concentration, are considered to be hazardous to health

3. HAZARDS IDENTIFICATION

Emergency Overview
The product contains no substances which at their given concentration, are considered to be hazardous to health

Form
Liquid

Principle Routes of Exposure/ Potential Health effects

Eyes	No information available
Skin	No information available
Inhalation	No information available

Environmental exposure controls	Prevent product from entering drains.

9. PHYSICAL AND CHEMICAL PROPERTIES

General Information

Form	Liquid

Important Health Safety and Environmental Information

Boiling point/range	**°C** No data available	**°F** No data available
Melting point/range	**°C** No data available	**°F** No data available
Flash point	**°C** No data available	**°F** No data available
Autoignition temperature	**°C** No data available	**°F** No data available
Oxidizing properties	No information available	
Water solubility	No data available	

10. STABILITY AND REACTIVITY

Stability	Stable.
Materials to avoid	No information available
Hazardous decomposition products	No information available
Polymerization	Hazardous polymerisation does not occur.

11. TOXICOLOGICAL INFORMATION

Acute toxicity

Principle Routes of Exposure/ Potential Health effects

Eyes	No information available
Skin	No information available
Inhalation	No information available
Ingestion	No information available

Specific effects

Carcinogenic effects	No information available
Mutagenic effects	No information available
Reproductive toxicity	No information available
Sensitization	No information available

Target Organ Effects No information available

12. ECOLOGICAL INFORMATION

Ecotoxicity effects	No information available.
Mobility	No information available.
Biodegradation	Inherently biodegradable.
Bioaccumulation	Does not bioaccumulate.

13. DISPOSAL CONSIDERATIONS

Dispose of in accordance with local regulations

invitrogen™

Material Safety Data Sheet

Revision Date: 17-Dec-2007

1. IDENTIFICATION OF THE SUBSTANCE/PREPARATION AND THE COMPANY/UNDERTAKING

Product code 500156
Product name GS115 Stab yeast

Company/Undertaking Identification

INVITROGEN CORPORATON
1600 FARADAY AVENUE
PO BOX 6482
CARLSBAD, CA 92008
760-603-7200

INVITROGEN CORPORATION
2270 INDUSTRIAL STREET
BURLINGTON, ONT
CANADA L7P 1A1
800-263-6236

GIBCO PRODUCTS
INVITROGEN CORPORATION
3175 STALEY ROAD P.O. BOX 68
GRAND ISLAND, NY 14072
716-774-6700

2. COMPOSITION/INFORMATION ON INGREDIENTS

Hazardous/Non-hazardous Components
The product contains no substances which at their given concentration, are considered to be hazardous to health

3. HAZARDS IDENTIFICATION

Emergency Overview
The product contains no substances which at their given concentration, are considered to be hazardous to health

Form
Solid

Principle Routes of Exposure/ Potential Health effects

Eyes	No information available
Skin	No information available
Inhalation	No information available

Environmental exposure controls	Prevent product from entering drains.

9. PHYSICAL AND CHEMICAL PROPERTIES

General Information

Form	Solid

Important Health Safety and Environmental Information

Boiling point/range	**°C** No data available	**°F** No data available
Melting point/range	**°C** No data available	**°F** No data available
Flash point	**°C** No data available	**°F** No data available
Autoignition temperature	**°C** No data available	**°F** No data available
Oxidizing properties	No information available	
Water solubility	No data available	

10. STABILITY AND REACTIVITY

Stability	Stable.
Materials to avoid	No information available
Hazardous decomposition products	No information available
Polymerization	Hazardous polymerisation does not occur.

11. TOXICOLOGICAL INFORMATION

Acute toxicity

Principle Routes of Exposure/ Potential Health effects

Eyes	No information available
Skin	No information available
Inhalation	No information available
Ingestion	No information available

Specific effects

Carcinogenic effects	No information available
Mutagenic effects	No information available
Reproductive toxicity	No information available
Sensitization	No information available

Target Organ Effects No information available

12. ECOLOGICAL INFORMATION

Ecotoxicity effects	No information available.
Mobility	No information available.
Biodegradation	Inherently biodegradable.
Bioaccumulation	Does not bioaccumulate.

13. DISPOSAL CONSIDERATIONS

Dispose of in accordance with local regulations

life technologies™

KM71H

(Invitrogen™)

Description

Several *Pichia pastoris* strains are available to allow you to optimize expression and recovery of your protein of interest. Table 1 provides information to help you choose the appropriate strain.

Catalog Number	**C182-00**
Size	**1 stab**
List Price	**(CAD) 461.00**

Specifications

General Specifications

Regulatory Statement:	For Research Use Only. Not for any animal or human therapeutic or diagnostic use.
Species:	P. pastoris
Cell Line:	Yeast Cell Line
Product Size:	1 stab
Bacterial or Yeast Strain:	KM71H

Documents

Manuals & Protocols

Pichia Fermentation Guidelines

Certificates of Analysis (COA)

Product Literature

Pichia pastoris Expression System

Product Reviews (1)

VECTOR BIOLABS
THE ADENOVIRUS COMPANY

MATERIAL SAFETY DATA SHEET

EMERGENCY TELEPHONES: 1- 877-BioLabs 1-215-966-6045

Cultures of replication defective AAV vectors are non-infectious and are not hazardous materials as defined by OSHA 1919.1200. However, these materials are produced in cells where there is the possibility of recombination to form wild type virus. As such, they should be handled as potentially infectious material.

Description:
AAV vectors consist of recombinant transgene sequences (e.g., marker or human genes) flanked by the AAV inverted terminal repeats. The removal of the majority of viral structural genes renders the vector replication-defective and dependent on an AAV helper virus. AAV cultures are normally provided as purified viral particles in phosphate buffered saline at a concentration of up to $1x10^{13}$ particles/ml. The viral stock consists of particles containing the vector genome (full capsids) and a variable number of empty viral capsids in PBS. Other trace components present include, but are not limited to, inorganic salts, vitamins and other nutrients, and human cellular proteins, carbohydrates, amino acids, and fats. The material is normally shipped and stored frozen.

SECTION I
Hazardous Ingredients
None

SECTION II
Physical Data
Liquid or frozen particle suspensions

SECTION III
Health Hazards
AAV cultures are not known to cause any diseases in humans or animals

SECTION IV
Fire and Explosion
None

SECTION V
Reactivity
Stable. Will enter mammalian cells in the presence of adenovirus and can integrate into host cell DNA.

SECTION VI
Method of Disposal
Spill: Contain spill and decontaminate the area using a disinfectant such as chlorine bleach (10% f.c.), Wescodyne, or detergent-based disinfectant.
Waste Disposal: Dispose of viral stock by autoclaving at 121°C for 30-45 minutes

Dispose of infected liquid cultures by decontamination with chlorine bleach (10% f.c.) for 10 minutes and then dispose of in sink.
Dispose of infected animal carcasses or tissues by incineration
Follow all Federal, State, and Local regulations.

SECTION VII
Special Protective Information
Handle as biohazardous material under Biosafety Level 2 containment

SECTION VIII
Special Precautions or Comments

Vectot BioLabs recommends that all AAV vectors and cultures be handled by qualified biologists using appropriate safety procedures and precautions. Detailed discussions of laboratory safety procedures are provided in **Laboratory Safety: Principles and Practice** (Fleming et al., ASM Press, Washington D.C., 1995), and in the U.S. Government Publication, **Biosafety in Microbiological and Biomedical Laboratories** (CDC, 1999). This and other publications are available at the Centers for Disease Control Office of Health and Safety's website at
http://www.cdc.gov/od/ohs/biosfty/bmb14/bmb14toc.htm

Information on the classification of human etiologic agents on the basis of hazard can be found as Appendix B in the NIH **Guidelines for Research Involving Recombinant DAN Molecules** at
http://www.grants.nih.gov/grants/policy/recombinentdnaguidelines.htm

The above information is accurate to the best of our knowledge. All materials and mixtures may present unknown hazards and should be used with caution. The user should exercise independent judgment as to the hazards based on all sources of information available. Vector BioLabs shall not be held liable for any damage resulting from the handling or use of the above product

Date of revision: May 24, 2006

ATCC™

MATERIAL SAFETY DATA SHEET

MSDS FOR ANIMAL CELL CULTURES (Biosafety Level 1 or 2)

MATERIAL SAFETY DATA SHEET

SECTION 1 - SUBSTANCE IDENTITY AND COMPANY INFORMATION

Product Name: Various Animal Cell Cultures at Biosafety Level 1 or 2
ATCC Catalog #: Various

COMPANY INFORMATION: AMERICAN TYPE CULTURE COLLECTION
PO BOX 1549
MANASSAS, VA 20108

FOR INFORMATION CALL: 800-638-6597 or 703-365-2700
AFTER-HOURS CONTACT: 703-365-2710
CHEMTREC EMERGENCY: 800-424-9300 or 703-527-3887

SECTION 2 - COMPOSITION/INFORMATION ON INGREDIENTS

Either frozen or growing cells shipped in liquid cell culture medium (a mixture of components that may include, but is not limited to: inorganic salts, vitamins, amino acids, carbohydrates and other nutrients dissolved in water). Frozen Cultures may also contain a 5%-10% solution of Dimethyl sulfoxide as a cryoprotectant.

SECTION 3 - HAZARD IDENTIFICATION

HMIS Rating:	Health: 0	Flammability: 0	Reactivity:0
NFPA Rating:	Health:0	Flammability:0	Reactivity:0

This substance is not hazardous as defined by OSHA 29CFR 1910.1200 however this product should be handled according to good lab practices, with proper personal protective equipment, proper engineering controls and within the parameters of the purchaser's safety program.

Health Hazards

For Biosafety Level 1 Cell Cultures
Handle as a potentially biohazardous material under at least Biosafety Level 1 containment.
This cell line is not known to cause disease in healthy adult humans. These cells have **NOT** been screened for Hepatitis B, human immunodeficiency viruses or other adventitious agents, unless otherwise reported on the Certificate of Analysis. Regardless of results reported on the Certificate of Analysis Universal Precautions according to 29 CFR 1910.1030 should be followed at all times when manipulating these cell lines.

See next page for Biosafety Level 2 cell cultures.

For Biosafety Level 2 Cell Cultures
Handle as a potentially biohazardous material under at least Biosafety Level 2 containment.
These cell lines are associated with human disease, hazards include: percutaneous injury, ingestion, mucous membrane exposure (U.S. Government Publication **Biosafety in Microbiological and Biomedical Laboratories)**. These cells have **NOT** been screened for Hepatitis B, human immunodeficiency viruses or other adventitious agents, unless otherwise reported on the Certificate of Analysis. Regardless of results reported on the Certificate of Analysis Universal Precautions according to 29 CFR 1910.1030 should be followed at all times when manipulating these cell lines.

SECTION 4 - FIRST AID MEASURES

Report to your Safety Office and Seek Medical Attention as Soon as Possible

Ingestion: If person is unconscious seek emergency medical attention; never give anything by mouth to an unconscious person. If the person is conscious wash mouth out with copious amounts of water and call a physician then administer three cupfuls of water. Do not induce vomiting unless directed to do so by a physician.

Inhalation: If person is unconscious seek emergency medical attention, if person is conscious remove to fresh air and call a physician.

Dermal exposure: Immediately wash skin with copious amounts of water followed by washing with soap and copious amounts of water. Remove all contaminated clothing.

Eye exposures: Flush eyes with copious amounts of water for at least 15 minutes with eyelids separated and call a physician.

SECTION 5 - FIRE FIGHTING MEASURES

Flammability: Data not available

Suitable Extinguishing Media: Water spray, carbon dioxide, dry chemical powder, Halon (where regulations permit), or appropriate foam.

Protective Equipment: Wear self-contained breathing apparatus and protective clothing to prevent inhalation, ingestion, skin and eye contact.

Specific Hazard(s): Responders should take into consideration the biohazard risk associated with responding to a fire in the area where the material may be stored or handled.

SECTION 6 - ACCIDENTAL RELEASE MEASURES

Procedure(s) of Personal Precaution(s): At a minimum use PPE listed in Section 8. Wear laboratory coat, gloves and eye protection. Avoid all contact.

Methods for Cleaning Up

Patient/Victim: Wash with soap and water. Work clothes should be laundered separately. Launder contaminated clothing before re-use. Do not take clothing home.
Equipment/Environment: Allow aerosols to settle; wearing protective clothing, gently cover spill with paper towel and apply 1% sodium hypochlorite, starting at perimeter and working towards the center; allow sufficient contact time before clean up (30 min).
Note: The use of additional PPE may be necessary for cleaning solutions.

SECTION 7 - HANDLING AND STORAGE

Handle and store according to instructions on product information sheet and label.
Special Requirements:
Follow established laboratory procedures when handling material.

SECTION 8 - EXPOSURE CONTROLS/PERSONAL PROTECTION

Use Personal Protective Equipment: Including Eye Protection, Chemical Resistant Gloves, and appropriate clothing to prevent skin exposure. In addition, a Respiratory protection program that complies with OSHA 29 CFR 1910.134 and ANSI Z88.2 requirements or European Standard EN 149 must be followed whenever workplace conditions warrant respirator use.

Engineering Controls: The use and storage of this material requires user to maintain and make available appropriate eyewash and safety shower facilities. Use fume hood or other appropriate ventilation method to keep airborne concentrations a low as possible.

Exposure Limits: No exposure limits for this material have been established by ACGIH, NIOSH, or OSHA.

SECTION 9 - PHYSICAL AND CHEMICAL PROPERTIES

Data Not Available

SECTION 10 - STABILITY AND REACTIVITY

Hazardous polymerization will not occur.

SECTION 11 - TOXICOLOGICAL INFORMATION

Route of Exposure

Eye Contact: Data not available. Avoid eye contact.
Skin Contact: Data not available. Avoid skin contact.
Skin Absorption: Data not available. Avoid skin absorption.
Inhalation: Data not available. Avoid inhalation.
Ingestion: Data not available. Avoid ingestion.
Parenteral Exposure: Data not available. Avoid parenteral exposure.

Sensitization
Skin: Data not available
Respiratory: Data not available

Target Organ(s) or System(s): Data not available

Signs and Symptoms of Exposure
Skin and Mucous Membranes: Data not available
Respiratory: Data not available
Gastrointestinal: Data not available

Toxicity Data: Data not available
Effects of Long Term or Repeated Exposure: Data not available
Chronic Exposure–Teratogen: Data not available
Chronic Exposure–Mutagen: Data not available
Chronic Exposure–Reproductive Hazard: Data not available

SECTION 12 - ECOLOGICAL INFORMATION

No ecological information available.

SECTION 13 - DISPOSAL CONSIDERATIONS

Decontaminate all wastes before disposal (steam sterilization, chemical disinfection, and/or incineration).

Dispose of in accordance with applicable regulations.

SECTION 14 - TRANSPORT INFORMATION

Contact ATCC for transport information.

SECTION 15 - REGULATORY INFORMATION

Contact ATCC for regulatory information.

SECTION 16 - OTHER INFORMATION

ATCC

MATERIAL SAFETY DATA SHEET

THE INFORMATION PRESENTED IN THIS DOCUMENT IS BELIEVED TO BE CORRECT BASED UPON DATA AVAILABLE TO ATCC. USERS SHOULD MAKE AN INDEPENDENT DECISION REGARDING THE ACCURACY OF THIS INFORMATION BASED ON THEIR NEEDS AND DATA AVAILABLE TO THEM. ALL SUBSTANCES AND MIXTURES MAY PRESENT UNKNOWN HAZARDS AND ALL NECESSARY SAFETY PRECAUTIONS SHOULD BE TAKEN. ATCC ASSUMES NO LIABILITY RESULTING FROM USING OR COMING IN CONTACT WITH THIS SUBSTANCE.

ATCC

Product Information Sheet for ATCC® CRL-1573™

Cell Line Designation: 293 (HEK293)
ATCC® Catalog No. CRL-1573™

Table of Contents:

Cell Line Description

Organism: *Homo sapiens* (human)
Tissue: kidney; transformed with adenovirus 5 DNA
Age: fetus
Morphology: epithelial
Growth properties: adherent
Doubling time: about 19 hours
Tumorigenic: tumors developed within 21 days at 100% frequency (5/5) in nude mice inoculated subcutaneously with 10(7) cells.
Receptors expressed: vitronectin
Virus susceptibility: human adenoviruses
DNA profile (STR analysis)

Amelogenin: X
CSF1PO: 11,12
D13S317: 12,14
D16S539: 9,13
D5S818: 8,9
D7S820: 11,12
TH01: 7,9.3
TPOX: 11
vWA: 16,19

Depositors: F.L. Graham
Comments: Although an earlier report suggested that the cells contained Adenovirus 5 DNA from both the right and left ends of the viral genome, it is now clear that only left end sequences are present. The line is excellent for titrating human adenoviruses.
The cell line does not adhere to the substrate when left at room temperature for any length of time, therefore, live cultures may be received with the cells detached. The cells will re-attach to the flask over a period of several days in culture at 37C.
The cells express an unusual cell surface receptor for vitronectin composed of the integrin beta-1 subunit and the vitronectin receptor alpha-v subunit.
The Ad5 insert was cloned and sequenced, and it was determined that a colinear segment from nts 1 to 4344 is integrated into chromosome 19 (19q13.2).

Karyotype: This is a hypotriploid human cell line. The modal chromosome number was 64, occurring in 30% of cells. The rate of cells with higher ploidies was 4.2 %.
The der(1)t(1;15) (q42;q13), der(19)t(3;19) (q12;q13), der(12)t(8;12) (q22;p13), and four other marker chromosomes were common to most cells. Five other markers occurred in some cells only. The marker der(1) and M8 (or Xq+) were often paired.
There were four copies of N17 and N22. Noticeably in addition to three copies of X chromosomes, there were paired Xq+, and a single Xp+ in most cells.
Note: Cytogenetic information is based on initial seed stock at ATCC. Cytogenetic instability has been reported in the literature for some cell lines.
Purified DNA: from this line is available as ATCC Catalog No. CRL-1573D™ (10 µg).

Biosafety Level: 2

Appropriate safety procedures should always be used with this material. Laboratory safety is discussed in the following publication: *Biosafety in Microbiological and Biomedical Laboratories*, 5th ed. HHS Publication No. (CDC) 93-8395. U.S. Department of Health and Human Services, Centers for Disease Control and Prevention. Washington DC: U.S. Government Printing Office; 2007. The entire text is available online at www.cdc.gov/od/ohs/biosfty/bmbl4/bmbl4toc.htm.

Use Restrictions

These cells are distributed for research purposes only. 293 cells, their products, or their derivatives may not be distributed to third parties. ATCC recommends that individuals contemplating commercial use of any cell line first contact the originating investigator to negotiate an agreement.

Handling Procedure for Frozen Cells

To insure the highest level of viability, thaw the vial and initiate the culture as soon as possible upon receipt. If upon arrival, continued storage of the frozen culture is necessary, it should be stored in liquid nitrogen vapor phase and not at –70°C. Storage at –70°C will result in loss of viability.

SAFETY PRECAUTION: ATCC highly recommends that protective gloves and clothing always be used and a full face mask always be worn when handling frozen vials. *It is important to note that some vials leak when submersed in liquid nitrogen and will slowly fill with liquid nitrogen. Upon thawing, the conversion of the liquid nitrogen back to its gas phase may result in the vessel exploding or blowing off its cap with dangerous force creating flying debris.*

1. Thaw the vial by gentle agitation in a **37°C** water bath. To reduce the possibility of contamination, keep the O-ring and cap out of the water. Thawing should be rapid (approximately 2 minutes).

2. Remove the vial from the water bath as soon as the

American Type Culture Collection
P.O. Box 1549
Manassas, VA 20108 USA
www.atcc.org

800-638-6597 or 703-365-2700
Fax: 703-365-2750
E-mail: tech@atcc.org
Or contact your local distributor.

contents are thawed, and decontaminate by dipping in or spraying with 70% ethanol. *All of the operations from this point on should be carried out under strict aseptic conditions.*

3. Transfer the vial contents to a centrifuge tube containing 9.0 ml complete growth medium and spin at approximately 125 xg for 5 to7 minutes.

4. Resuspend cell pellet with the recommended complete growth medium (see the specific batch information for the culture recommended dilution ratio) and dispense into a 25 cm^2 or a 75 cm^2 culture flask. *It is important to avoid excessive alkalinity of the medium during recovery of the cells. It is suggested that, prior to the addition of the vial contents, the culture vessel containing the complete growth medium be placed into the incubator for at least 15 minutes to allow the medium to reach its normal pH (7.0 to 7.6).*

5. Incubate the culture at 37°C in a suitable incubator. A 5% CO_2 in air atmosphere is recommended ifusing the medium described on this product sheet.

Handling Procedure for Flask Cultures

The flask was seeded with cells (see specific batch information) grown and completely filled with medium at ATCC to prevent loss of cells during shipping.
The cell line does not adhere to the substrate when left at room temperature for any length of time, therefore, live cultures may be received with the cells detached. The cells will re-attach to the flask over a period of several days in culture at 37°C.

1. Upon receipt visually examine the culture for macroscopic evidence of any microbial contamination. Using an inverted microscope (preferably equipped with phase-contrast optics), carefully check for any evidence of microbial contamination. Also check to determine if the majority of cells are still attached to the bottom of the flask; during shipping the cultures are sometimes handled roughly and many of the cells often detach and become suspended in the culture medium (but are still viable).

2. **If the cells are still attached,** aseptically remove all but 5 to 10 ml of the shipping medium. The shipping medium can be saved for reuse. Incubate the cells at 37°C in a 5% CO_2 in air atmosphere until they are ready to be subcultured.

3. **If the cells are not attached,** aseptically remove the entire contents of the flask and centrifuge at 125 xg for 5 to 10 minutes. Remove shipping medium and save. Resuspend the pelleted cells in 10 ml of this medium and add to 25 cm^2 flask. Incubate at 37°C in a 5% CO_2 in air atmosphere until cells are ready to be subcultured.

Subculturing Procedure

Volumes used in this protocol are for 75 cm^2 flasks; proportionally reduce or increase amount of dissociation medium for culture vessels of other sizes.

1. Remove and discard culture medium.

2. Add 2.0 to 3.0 ml of 0.25% (w/v) Trypsin-0.53mM EDTA solution to flask and observe cells under an inverted microscope until cell layer is dispersed (usually within 5 to 10 minutes).

   Note: To avoid clumping do not agitate the cells by hitting or shaking the flask while waiting for the cells to detach. Cells that are difficult to detach may be placed at 37°C to facilitate dispersal.

3. Add 6.0 to 8.0 ml of complete growth medium and aspirate cells by gently pipetting.

4. Add appropriate aliquots of the cell suspension to new culture vessels. An inoculum of 2 X 10^3 to 6 X 10^3 viable cells/cm^2 is recommended.
   Subcultivation Ratio: 1:6 to 1:10 weekly

5. Incubate cultures at 37°C.

6. Subculture when cell concentration is between 6 and 7 X 10^4 cells/cm^2.

Note: For more information on enzymatic dissociation and subculturing of cell lines consult Chapter 13 in **Culture Of Animal Cells: A Manual Of Basic Technique** by R. Ian Freshney, 5th edition, published by Wiley-Liss, N.Y., 2005.

Medium Renewal

Two to three times weekly

Complete Growth Medium

The base medium for this cell line is ATCC-formulated Eagle's Minimum Essential Medium, Catalog No. 30-2003. To make the complete growth medium, add the following components to the base medium:

- fetal bovine serum to a final concentration of 10%

This medium is formulated for use with a 5% CO_2 in air atmosphere.
ATCC tested fetal bovine serum is available as ATCC Catalog No. 30-2020 (500ml) and ATCC Catalog No. 30-2021 (100ml).

Cryoprotectant Medium

Complete growth medium described above supplemented with 5% (v/v) DMSO.
Cell culture tested DMSO is available as ATCC Catalog No. 4-X.

Additional Information

Additional product and technical information can be obtained from the catalog references and the ATCC Web site at www.atcc.org, or by e-mail at tech@atcc.org.

References

(additional references may be available in the catalog description at www.atcc.org)

Da Costa LT, et al. **Converting cancer genes into killer genes.** Proc. Natl. Acad. Sci. USA 93: 4192-4196, 1996 PubMed: 96210616

Graham FL et al. **Characteristics of a human cell line transformed by DNA from human adenovirus type 5.** J. Gen. Virol. 36: 59-72, 1977 PubMed: 77229557

Graham FL et al. **Defective transforming capacity of adenovirus type 5 host-range mutants.** Virology 86: 10-21, 1978 PubMed: 78205587

Harrison T et al. **Host-range mutants of adenovirus type 5 defective for growth in HeLa cells.** Virology 77: 319-329, 1977 PubMed: 77129592

Bodary SC and McLean JW. **The integrin beta 1 subunit associates with the vitronectin receptor alpha v subunit to form a novel vitronectin receptor in a human embryonic kidney cell line.** J. Biol. Chem. 265: 5938-5941, 1990 PubMed: 90202850

Goodrum FD and Ornelles DA. **The early region 1B 55-kilodalton oncoprotein of adenovirus relieves growth restrictions imposed on viral replication by the cell cycle.** J. Virol. 71: 548-561, 1997 PubMed: 97138357

Loffler S et al. **CD9, a tetraspan transmembrane protein, renders cells susceptible to canine distemper virus.** J. Virol. 71: 42-49, 1997 PubMed: 97138295

Hu SX et al. **Development of an adenovirus vector with tetracycline-regulatable human tumor necrosis factor alpha gene expression.** Cancer Res. 57: 3339-3343, 1997 PubMed: 97413605

Kolanus W et al. **alphaLbeta2 integrin/LFA-1 binding to ICAM-1 induced by cytohesin-1 a cytoplasmic regulatory molecule.** Cell 86: 233-242, 1996 PubMed: 96319726

Stauderman KA et al. **Characterization of human recombinant neuronal nicotinic acetylcholine receptor subunit combinations alpha 2 beta 4, alpha 3 beta 4 and alpha 4 beta 4 stably expressed in HEK293 cells.** J. Pharmacol. Exp. Ther. 284: 777-789, 1998 PubMed: 98122961

Bartz SR et al. **Human immunodeficiency virus type 1 cell cycle control: Vpr is cytostatic and mediates G2 accumulation by a mechanism which differs from DNA damage checkpoint control.** J. Virol. 70: 2324-2331, 1996 PubMed: 96183878

Sandri-Goldin RM and Hibbard MK. **The herpes simplex virus type 1 regulatory protein ICP27 coimmunoprecipitates with anti-sm antiserum, and the C terminus appears to be required for this interaction.** J. Virol. 70: 108-118, 1996 PubMed: 96099420

Ansieau S et al. **Tumor necrosis factor receptor-associated factor (TRAF)-1, TRAF-2, and TRAF-3 interact in vivo with the CD30 cytoplasmic domain; TRAF-2 mediates CD30-induced nuclear factor kappa B activation.** Proc. Natl. Acad. Sci. USA 93: 14053-14058, 1996 PubMed: 97098519

Zhang J et al. **Dynamin and beta-arrestin reveal distinct mechanisms for G protein-coupled receptor internalization.** J. Biol. Chem. 271: 18302-18305, 1996 PubMed: 96324889

Oppermann M et al. **Monoclonal antibodies reveal receptor specificity among G-protein-coupled receptor kinases.** Proc. Natl. Acad. Sci. USA 93: 7649-7654, 1996 PubMed: 96353872

Xia Y et al. **Nitric oxide synthase generates superoxide and nitric oxide in arginine-depleted cells leading to peroxynitrite-mediated cellular injury.** Proc. Natl. Acad. Sci. USA 93: 6770-6774, 1996 PubMed: 96270618

Zhu X et al. **Cell cycle-dependent modulation of telomerase activity in tumor cells.** Proc. Natl. Acad. Sci. USA 93: 6091-6095, 1996 PubMed: 96234095

Uebele VN et al. **Functional differences in Kv1.5 currents expressed in mammalian cell lines are due to the presence of endogenous Kvbeta2.1 subunits.** J. Biol. Chem. 271: 2406-2412, 1996 PubMed: 96161969

Abell A et al. **Deletions of portions of the extracellular loops of the lutropin/choriogonadotropin receptor decrease the binding affinity for ovine luteinizing hormone, but not human choriogonadotropin, by preventing the formation of mature cell surface receptor.** J. Biol. Chem. 271: 4518-4527, 1996 PubMed: 96224039

Tiberi M et al. **Differential regulation of dopamine D1A receptor responsiveness by various G protein-coupled receptor kinases.** J. Biol. Chem. 271: 3771-3778, 1996 PubMed: 96216484

Shahrestanifar M et al. **Studies on inhibition of mu and delta opioid receptor binding by dithiothreitol and N-ethylmaleimide. His223 is critical for mu opioid receptor binding and inactivation by N-ethylmaleimide.** J. Biol. Chem. 271: 5505-5512, 1996 PubMed: 96215005

Boring L et al. **Molecular cloning and functional expression of murine JE (monocyte chemoattractant protein 1) and murine macrophage inflammatory protein 1alpha receptors.** J. Biol. Chem. 271: 7551-7558, 1996 PubMed: 96205938

Noonberg SB et al. **Evidence of post-transcriptional regulation of U6 small nuclear RNA.** J. Biol. Chem. 271: 10477-10481, 1996 PubMed: 96209965

Fox JC and Shanley JR. **Antisense inhibition of basic fibroblast growth factor induces apoptosis in vascular smooth muscle cells.** J. Biol. Chem. 271: 12578-12584, 1996 PubMed: 96218185

Lee MJ et al. **The inducible G protein-coupled receptor edg-1 signals via the Gi/mitogen-activated protein kinase pathway.** J. Biol. Chem. 271: 11272-11279, 1996 PubMed: 96212194

Marchand P et al. **Cysteine mutations in the MAM domain result in monomeric meprin and alter stability and activity of the proteinase.** J. Biol. Chem. 271: 24236-24241, 1996 PubMed: 96394562

Arai H and Charo IF. **Differential regulation of G-protein-mediated signaling by chemokine receptors.** J. Biol. Chem. 271: 21814-21819, 1996 PubMed: 96355570

Huang Q et al. **Substrate recognition by tissue factor-factor VIIa.** J. Biol. Chem. 271: 21752-21757, 1996 PubMed: 96355561

Monteclaro FS and Charo IF. **The amino-terminal extracellular domain of the MCP-1 receptor, but not the RANTES/MIP-1alpha receptor, confers chemokine selectivity.** J. Biol. Chem. 271: 19084-19092, 1996 PubMed: 96325007

Keith DE et al. **Morphine activates opioid receptors without causing their rapid internalization.** J. Biol. Chem. 271: 19021-19024, 1996 PubMed: 96324996

Louis N et al. **Cloning and sequencing of the cellular-viral junctions from thehuman adenovirus type 5 transformed 293 cell line.** Virology 233: 423-429, 1997 PubMed: 97360037

Hay, R. J., Caputo, J. L., and Macy, M. L., Eds. (1992), **ATCC Quality Control Methods for Cell Lines**. 2nd edition, Published by ATCC.

Caputo, J. L., **Biosafety procedures in cell culture**. J. Tissue Culture Methods 11:223-227, 1988.

Fleming, D.O., Richardson, J. H., Tulis, J.J. and Vesley, D., (1995) **Laboratory Safety: Principles and Practice**. Second edition, ASM press, Washington, DC.

ATCC Warranty

The viability of ATCC products is warranted for 30 days from the date of shipment. If you feel there is a problem with this product, contact Technical Services by phone at 800-638-6597 or 703-365-2700 or by e-mail at tech@atcc.org. Or you may contact your local distributor.

Disclaimers

This product is intended for laboratory research purposes only. It is not intended for use in humans.

While ATCC uses reasonable efforts to include accurate and up-to-date information on this product sheet, ATCC makes no warranties or representations as to its accuracy. Citations from scientific literature and patents are provided for informational purposes only. ATCC does not warrant that such information has been confirmed to be accurate.

This product is sent with the condition that you are responsible for its safe storage, handling, and use. ATCC is not liable for any damages or injuries arising from receipt and/or use of this product. While reasonable effort is made to insure authenticity and reliability of strains on deposit, ATCC is not liable for damages arising from the misidentification or misrepresentation of cultures.

Please see the enclosed Material Transfer Agreement (MTA) for further details regarding the use of this product. The MTA is also available on our Web site at www.atcc.org.

06/11

Reference for CF10 cells

Neurobiology of Disease

Endocytosis of Prion Protein Is Required for ERK1/2 Signaling Induced by Stress-Inducible Protein 1

Fabiana A. Caetano,[1]* Marilene H. Lopes,[4]* Glaucia N. M. Hajj,[4]* Cleiton F. Machado,[4] Camila Pinto Arantes,[4,5] Ana C. Magalhães,[1] Mônica De Paoli B. Vieira,[1] Tatiana A. Américo,[6] Andre R. Massensini,[2] Suzette A. Priola,[7] Ina Vorberg,[8] Marcus V. Gomez,[1] Rafael Linden,[6] Vania F. Prado,[3] Vilma R. Martins,[4] and Marco A. M. Prado[1]

[1]Programa de Farmacologia Bioquímica e Molecular, Departamento de Farmacologia, [2]Departamento de Fisiologia e Biofísica and [3]Departamento de Bioquímica-Imunologia, Instituto de Ciências Biológicas, Universidade Federal de Minas Gerais, MG 30270-910, Belo Horizonte, Brazil, [4]Ludwig Institute for Cancer Research–Hospital Alemão Oswaldo Cruz, SP 01323-903, São Paulo, Brazil, [5]Departamento de Bioquímica, Instituto de Química, Universidade de São Paulo, 05508-900, São Paulo, Brazil, [6]Instituto de Biofísica Carlos Chagas Filho, Universidade Federal do Rio de Janeiro, 21949-900, Rio de Janeiro, Brazil, [7]Laboratory of Persistent Viral Diseases, National Institutes of Health, National Institute of Allergy and Infectious Diseases Rocky Mountain Laboratories, Hamilton, Montana 59840, and [8]Institute of Virology, Technical University of Munich, 81675 Munich, Germany

The secreted cochaperone STI1 triggers activation of protein kinase A (PKA) and ERK1/2 signaling by interacting with the cellular prion (PrP^C) at the cell surface, resulting in neuroprotection and increased neuritogenesis. Here, we investigated whether STI1 triggers PrP^C trafficking and tested whether this process controls PrP^C-dependent signaling. We found that STI1, but not a STI1 mutant unable to bind PrP^C, induced PrP^C endocytosis. STI1-induced signaling did not occur in cells devoid of endogenous PrP^C; however, heterologous expression of PrP^C reconstituted both PKA and ERK1/2 activation. In contrast, a PrP^C mutant lacking endocytic activity was unable to promote ERK1/2 activation induced by STI1, whereas it reconstituted PKA activity in the same condition, suggesting a key role of endocytosis in the former process. The activation of ERK1/2 by STI1 was transient and appeared to depend on the interaction of the two proteins at the cell surface or shortly after internalization. Moreover, inhibition of dynamin activity by expression of a dominant-negative mutant caused the accumulation and colocalization of these proteins at the plasma membrane, suggesting that both proteins use a dynamin-dependent internalization pathway. These results show that PrP^C endocytosis is a necessary step to modulate STI1-dependent ERK1/2 signaling involved in neuritogenesis.

Key words: neurodegeneration; endocytosis; clathrin; raft; prion diseases; flotillin; ERK

Introduction

Prions are believed to be the causal agent of transmissible spongiform encephalopathies that affect humans and other species. These neurological disorders have in common the corruption of a glycosylphosphatidylinositol (GPI)-anchored host protein known as the prion protein (PrP^C). It is widely accepted that a misfolded conformer of PrP^C, PrP^{Sc} (here to denote infectious, β sheet-enriched prion), is the major component of the infectious particle (Prusiner, 1998; Weissmann, 1999). PrP^{Sc} interacts with PrP^C at the cell surface or along the endocytic pathway (Caughey and Raymond, 1991; Caughey and Baron, 2006), but how this interaction imprints novel information to cause disease in the host is a matter of debate. The proposal that PrP^{Sc} represents a gain-of-function, toxic conformer has received much attention, whereas the possibility that alterations in physiological functions of PrP^C contribute to the disease has only recently started to be addressed (Samaia and Brentani, 1998; Martins et al., 2002; Linden et al., 2008).

One of the major difficulties has been to attribute defined physiological roles for PrP^C. Nonetheless, studies in yeast, mammalian cells, and mice models support the hypothesis that PrP^C plays a major role in neuroprotection (for review, see Westergard et al., 2007). Recent data pointed at specific domains of the molecule that are essential for PrP^C-mediated protection. Mice expressing a PrP^C mutant without amino acids 105–125 (hydrophobic domain) in a PrP^C-null background spontaneously developed severe neurodegenerative illness that was lethal within 1 week after birth (Li et al., 2007). Additionally, the presence of a PrP^C variant lacking residues 94–134 induced a rapidly progressive lethal phenotype with extensive central and peripheral myelin degeneration (Baumann et al., 2007).

Received Oct. 22, 2007; accepted May 7, 2008.

This work was supported by Conselho Nacional de Desenvolvimento Científico e Tecnológico (CNPq), Fundação de Amparo à Pesquisa do Estado Minas Gerais–Programa de Apoio a Núcleos de Excelência (PRONEX)-MG, Millennium Institute (MCT/Brazil), Financiadora de Estudos e Projetos, and National Institutes of Health–Fogarty International Center Grants R03 TW007025-01 and R21 TW007800-01 (M.A.M.P., V.F.P., M.V.G.). R.L. and T.A.A. were supported by CNPq, Fundação de Amparo à Pesquisa do Estado do Rio de Janeiro, Coordenação de Aperfeiçoamento de Pessoal de Nível Superior, and PRONEX-RJ. V.R.M. is an International Scholar of the Howard Hughes Medical Institute and received support from Fundação de Amparo à Pesquisa do Estado de São Paulo.

*F.A.C., M.H.L., and G.N.M.H. contributed equally to this work.

Correspondence should be addressed to either of the following: Vilma R. Martins, Ludwig Institute for Cancer Research, Rua Joao Julião 245 1A, SP 01323-903, São Paulo, Brazil, E-mail: vmartins@ludwig.org.br; or Marco A. M. Prado, Departamento de Farmacologia, Instituto de Ciências Biológicas, Universidade Federal de Minas Gerais, Avenida Antonio Carlos 6627, MG 30270-910, Belo Horizonte, Brazil, E-mail: mprado@icb.ufmg.br.

Ana C. Magalhães's, Vania F. Prado's, and Marco A. M. Prado's present address: Robarts Research Institute, University of Western Ontario, London, Ontario, Canada N6A 5K8.

DOI:10.1523/JNEUROSCI.1701-08.2008

 0270-6474/08/286691-12$15.00/0

We have demonstrated that the PrP^C domain, which includes amino acids 113–128, is the binding site for the cochaperone stress-inducible phosphoprotein 1 (STI1). PrP^C engagement with STI1 rescued retinal and hippocampal neurons from programmed cell death through activation of protein kinase A (PKA) (Chiarini et al., 2002; Zanata et al., 2002; Lopes et al., 2005). Additionally, PrP^C–STI1 binding also induced the differentiation of hippocampal neurons by ERK1/2 activation (Lopes et al., 2005). Understanding the fate of both STI1 and PrP^C after their association at the cell surface may help clarify the mechanisms associated with the neurotrophic roles of PrP^C, and its possible bearing on loss-of-function components of prion diseases.

To address these questions, we initially tested whether STI1 alters PrP^C trafficking. Indeed, we found that interaction of these proteins at the cell surface triggered PrP^C endocytosis. Remarkably, the transient ERK1/2 activity induced by PrP^C interaction with either recombinant STI1 or endogenous STI1 secreted by astrocytes depended on PrP^C endocytosis, whereas activation of PKA was not affected when PrP^C trafficking was impaired. STI1 localized in PrP^C-positive organelles only in the initial periods of internalization, suggesting that signaling is triggered by the interaction of these two proteins at the cell surface or shortly after. These data show for the first time that ligand-induced endocytosis of PrP^C is important for cellular signaling.

Materials and Methods

Animals

The *Principles of Laboratory Animal Care* (National Institutes of Health publication number 85-23, 1996) was strictly followed in all experiments. ZrchI *Prnp*$^{0/0}$ mice were provided by Dr. C. Weissmann (Scripps Florida, Jupiter, FL) (Bueler et al., 1992), and the wild-type control mice (ZrchI *Prnp*$^{+/+}$) were generated by crossing F1 descendants from 129/SV and C57BL/6J mating.

Cell culture

SN56 cells are derived from mouse septum neurons (Hammond et al., 1990) and were cultured as described previously (Santos et al., 2001). CF-10, a PrP^C-null neuronal cell line derived from 129/Ola *Prnp*$^{0/0}$ mice (Manson et al., 1994) and positive for the neuroectodermal stem cell marker nestin (I. Vorberg and S. A. Priola, unpublished observation), was used for reconstitution of PrP^C signaling. CF-10 cells were cultured in OptiMEM (Invitrogen) containing glutamine (2 mM; Invitrogen), penicillin (100 IU), and streptomycin (100 μg/ml; Invitrogen) supplemented with 10% fetal bovine serum.

Primary hippocampal cultures were obtained from embryonic day 17 brains of either wild-type (*Prnp*$^{+/+}$) or *Prnp*$^{0/0}$ mice (Bueler et al., 1992). The hippocampus was aseptically dissected in HBSS (Invitrogen) and treated with trypsin (0.06%) in HBSS for 20 min at 37°C. The protease was inactivated with 10% FCS in Neurobasal medium (Invitrogen) for 5 min. After three washes with HBSS, cells were mechanically dissociated in Neurobasal medium containing B-27 supplement (Invitrogen), glutamine (2 mM; Invitrogen), penicillin (100 IU), and streptomycin (100 μg/ml; Invitrogen). Cells (0.5×10^6 cells) were plated onto coverslips (22 mm) coated with 5 μg/ml poly-L-lysine (Sigma).

Plasmids

The GFP-PrP^C vector, GFP-Rab5, dynamin I, the dominant-negative dynamin I K44A, and GFP-Rab7 mutant plasmids have been described previously (Lee et al., 2001; Santos et al., 2001; Barbosa et al., 2002; Magalhães et al., 2002, 2005; Ribeiro et al., 2005). Flotillin1–green fluorescent protein (GFP) and caveolin-1–GFP were kindly provided by Dr. B. J. Nichols (MRC Laboratory of Molecular Biology, Cambridge, UK). The 3F4-tagged plasmids, PrP3F4, and the N-PrP3F4 (N-terminally mutated, altered from ^{23}KKRPKP^{28} to ^{23}KQHPSP^{28}) (Sunyach et al., 2003) were kindly provided by R. Morris (Wolfson Centre for Age Related Diseases, Guy's Hospital Campus, King's College, London, UK). It is important to note that in the N-PrP3F4 mutant, a serine is present at the position 27 and not histidine as published previously (Sunyach et al., 2003) (R. Morris, personal communication).

Transfection of cell lines and isolation of PrP^C-expressing cells

SN56 cells were plated on coverslips for 2 d and transfected using the liposome-mediated method (Effectene; Qiagen) according to the manufacturer's instruction using a 1:10 ratio of DNA to Effectene. After 6 h of transfection, cells were differentiated in serum-free medium supplemented with 1 mM dibutyryl-cAMP (Sigma) for 2 or 3 d with medium changes every day. In cotransfection experiments, a total of 3–5 μg of DNA was used with a plasmid ratio of 1:4 of clathrin–GFP, flotillin1–GFP, and caveolin-1–GFP and a ratio of 1:2 for GFP-PrP^C and dynamin I or dynamin I K44A.

CF-10 cells were transfected with either 3F4-tagged PrP^C (PrP3F4) or the mutant PrP^C N-PrP3F4 (Sunyach et al., 2003) using a liposome-mediated method (Lipofectamine 2000; Invitrogen) according to the manufacturer's instructions using a 1:3 ratio of DNA to lipofectamine. After transfection, the cells were selected with G418 (2 mg/ml; Invitrogen) for 15 d, and resistant cells (10^7) were incubated with mouse anti-PrP^C serum (Zanata et al., 2002) at a 1:100 dilution for 1 h at 4°C. As a negative control, the cells were incubated with preimmune serum. After three washes with PBS, cells were incubated with anti-mouse IgG R-phycoerythrin conjugated at a 1:200 dilution for 1 h at 4°C. Cell sorting was performed using a FACSCalibur flow cytometer (BD Biosciences). Fluorescence was measured using a 488 nm argon laser and FL2-H channel (red fluorescence, 585/42 nm), and data acquisition from 10,000 events was analyzed using CellQuest software (BD Biosciences). Sorting was accomplished using logical gating of the cells in the forward scatter (FSC) versus side scatter and the FSC versus FL2 dot plots. Only events that entered a gate consisting of both cell regions were sorted.

Alexa Fluor 594, 568, or 488 protein labeling

Recombinant STI1 [wild type or deleted in residues 230–245 ($STI1_{\Delta 230-245}$)] was expressed and purified as described previously (Zanata et al., 2002). STI1 labeling was performed using an Alexa Fluor 594 (AF594), Alexa Fluor 568 (AF568), or Alexa Fluor 488 (AF488) labeling kit (Invitrogen). Briefly, STI1 (2 mg/ml) diluted in PBS containing 100 mM sodium bicarbonate was labeled with the reactive dye for 1 h at room temperature, and free dye was separated from the labeled protein by size exclusion chromatography using a PD-10 column (GE Healthcare). Protein concentration was determined with Bradford reagent (Bio-Rad).

Protein detection

Fluorescent-labeled proteins (STI1 and $STI1_{\Delta 230-245}$; 2 μg) were submitted to 10% SDS-PAGE. To visualize labeled proteins, the gel was irradiated with ultraviolet light, and images were acquired using a UV transilluminator MultiDoc-It-Digital Imaging System (Bioimaging Systems). Alternatively, proteins resolved in 10% SDS-PAGE were subjected to immunoblotting with polyclonal antibody anti-STI1 (1:10,000) (Zanata et al., 2002). Rabbit nonimmune-purified IgG was used as the immunoblotting negative control. For detection of PrP^C, cell extracts were prepared by homogenizing the cell pellet in lysis buffer (100 mM Tris, pH 7.4, 150 mM NaCl, 1 mM EDTA, 1% Triton X-100, 0.1% SDS, and 1% acid deoxycholic) and a protease inhibitor mixture (complete protease inhibitor tablets; Roche Diagnostics) or a protease inhibitor mixture (Sigma) at twice the concentration suggested by the manufacturers. Proteins from cells were resolved in SDS-PAGE, transferred to nitrocellulose or Immobilon-P transfer membranes (Millipore), and incubated with mouse anti-PrP^C antibody (Zanata et al., 2002). Staining was revealed by enhanced chemiluminescence (ECL Plus; GE Healthcare) or Super Signal Chemiluminescent Substrate (Pierce).

Fluorescence imaging

Confocal microscopy was performed using a Bio-Rad MRC 1024 laser-scanning confocal system running the Lasersharp 3.0 software coupled to a Zeiss microscope (Axiovert 100) with a 100 × 1.4 numerical aperture (NA) or 63 × 1.3 NA oil-immersion lens (Zeiss), a Bio-Rad Radiance 2100 laser-scanning confocal system coupled to a Nikon microscope (TE2000-U), and a Leica SP5 laser-scanning confocal microscope using a

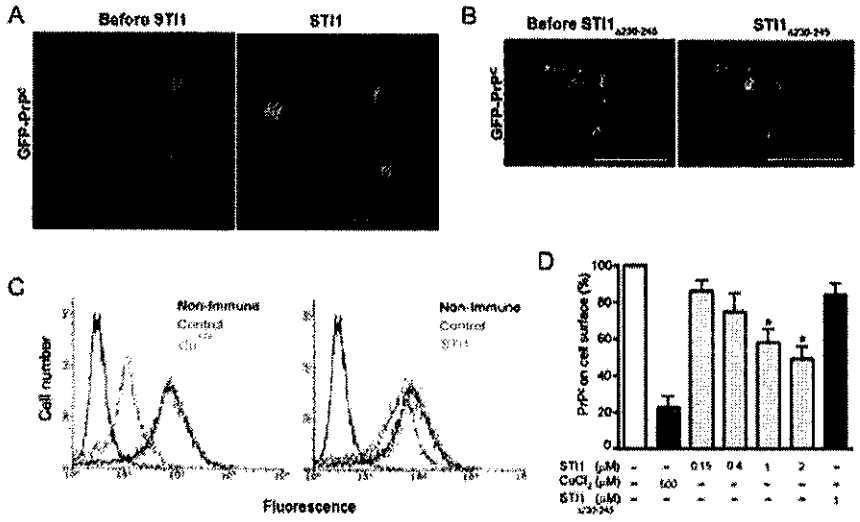

Figure 1. *A*, *B*, STI1 induces PrP^C internalization. SN56 cells expressing GFP-PrP^C were treated with 1 μM STI1 (*A*) or STI1$_{\Delta 230-245}$ (*B*) for 45 min at 37°C. The left and right panels show the green fluorescence from GFP-PrP^C before and after the incubation with STI1 or STI1$\Delta_{230-245}$, respectively. *A* and *B* represent *Z* projections acquired before and after the perfusion. Images are representative of nine and five independent experiments with multiple culture plates in which 40 and 12 cells were analyzed. Scale bars, 20 μm. *C*, Flow cytometry assay from SN56 cells treated with 500 μM Cu^{2+}, 1 μM wild-type STI1, or 1 μM STI1$_{\Delta 230-245}$ for 40 min. Cells were incubated with nonimmune or anti-PrP^C mouse serum followed by R-phycoerythrin-labeled anti-mouse IgG. *D*, The fluorescence for cell-surface PrP^C in untreated cells as described in *C* was set up to 100%, and the levels of PrP^C cell-surface expression after treatment with the indicated concentrations of Cu^{2+}, STI1, or STI1$_{\Delta 230-245}$ were normalized to untreated cells. The results shown are the mean values of six independent experiments. Error bars represent SEM. ANOVA followed by Tukey's HSD test was used for comparisons. *$p < 0.05$.

63 × 1.2 NA water-immersion or a 63 × 1.4 oil-immersion lens (Leica). Cells on coverslips were washed and maintained in serum-free medium or Krebs–Ringer–HEPES (KRH) buffer (124 mM NaCl, 4 mM KCl, 1.2 mM $MgSO_4$, 25 mM HEPES, 10 mM glucose, and 1 mM $CaCl_2$) during image acquisition. In live cell experiments, a FCS2 chamber and objective heater system (Bioptechs) were used to maintain cells at 37°C. Image analysis and processing were performed with Lasersharp (Bio-Rad), Confocal Assistant, Adobe Photoshop, Metamorph, Leica Application Suite Advanced Fluorescent Lite, and ImageJ (version 1.24) software.

Internalization of STI1 and PrP^C

SN56 cells were incubated with 1 μM fluorescent STI1 for different periods at 37°C in 5% CO_2, washed three times with serum-free medium, and visualized by confocal microscopy. For competition assays, cells were incubated with 10 μM STI1 or albumin in DMEM for 1 h at 4°C, followed by 1 μM fluorescent STI1. The coverslips were washed with serum-free medium and visualized by confocal microscopy.

Cells expressing GFP-PrP^C or coexpressing GFP-PrP^C and dynamin I K44A were maintained in a FCS2 chamber at 37°C and perfused with KRH to obtain the first image. After that, cells were perfused with 1 μM fluorescent STI1 or STI1$_{\Delta 230-245}$, and additional optical sections were acquired each minute for 50 min.

For cell-surface labeling, CF-10 PrP3F4 or N-PrP3F4 cells were treated with STI1 or STI1$_{\Delta 230-245}$, as described in the figure legends, for 20 min, washed in PBS three times, and fixed in 3.5% paraformaldehyde without any detergent for 20 min. Cells were incubated simultaneously with monoclonal 3F4 antibodies (1:100; Dako), and after washing with PBS, cells were incubated goat anti-mouse AF488 secondary antibodies (Invitrogen), mounted in coverslips with Hydromount (National Diagnostics), and imaged with the SP5 confocal microscope. In these experiments, nuclei were stained with Syto60Red (Invitrogen).

Biotinylation of cell-surface proteins was performed as described previously (Ribeiro et al., 2005; Lee et al., 2007). Briefly, cells were incubated with STI1 or 500 μM Cu^{2+} for 5 or 10 min, respectively, transferred to ice, washed, and incubated on ice in PBS/CM (PBS supplemented with 1.0 mM $MgCl_2$ and 0.1 mM $CaCl_2$). Cell-surface proteins were biotinylated with 1 mg/ml sulfo-NHS-SS-biotin (Pierce) for 1 h on ice. To quench the biotinylation reaction, cells were washed and incubated for 30 min with cold 100 mM glycine in PBS/CM, followed by three washes with cold PBS/CM, and proteins were extracted using 10 mM Tris, pH 7.8, 0.1 M NaCl, 10 mM EDTA, 0.5% Triton X-100, and 0.5% acid deoxycholic. Biotinylated proteins were separated from nonbiotinylated proteins by Neutravidin bead pull-down from equivalent amounts of total cellular protein (800 μg) from each sample. The biotinylated proteins were subjected to SDS-PAGE, followed by electroblotting onto polyvinylidene fluoride membranes, and revealed using a mouse anti-PrP^C antibody (Zanata et al., 2002). For quantification, the major glycosylated band of PrP^C in nonsaturated blots was analyzed using ImageQuant TL and normalized by the expression of PrP^C in the lysates.

Labeling of organelles

Labeling of endosomes was performed by incubating cells with 40 μg/ml AF488-labeled transferrin (Invitrogen) at 37°C in 5% CO_2 for 40 min. After incubation, cells were washed three times with PBS and fixed with 3% paraformaldehyde in PBS for 20 min for posterior imaging. Labeling of late endosomes/lysosomes was done by incubating cells with 1 μM Lysosensor Green DND-189 (Invitrogen) at 37°C in 5% CO_2 for 1 h, and cells were washed as described above and imaged.

Quantification of fluorescence

The effect of dynamin K44A expression on STI1 internalization was evaluated using the ImageJ software or MetaMorph. The total fluorescence inside cells after a 40 min incubation with STI1-AF568 was quantified. Images were thresholded, and the total fluorescence was detected automatically and independently by the software. The results were expressed as the mean of total fluorescence per cell. For colocalization indices, cells were analyzed using MetaMorph, by independently counting fluorescent objects (vesicles) and analyzing the percentage of colocalization independently by the software.

Conditioned medium from astrocytes

Primary mouse astrocyte cultures were obtained as described previously (Lima et al., 2007). After reaching confluence, cells were maintained in DMEM without serum for 48 h. The conditioned medium (CM) was collected, centrifuged for 10 min to remove cellular debris, and filtered in 0.2 μm membranes. CM (total volume of 30 ml) was concentrated to a final volume of 150 μl (200×) in Minicon Static concentrator B12 (Millipore). A total of 30 μl of the 200× concentrated CM was used to measure STI1 concentration. Alternatively, 50 μl of the 200× concentrated CM was immunodepleted of STI1 using a rabbit anti-STI1 antibody (IgG, 4 μg/ml) overnight at 4°C (Lima et al., 2007), mixed with protein A-Sepharose for 2 h at 4°C, and centrifuged. The pellets (washed three times) and supernatants were analyzed for the presence of STI1.

Kinase assays

P44/42 extracellular signal-regulated kinase phosphorylation. Phosphorylation assays were performed using the PhosphoPlus p44–42 extracellular signal-regulated kinase (ERK) (Thr202/Tyr204) antibody kit (Cell Signaling Technology) according to the manufacturer's instructions. Briefly, CF-10 cell lines (5×10^4 cells, serum starved for 48 h with medium change every 24 h) and hippocampal primary culture (10^6 cells) were stimulated or not with recombinant STI1 (0.5 μM) or 50 μl of the 200× concentrated CM to a final volume of 1 ml (5 nM STI1), rinsed once with ice-cold PBS, and lysed in Laemmli buffer. Cell extracts were subject to SDS-PAGE, followed by immunoblotting with anti-phospho-ERK1/2 and anti-ERK1/2 antibodies (Cell Signaling Technology). The bands obtained after x-ray film exposure to the membranes were analyzed by densitometric scanning and quantified using the Scion Image software.

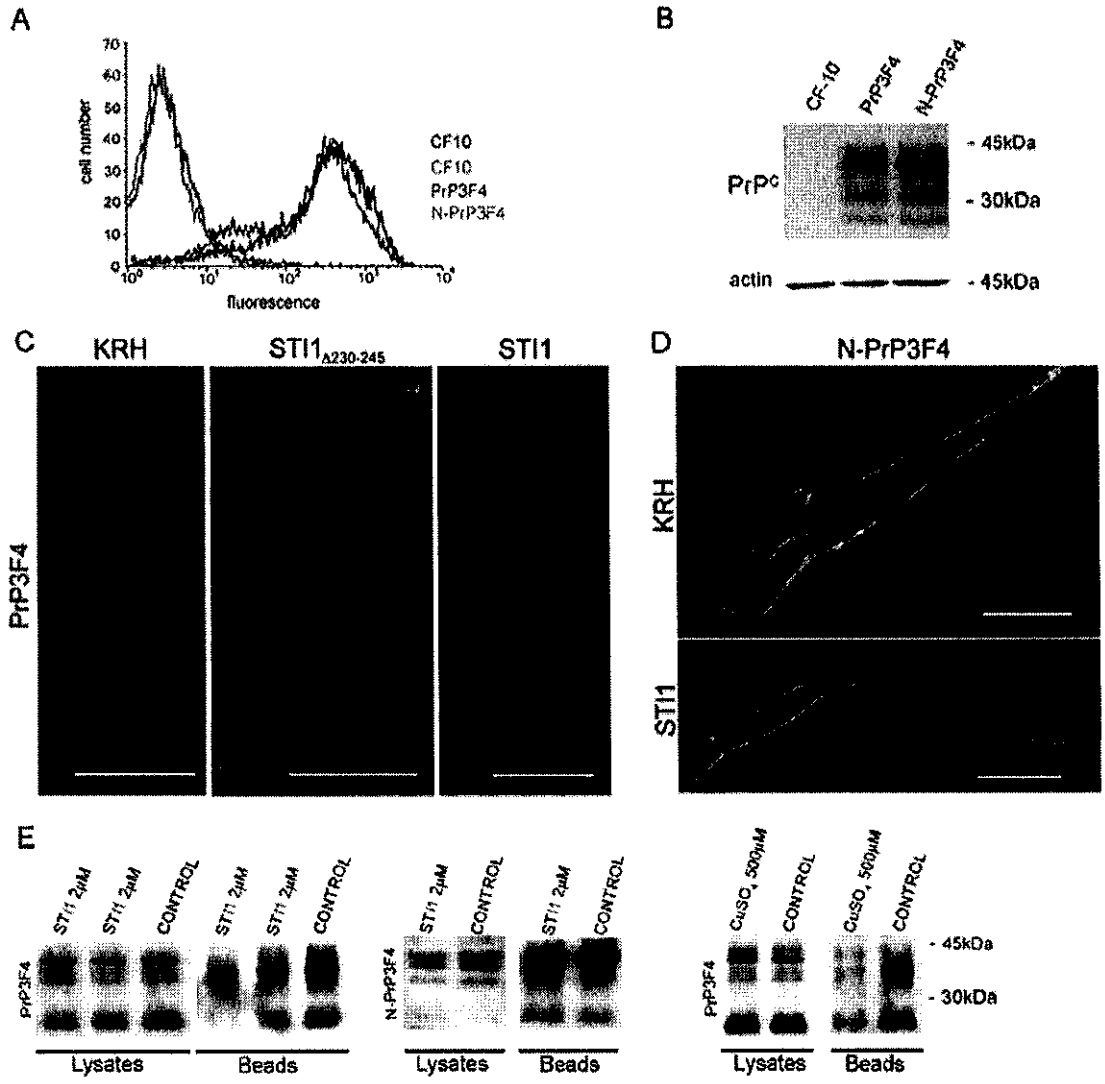

Figure 2. Internalization of PrP^C is dependent of the N-terminal basic motif. The PrP^C-null cell line CF-10 was transfected with an expression vector encoding wild-type PrP^C (PrP3F4) or a mutated PrP^C (N-PrP3F4) protein, the internalization of which is impaired, and stably transfected cells were sorted. ***A***, Flow cytometry of nonpermeabilized cells detected using anti-PrP^C antibodies (except in CF-10 cells, black lines that were incubated only with secondary antibodies). ***B***, Western blot assays using anti-PrP^C antibodies show similar expression of ectopic proteins. ***C***, PrP3F4 cells were kept in KRH or treated with 2 μM STI1$_{\Delta 230-245}$ (second column) or STI1 (third column) for 20 min at 37°C. After treatment, cells were fixed and immunostained for cell-surface PrP^C using the 3F4 antibody. ***D***, As in ***C***, the N-PrP3F4 mutant cells were treated with 2 μM STI1 for 20 min at 37°C. Scale bars, 20 μm. ***E***, PrP3F4- or N-PrP3F4-expressing cells were treated with STI1 or KRH for 5 min and iced. Cell-surface PrP^C after these treatments was detected by biotinylation of cell-surface proteins. Biotinylated proteins were isolated using Neutravidin beads, subjected to SDS-PAGE, and immunobloted using a mouse anti-PrP^C antibody. The lysates represent the expression of PrP3F4 or N-PrP3F4 proteins, and beads represent biotinylated cell-surface PrP^C after treatment with STI1 or KRH (control). Note that STI1 decreased the amount of PrP3F4 in the membrane in the two lanes (duplicates) labeled STI1 compared with control, whereas N-PrP3F4 was not decreased. Treatment with 500 μM $CuSO_4$ for 10 min was used to test for efficient detection PrP^C cell-surface sequestration. The blots are representative of six or seven experiments, respectively.

PKA activation. Primary hippocampal neurons (10^6 cells), the SN56 cell line (10^6 cells, medium starved 24 h), or the CF-10 cell line (10^5 cells, serum starved for 48 h with medium change every 24 h) were preincubated with 100 μM IBMX (Sigma) for 1 h at 37°C and 5% CO_2 and treated with STI1 (1 μM) or forskolin (10 μM) for 20 min at 37°C. The cells were washed with PBS and homogenized with ice-cold extraction buffer (150 mM NaCl, 20 mM $MgCl_2$, 1% Triton X-100, and 25 mM Tris-HCl, pH 7.4) plus Complete Protease Inhibitor Cocktail (Roche). Cellular debris was removed by centrifugation at 6000 × *g* for 10 min. The PKA activity was determined by $\gamma[P^{32}]$-ATP incorporation to a PKA-specific substrate provided by the PKA assay system kit (Millipore). The reaction was performed according to the manufacturer's instructions.

Flow cytometry assay

SN56 cells were preincubated with blocking solution (0.5% BSA in PBS) in the absence or presence of STI1 or copper sulfate for 20 or 40 min at 37°C. Cells were washed and incubated with an anti-PrP^C antibody (1:100) (Zanata et al., 2002), followed by anti-mouse IgG conjugated to R-phycoerythrin (1:200; Dako), both for 1 h at 4°C. Analyses were performed using a FACSCalibur flow cytometer (BD Biosciences), and data acquisition from 10,000 events was analyzed using CellQuest software (BD Biosciences).

Statistical analysis

The mean values of at least three independent datasets are shown in the figures; the error bars represent SEM. ANOVA followed by Tukey's honestly significant difference (HSD) test or Kruskal–Wallis one-way ANOVA followed by a Dunn's *post hoc* test were used for multiple comparisons. For all tests, results were considered statistically significant when p was <0.05.

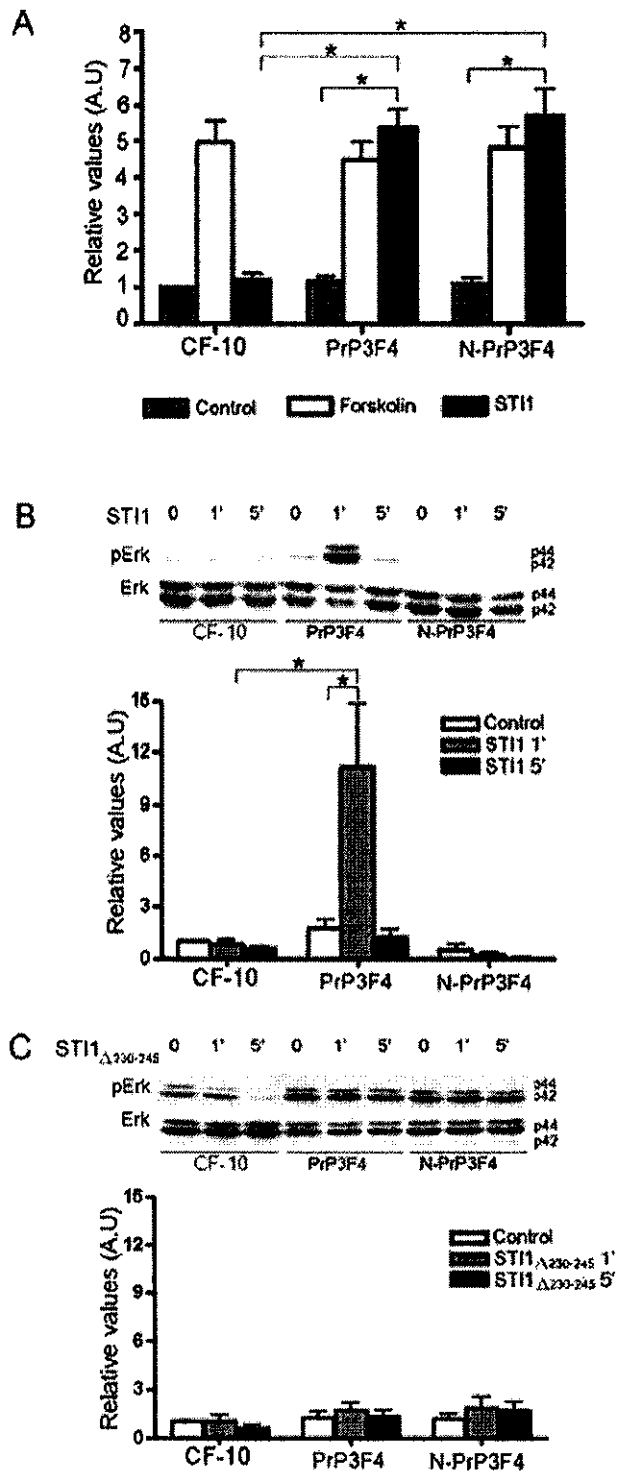

Figure 3. PrP^C endocytic trafficking is necessary for STI-PrP^C-dependent ERK1/2 but not for PKA activation. ***A***, Cells were treated with forskolin or 1 μM of STI1, and the PKA activity was evaluated. ***B***, Cells were treated with 0.5 μM STI1 for 1 or 5 min, and ERK1/2 activity (pErk) was analyzed. ***C***, Cells were treated with 0.5 μM STI1$_{\Delta 230-245}$ for 1 or 5 min, and ERK1/2 activity was analyzed. The basal activity of CF-10 cells without treatment was normalized to 1, and the other values are relative to it. The results show the mean values of five (***A***) or four (***B***, ***C***) independent datasets. Error bars represent SEM. ANOVA followed by Tukey's HSD test was used for comparisons. *$p < 0.05$. A.U., Arbitrary units.

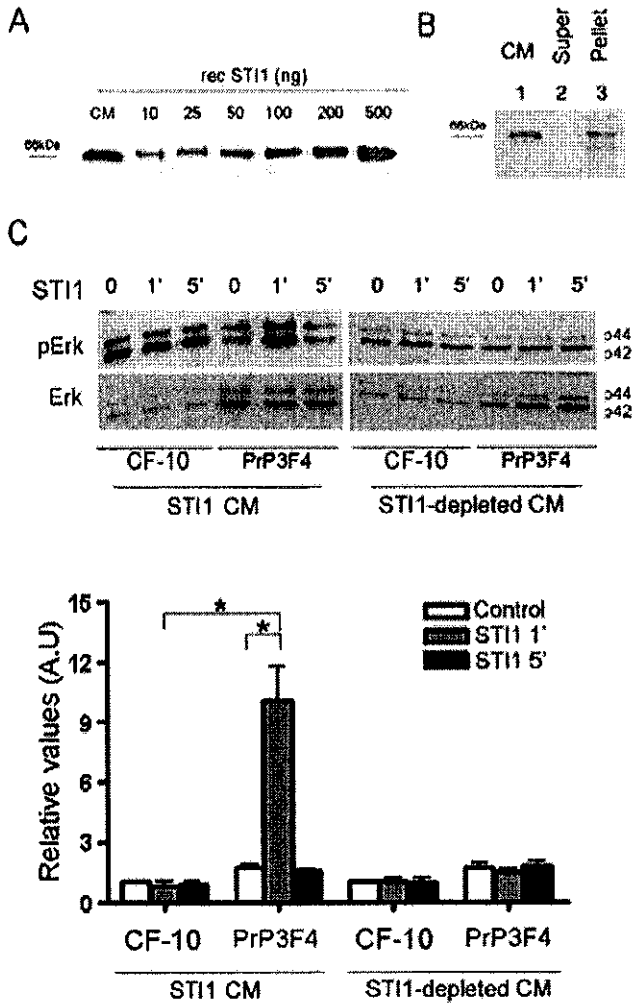

Figure 4. STI1 secreted by astrocytes induces ERK1/2 activation. ***A***, Increasing amounts of recombinant STI1 (from 10 to 500 ng) and 30 μl of 200× concentrated CM was loaded onto SDS-PAGE. Immunoblotting was developed with anti-STI1 antibodies. ***B***, STI1 was immunoprecipitated from 150 μl of concentrated CM. The supernatant and the pellet were resolved by SDS-PAGE and detected with anti-STI1 antibodies: lane 1, 30 μl of concentrated CM; lane 2, 30 μl of immunodepleted concentrated CM; lane 3, 30 μl pellet from immunoprecipitation. ***C***, CF-10 or CF-10-expressing PrP3F4 were treated with 50 μl of concentrated CM (STI1 final concentration of 5 nM) or immunodepleted concentrated CM for 1 or 5 min, and ERK1/2 activity was analyzed. The basal activity of CF-10 cells without treatment was normalized to 1, and the other values are relative to it. The results show the mean values of three independent datasets. Error bars represent SEM. ANOVA followed by Tukey's HSD test was used for comparisons. *$p < 0.05$. A.U., Arbitrary units.

Results

STI1 induces PrP^C internalization

To test whether interaction with STI1 causes any consequence for PrP^C localization in living cells, we expressed GFP-PrP^C ectopically. This fluorescent protein has been previously shown to respond to Cu^{2+} and to present identical localization as endogenous PrP^C. For these experiments, we used SN56 cells, in which the cellular trafficking of fluorescent PrP^C and PrP^{res} was studied and which have also been shown to be infected by PrP^{res} (Lee et al., 2001; Magalhães et al., 2005). Maximum projection images obtained from confocal stacks (data not shown) demonstrated that, as described previously (Lee et al., 2001), GFP-PrP^C is present at the cell surface and in the perinuclear region that represents the Golgi apparatus and endosomes (Magalhães et al., 2002). In control experiments, we reproduced the observation that Cu^{2+} evokes internalization of GFP-PrP^C (data not shown) (Lee et al., 2001; Magalhães et al., 2002). We then evaluated GFP-PrP^C distribution in SN56 cells after treatment with STI1 or a deletion mutant unable to bind PrP^C, STI1$_{\Delta 230-245}$ (Lopes et al.,

2005). We noted that a significant fraction of the green fluorescence representing PrP^C disappeared from the cell surface and accumulated inside cells after STI1 addition (Fig. 1*A*). Conversely, GFP-PrP^C was not internalized in cells similarly treated with STI1$_{\Delta 230-245}$ (Fig. 1*B*), indicating the need of STI1–PrP^C interaction for PrP^C endocytosis.

To test whether endogenous PrP^C was also internalized in cells in response to STI1 and to quantify this effect, flow cytometry assays were performed. SN56 cells express PrP^C (Lee et al., 2001; Magalhães et al., 2005; Baron et al., 2006), and treatment with 500 μM Cu^{2+} evoked sequestration of cell-surface PrP^C (Fig. 1*C*). STI1 also induced internalization of endogenous PrP^C in a dose-dependent manner (Fig. 1*D*), whereas STI1$_{\Delta 230-245}$ was unable to promote endocytosis of PrP^C (Fig. 1*D*). The present results show that interaction of STI1 and PrP^C at the cell surface triggers internalization of PrP^C, albeit at lower levels than copper. Control experiments showed that STI1 interaction with PrP^C does not shed the latter from the cell surface, because cultures treated with STI1 showed no increase in PrP^C in CM (data not shown).

Endocytic trafficking of PrP^C is required for STI–PrP^C-dependent ERK1/2 but not for activation of PKA

The endocytic trafficking of membrane receptors is important for attenuating ligand-induced signaling, but it can also be critical to trigger and modulate specific signaling pathways as shown, for example, for epidermal growth factor receptors (Vieira et al., 1996). Our previous data showed that PrP^C–STI1 interaction triggers both PKA and ERK1/2 activation promoting neuronal survival and differentiation, respectively (Chiarini et al., 2002; Lopes et al., 2005). To test for a role of STI1-induced PrP^C endocytic trafficking on these signaling pathways, we expressed either a mutant PrP^C, the internalization of which is impaired (N-PrP3F4), or its wild-type control (PrP3F4) (Sunyach et al., 2003) in PrP^C-null CF-10 neuronal cells. Transfected cells were selected for similar expression of either wild-type PrP3F4 or N-PrP3F4 mutated PrP^C, as verified by flow cytometry (Fig. 2*A*) and Western blot assays (Fig. 2*B*). As expected, no endogenous PrP^C expression was present in untransfected CF-10 cells (note that black and red lines represent CF-10 cells incubated without or with PrP^C antibodies, respectively) (Fig. 2*A*,*B*).

We initially tested whether in these cells STI1 would also induce endocytosis. Immunofluorescence analysis of cell-surface PrP3F4 indicates that STI1, but not STI1$_{\Delta 230-245}$, decreased cell-surface immunolabeling for PrP^C (Fig. 2*C*). In contrast, in N-PrP3F4-expressing cells, treatment with STI1 did not change cell-surface immunolabeling (Fig. 2*D*). To complement these experiments and quantify the effect of STI1, we used biotinylation of cell-surface PrP^C (Fig. 2*E*). In these experiments, we measured the amount of PrP3F4 remaining at the cell surface after the cells were treated with STI1 (Ribeiro et al., 2005; Lee et al., 2007). In control experiments, cells exposed to Cu^{2+} showed a decrease in cell-surface PrP^C (63 ± 10% of decrease; mean ± SEM for seven experiments). Treatment of cells with STI1 for 5 min caused sequestration of PrP3F4 with consequent decrease in cell-surface PrP^C (Fig. 2*E*) (34 ± 7%; mean ± SEM for six experiments). In contrast, N-PrP3F4 cells treated with STI1 showed no sign of internalization (Fig. 2*E*) (2 ± 2%; mean ± SEM of four experiments). Thus, the combination of live cell, flow cytometry, immunofluorescence, and biotinylation experiments showed that STI1 was able to induce PrP^C endocytosis in two distinct neuronal cell lines.

Incubation of PrP-null CF-10 cells with STI1 induced neither PKA nor ERK1/2 activation, consistent with dependence on PrP^C for STI1-dependent signaling, although the cells responded to forskolin (Fig. 3*A*). The expression of either the wild type (PrP3F4) or the internalization defective PrP^C (N-PrP3F4) reconstituted STI1-induced PKA activation (Fig. 3*A*). In contrast, transient activation of ERK1/2 by STI1 was rescued in CF-10 by wild-type PrP^C, but not by the mutated PrP^C, which lacks internalization signals (Fig. 3*B*). The STI1 deletion mutant defective for the PrP^C binding site, STI1$_{\Delta 230-245}$, is unable to activate either PKA or ERK1/2 signaling in hippocampal neurons (Lopes et al., 2005). In agreement with those observations, CF-10 cells expressing PrP3F4 or N-PrP3F4 presented no activation of ERK1/2 when treated with STI1$_{\Delta 230-245}$ (Fig. 3*C*).

Our recent data demonstrated that, similar to chaperones such as Hsp70, STI1 is secreted by astrocytes and presents neurotrophic activity (Lima et al., 2007). To test whether recombinant STI1 may mimic physiologically secreted STI1, we first estimated the amount of STI1 present in CM from astrocytes. Comparison of STI1 in CM with standards containing several concentrations of recombinant STI1 indicates that the amount of STI1 therein is equivalent to ~200 ng of protein (Fig. 4*A*), a STI1 final concentration of 33 ng/ml or 0.5 nM (see Materials and Methods for details). As shown previously (Lima et al., 2007), STI1 from the CM of astrocytes (Fig. 4*B*, lane 1) can be immunoprecipitated with specific antibodies (Fig. 4*B*, lane 3) resulting in a fraction of CM depleted of this protein (Fig. 4*B*, lane 2). The CM containing STI1 at a final concentration of 5 nM was able to induce ERK1/2 activation in PrP3F4-expressing cells, but not in the PrP-null parent CF-10 cells (Fig. 4*C*, left). Conversely, STI1-depleted CM did not activate ERK1/2 in any of the cell lines (Fig. 4*C*, right), suggesting that recombinant STI1 reproduces the effects of secreted protein found in CM derived from astrocytes. It should be noted that 100 times more recombinant STI1 (0.5 μM) (Fig. 3*B*) than astrocyte-secreted STI1 (5 nM) (Fig. 4*C*) is necessary to activate ERK1/2. This indicates either that some of the recombinant protein may not be properly folded or that posttranslational

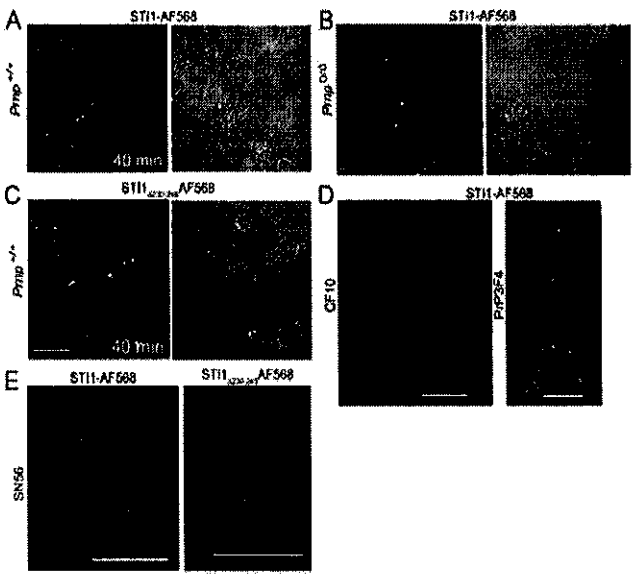

Figure 5. STI1 is internalized independently of PrP^C. ***A–E***, Wild-type *Prnp*$^{+/+}$ (***A***, ***C***); PrP^C-null, *Prnp*$^{0/0}$ primary hippocampal neurons (***B***), CF-10 and CF-10 PrP3F4 cells (***D***); or SN56 cells (***E***) were incubated with 1 μM STI1–AF568 or STI1$_{\Delta 230-245}$–AF568, as indicated, for 40 min at 37°C. Optical sections of representative cells from at least three independent experiments done in multiple cultures are shown. Scale bars, 20 μm.

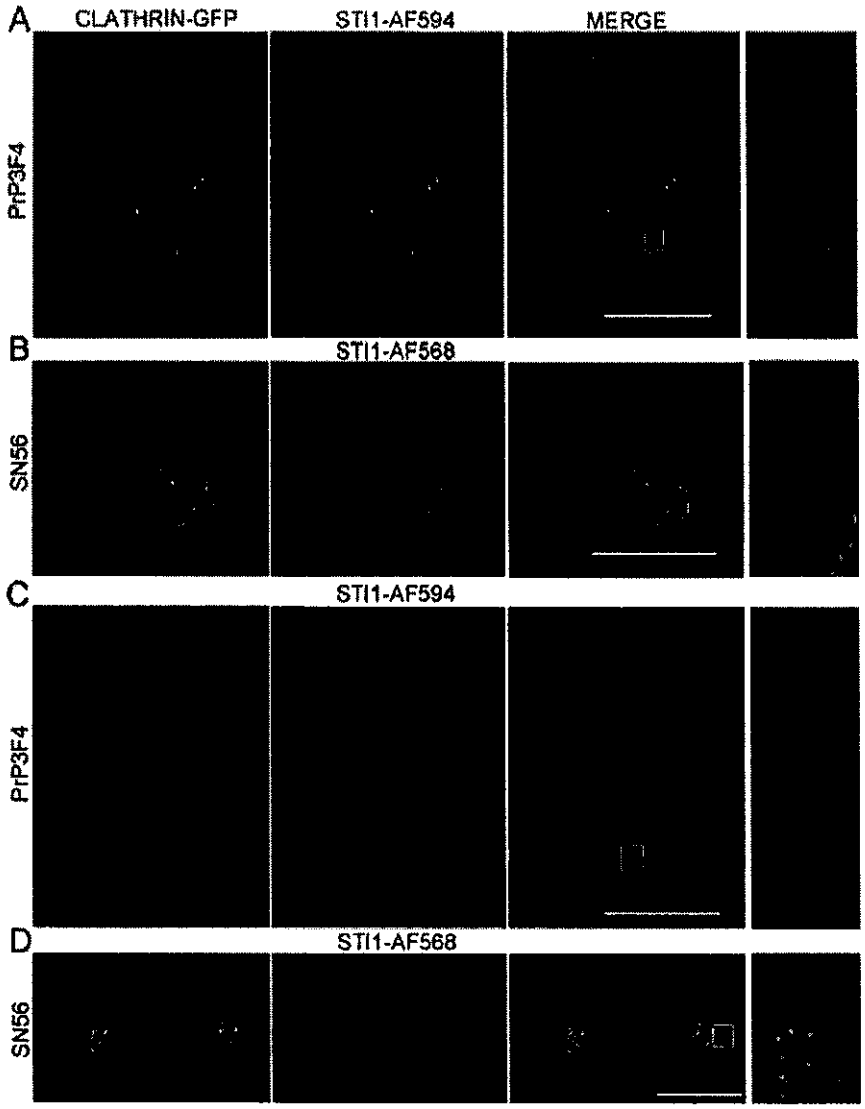

Figure 6. A fraction of internalized STI1 colocalizes with clathrin. PrP3F4 or SN56 cells, as indicated, were transfected with clathrin–GFP and incubated with 1 μM STI1–AF594 or STI1–AF568 for various periods of time. ***A***, ***B***, Representative images for the first minutes after incubation with STI1. Arrows point to some vesicles where clathrin–GFP and fluorescent STI1 are found. ***C***, ***D***, Representative images of transfected cells 20 min after incubation with STI1. Right panels present a magnified view of the region indicated in the merged images. Arrows indicate some of the colocalization spots. Images are representative of at least 30 cells from several culture dishes on 3 different days. Scale bars, 20 μm.

modifications in secreted STI1 as well as the presence of coactivators in the CM may contribute for this higher activity compared with the recombinant protein.

STI1 binds to cells in a specific manner and is internalized

To evaluate STI1 interaction with the cell membrane and its possible dependency on expression of PrP^C at the cell surface, recombinant STI1 or the deletion mutant unable to bind PrP^C, STI1$_{\Delta 230-245}$ (Lopes et al., 2005), were labeled using AF488, AF568, or AF594. Control experiments showed that labeling STI1 as well as STI1$_{\Delta 230-245}$ did not produce any degradation (supplemental Fig. 1*A*,*B*, available at www.jneurosci.org as supplemental material) and labeled proteins are able to evoke PKA activity in cultured hippocampal neurons (supplemental Fig. 1*C*, available at www.jneurosci.org as supplemental material) and are therefore functional. Interestingly, STI1–AF568 bound to hippocampal neurons from both wild-type (*Prnp*$^{+/+}$) (Fig. 5*A*) and PrP^C-null (*Prnp*$^{0/0}$) (Fig. 5*B*) mice was internalized. In agreement with these observations, STI1$_{\Delta 230-245}$–AF568 was also effectively internalized by wild-type neurons (Fig. 5*C*). These observations were confirmed in PrP-null CF-10 cells and CF-10 cells expressing PrP3F4 treated with STI1–AF488 (Fig. 5*D*) and also in SN56 cells exposed to STI1–AF568 or STI1$_{\Delta 230-245}$–AF568 (Fig. 5*E*). Therefore, these data suggest that STI1 binds to neuronal cells and is internalized by a PrP^C-independent pathway.

Intracellular localization of internalized STI1

Although the interaction of STI1 with cells appears to be independent of the presence of PrP^C, signaling is strictly dependent on PrP^C expression, and ERK1/2 activation depends on PrP^C internalization. Hence, it is possible that engagement of these proteins occurs at the cell surface and continues in intracellular organelles to activate ERK1/2. We investigated this possibility by examining the localization of fluorescent STI1. Confocal images of CF-10 PrP3F4 cells or SN56 cells showed that we could clearly detect internalized fluorescent STI1 after 10 min of incubation, and additional exposure to medium containing the fluorescent protein lead to increased intracellular accumulation in vesicles (supplemental Fig. 2*A*,*B*, available at www.jneurosci.org as supplemental material). The interaction of STI1–AF568 with cells and its sequestration in intracellular organelles showed specificity, because no internalization of STI1–Alexa Fluor was detected in experiments done at 4°C (data not shown). Moreover, intracellular labeling with fluorescent STI1 was blocked when CF-10 PrP3F4 or SN56 cells (supplemental Fig. 2*C*,*D*, available at www.jneurosci.org as supplemental material) were incubated with a 10-fold excess of nonfluorescent protein (STI1) for 1 h, followed by incubation with fluorescent STI.

To test whether fluorescent STI1 is present in the same organelles as PrP^C, we did a series of double-labeling experiments in living cells using GFP-tagged markers of internalization pathways. We chose to study trafficking in living cells to avoid possible fixation artifacts, because GPI-anchored proteins such as PrP^C may change location after fixation, and we noted that fixed STI1–AF568-labeled cells showed a distinct pattern of localization compared with live cells (data not shown). Cells were transfected with clathrin light chain–GFP, which labels both coated pits and clathrin-coated vesicles (Gaidarov et al., 1999). These experiments indicated that STI1 (AF568 or AF594) internalized in cells in the initial period (<15 min) after incubation showed some colocalization with GFP–clathrin-labeled vesicles both in CF-10 PrP3F4 cells (Fig. 6*A*) and in SN56 cells (Fig. 6*B*). In contrast, incubation of STI1–AF568 for 20 or 40 min (data not shown) with CF-10 PrP3F4 cells (Fig. 6*C*) or SN56 cells (Fig. 6*D*) showed

no colocalization of internalized STI1 (red) with clathrin-coated vesicles (green). Quantification of these colocalization experiments indicated that 41 ± 8% of STI1-positive vesicles also show clathrin labeling in the initial periods of incubation, but this colocalization decreased to 9 ± 1% after cells were exposed to fluorescent STI1 for >20 min.

We also investigated a role of raft-derived organelles in the trafficking of STI1, by using either caveolin–GFP (Fig. 7*A*) or flotillin–GFP (Fig. 7*B*) in CF-10 PrP3F4 cells and in SN56 cells (Fig. 7*C*,*D*). Strikingly, STI1–AF568 (red) partly colocalized with caveolin-1–GFP (green; 36 ± 8% of colocalization in CF-10 PrP3F4 cells in the initial periods of incubation), but quantification of colocalization after additional periods of incubation in CF-10 PrP3F4 cells showed decreased colocalization (15 ± 2% after 20 min incubation). In contrast, STI1–AF568 or STI1–AF594 (red) showed extensive colocalization with flotillin1–GFP (green)-labeled vesicles in all time periods examined (61 ± 5% in the initial 15 min incubation and 68 ± 2% after the 20 min incubation). In SN56 cells, fluorescent STI1 appeared to colocalize extensively with both caveolin- and flotillin-labeled vesicles.

These experiments suggest that internalized STI1 is found predominantly in flotillin organelles at steady state, but a fraction of the protein appears to use clathrin-coated vesicles for internalization, a pathway that also serves as the port of entry for PrP^C (Shyng et al., 1994, 1995; Sunyach et al., 2003; Taylor et al., 2005). To further understand the subcellular localization of STI1, we focused our experiments in SN56 cells, a cell line in which we have previously examined the trafficking of PrP^C and PrP^{res} (Lee et al., 2001; Magalhães et al., 2002, 2005). In agreement with an important role for a raft-derived organelle in the steady-state localization of STI1, we detected almost no colocalization between STI1–AF568 (red) incubated for 20 min (data not shown) or 40 min with AF488-labeled transferrin (green) (Fig. 8*A*) or GFP-Rab5 (green) (Fig. 8*B*), which are markers of classical early endosomes derived from clathrin-coated vesicles.

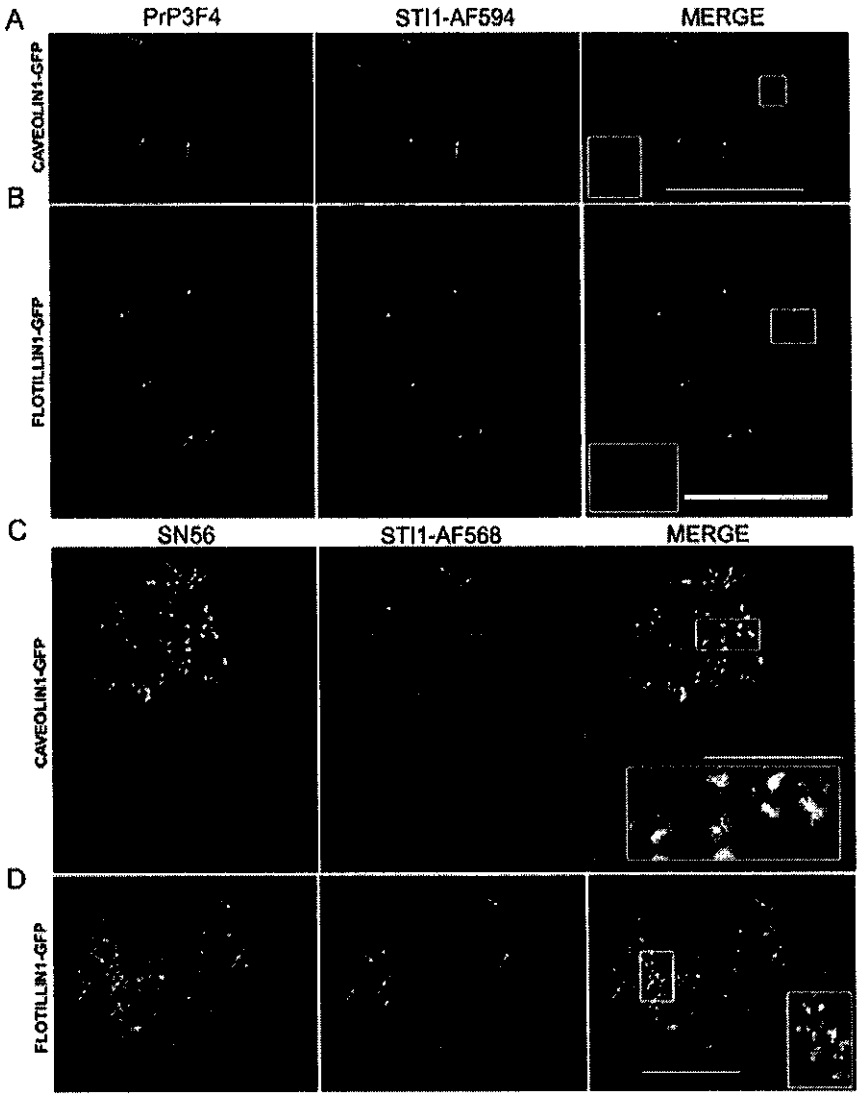

Figure 7. STI1 is also found in raft-derived vesicles. ***A***, ***B***, PrP3F4 cells were transfected with caveolin-1–GFP (***A***) or flotillin1–GFP (***B***), and living cells were perfused with STI1–AF594 for 30 min at 37°C. These images are representative examples of colocalization patterns in the first 15 min of incubation with STI1. ***C***, ***D***, SN56 cells were transfected with caveolin-1–GFP (***C***) or flotillin1–GFP (***D***) and incubated with STI1–AF568 for 40 min at 37°C. Insets show a magnified view of the designated box. Colocalization between STI1 and the two markers is seen in yellow in the superimposed images, and arrows show some of the colocalization spots. Images are representative of at least 40 cells from several dishes analyzed on 5 different days for each condition. Scale bars, 20 μm.

The above experiments suggest that STI1 may enter cells by two pathways: a smaller fraction of the fluorescent protein seems to use clathrin-mediated endocytosis, but a larger fraction uses a raft-mediated pathway (flotillin and perhaps caveolae in cells that endogenously express caveolin) for internalization. Proteins that are internalized by raft-mediated pathways are able to accumulate in acidic-late endosomal organelles, and flotillin1 (also known as reggie-2) itself is found also in acidic organelles (Stuermer et al., 2004; Pimpinelli et al., 2005). We tested the possibility that STI1 may be located in late endosomes by labeling STI1–AF568-treated cells (1 h) with lysosensor green, a marker of acidic vesicles. Figure 8*C* shows abundant colocalization between STI1–AF568 (red) and lysosensor green (green) in SN56 cells. We confirmed that STI1–AF568 was present in late endosomes/lysosomes by expressing GFP-RAB7Q67L, a constitutively active mutant that is preferentially located in these organelles (Bucci et al., 2000; Magalhães et al., 2005). STI1–AF568 (Fig. 8*D*, red) also colocalized with vesicles labeled with GFP-RAB7Q67L (green). Together, these observations suggest that a larger fraction of fluorescent STI1 accumulates in late endosomes.

STI1 interacts with PrP^C predominantly at the cell surface and in early endocytic intermediates

The above experiments suggest only a small fraction of fluorescent STI1 locates to organelles where PrP^C has been previously found in neurons and neuronal cells (i.e., clathrin-coated vesicles) (Sunyach et al., 2003). To also test in living cells whether both STI and PrP^C can be found in the same organelles, we used STI1–AF568 and GFP-PrP^C. Figure 9*A* (top) indicates that dur-

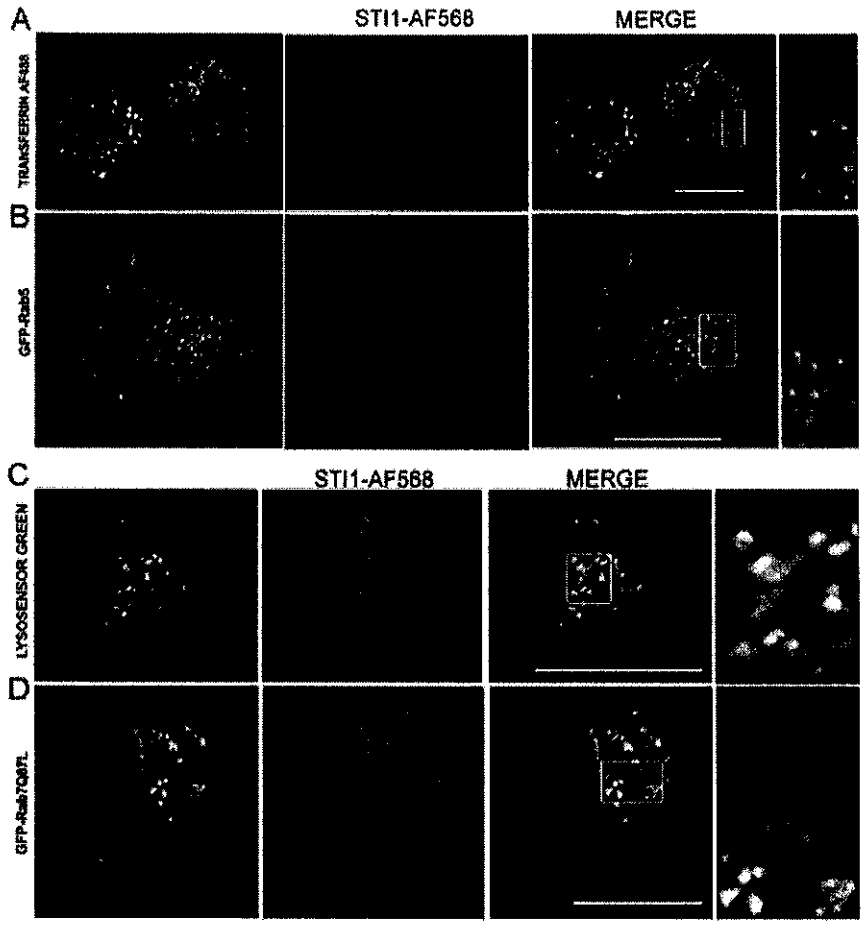

Figure 8. Subcellular localization of STI1. ***A***, SN56 cells were double labeled with STI1–AF568 and transferrin–AF488 for 40 min at 37°C. ***B***, Cells expressing GFP-Rab5 were incubated with STI1–AF568 for 40 min at 37°C. Right panels present a magnified view of the region indicated in the merged images. ***C***, SN56 cells were double labeled with STI1–AF568 and the aciditrophic probe Lysosensor Green (first panel) for 60 min. ***D***, Cells expressing constitutive active mutant GFP-Rab7Q67L were incubated with STI1–AF568 for 40 min at 37°C (second panel). The merged image shows colocalizations in yellow. The images are representative of three experiments with multiple dishes. At least 30 cells were analyzed in each condition. Scale bars, 20 μm.

ing the initial periods of incubation (14 min), a small fraction of STI1 and GFP-PrP^C can be found in similar organelles. Further incubation shows much less colocalization between these two fluorescent proteins (Fig. 9*A*, bottom).

We have previously demonstrated that GFP-PrP^C localization is affected by a dominant-negative mutant of dynamin I, dynamin K44A (Magalhães et al., 2002). We thus tested whether STI1 internalization would also be altered by dynamin I K44A. In this condition, but not in cells transfected with wild-type dynamin I, STI1–AF568 accumulated at the cell surface in spots (Fig. 9*B*). Quantification of internalized STI1–AF568 fluorescence suggests that cells transfected with the mutant, but not with wild-type dynamin I, sequestered <5% of the normal fluorescence found in nontransfected cells, whereas dynamin I had no significant effect in the internalization (Fig. 9*C*). In addition, we found that cells transfected with GFP-PrP^C and treated with STI1–AF568 showed almost no internalization of PrP^C when they were cotransfected with dynamin I K44A (Fig. 9*D*). Additionally, the decrease in endocytosis by this manipulation caused accumulation of STI1–AF568 at the cell surface in areas where GFP-PrP^C was also concentrated (Fig. 9*D*, merge). These results suggest that both proteins use a dynamin-dependent pathway for internalization and that block of endocytosis causes STI1 to remain bound to PrP^C at the cell surface.

Discussion

The present experiments allowed for the first time the direct visualization of the consequences of engagement between STI1 and PrP^C in living neuronal cells. We revealed that STI1, a PrP^C ligand that causes cellular signaling with consequences for neuronal survival and differentiation, triggers PrP^C sequestration and that this is critical for the activation of ERK1/2 but not PKA. We also noted that STI1 is internalized by cells independently of PrP^C and that although part of STI1 may be internalized together with PrP^C, the two proteins follow distinct downstream intracellular pathways. Finally, signaling by ERK1/2 induced by STI1 is fast and depends on endocytosis of PrP^C, but the interaction of the latter two proteins is likely to be transient once they are both internalized. These results have broad implications for understanding physiological functions of STI1–PrP^C interaction and provide information on how PrP^C trafficking can be affected by stimuli that promote PrP^C-dependent cell signaling.

Induction of heat shock proteins (HSPs) was initially described as an adaptive response that enhances the survival of cells exposed to environmental insults (Parsell and Lindquist, 1993). The evolutionarily conserved STI1, including its human homolog HSP70/HSP90 organizing protein (Hop), interacts with both HSP70 and HSP90 to facilitate the transfer of substrates, thus playing an important role in proper protein folding and maturation (Hernandez et al., 2002). The HSPs are abundantly expressed in both the cytoplasm and the nucleus (Honore et al., 1992; Lassle et al., 1997); however, growing evidence suggest that some HSPs, in particular HSP90 and HSP70, can be secreted by distinct cells (Eustace and Jay, 2004; Evdonin et al., 2006), including astrocytes (Guzhova et al., 2001; Robinson et al., 2005). Secreted HSP70 has been related to prevention of axotomy-induced death of spinal sensory and motor neurons (Houenou et al., 1996; Tidwell et al., 2004), as well as protection against light damage of photoreceptors (Yu et al., 2001) and enhancement of motoneuron survival *in vivo* during the period of naturally occurring programmed cell death (Robinson et al., 2005). Thus, HSP70 may function as a neurotrophic factor.

STI1 binds tightly to HSP70 and might be secreted similarly to the latter, although mechanisms of secretion for both proteins are poorly understood. STI1 is secreted from fibrosarcoma cells (Eustace and Jay, 2004), and we have recently found that the protein is also secreted from primary astrocyte cultures and engages PrP^C-dependent neuronal survival (Lima et al., 2007). Moreover, unbiased proteomic analysis of proteins secreted from cells has detected STI1 and HSPs, which are likely secreted by nonconventional pathways (Keller et al., 2008). Indeed, the recombinant

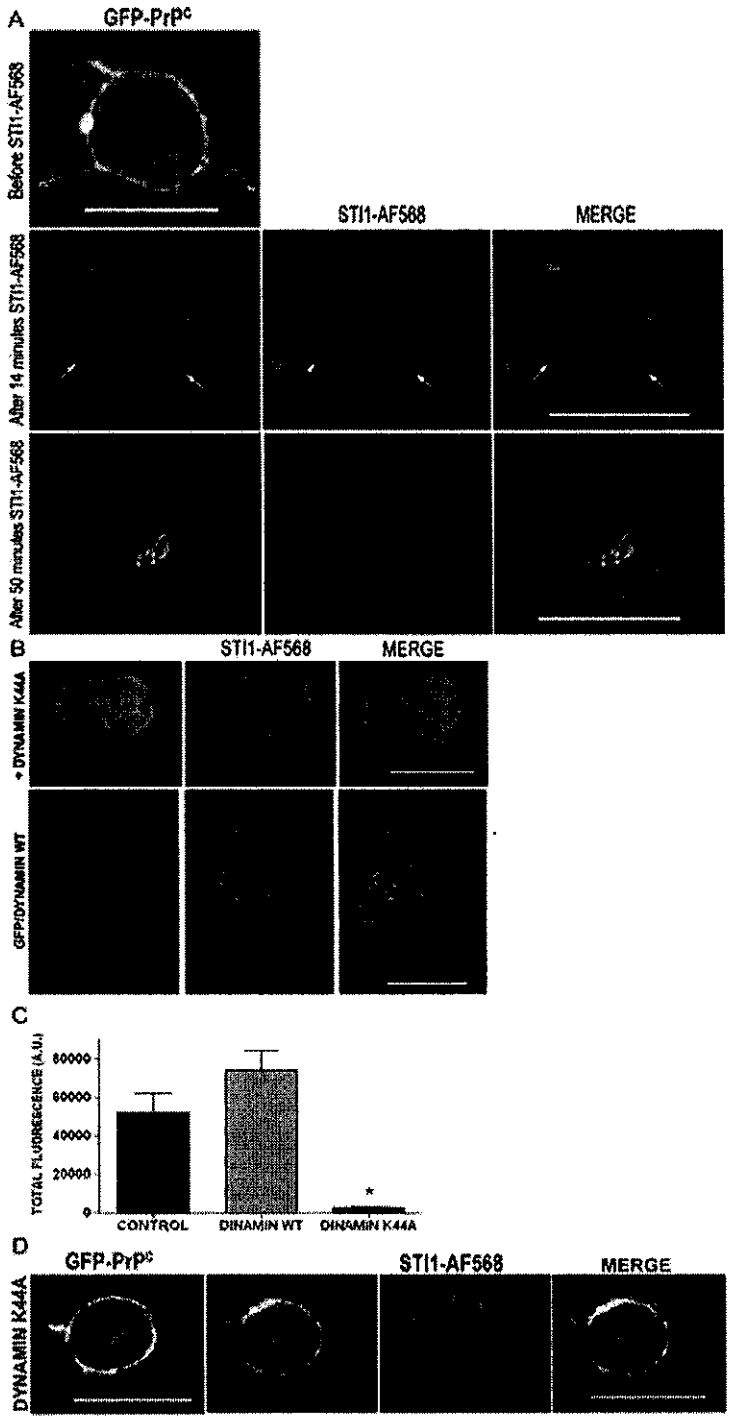

Figure 9. STI1 interacts with PrP^C predominantly at the cell surface. ***A***, SN56 cells expressing GFP-PrP^C (green) were treated with 1 μM STI1–AF568 (red) for distinct periods of time at 37°C. Images are representative five independent experiments with multiple dishes in which 40 and 12 cells were analyzed. Arrows indicate colocalization spots between GFP-PrPC^C (green) and STI1 (red) in forming vesicles. ***B***, SN56 cells were cotransfected with the constructs GFP and dynamin I K44A (top row) or wild-type (WT) dynamin I (bottom row), and living cells were incubated with 1 μM STI1–AF568 for 40 min at 37°C. ***C***, Quantitative analysis of the STI1–AF568 internalization in the presence of dynamin I K44A. Quantification was done using ImageJ software (control, $n = 27$ cells; dynamin I, $n = 67$ cells; dynamin I K44A, $n = 85$ cells) by scoring every cell for the total values of fluorescence internalized. The results are the mean values of fluorescence per cell from multiple dishes examined on 3 different days. Error bars represent SEM. For these experiments, a Kruskal–Wallis one-way ANOVA was used ($H = 120$; $p < 0.001$) followed by a Dunn's *post hoc* test (*$p < 0.05$). A.U., Arbitrary units. ***D***, SN56 cells coexpressing GFP-PrP^C and dynamin I K44A were treated with 1 μM STI1–AF568 at 37°C. *Z*-series were acquired before (GFP-PrP^C) and 40 min after (second to fourth panels) treatment with STI1. Images are representative of four independent experiments in which 15 cells were analyzed. Scale bars, 20 μm.

STI1 used in the current experiments mimics the extracellular secreted STI1 and induced PrP^C-mediated signal transduction, as expected, for a neurotrophic factor.

It is well known that the association between neurotrophic factors and cell-surface receptors induces diverse cellular signals. Some are triggered as the ligand binds to its cognate receptor at the cell surface, and others depend on the internalization of the receptor–ligand complex, a process known as endosomal signal transduction (Gonzalez-Gaitan, 2003). Indeed, evaluation of STI1 intracellular trafficking as well as its role on PrP^C internalization is of particular interest to understand cell signaling associated with the neurotrophic functions mediated by PrP^C–STI1 interaction. Previously, endocytosis of PrP^C had been linked to a pro-apoptotic activity mediated by p53 (Sunyach and Checler, 2005), but agonists that activate this process are unknown. Recently, it has been shown that signaling derived from STI1–PrP^C interactions and associated with proliferation of glioblastoma cells depends on general cellular endocytic activity (Americo et al., 2007; Erlich et al., 2007). The present study identifies a mechanism by which PrP^C is internalized and revealed that the endocytosis of PrP^C is a determinant of STI1-induced cellular signaling. These observations raise the possibility that other events of PrP^C-mediated signaling, such as those elicited by interaction with neural cell adhesion molecule (Santuccione et al., 2005) or antibody cross-linking of PrP^C (Mouillet-Richard et al., 2000; Stuermer et al., 2004), may also depend on the endocytosis of PrP^C. Recent observations have determined that hemin also interacts with PrP^C to induce endocytosis (Lee et al., 2007).

In addition to the downregulation of cell signaling (Drake et al., 2006), endocytosis of cell-surface receptors provides for the activity of signaling endosomes (Luttrell et al., 1999; Lefkowitz and Whalen, 2004). Similar to the dichotomous nature of signal transduction by β2-adrenergic receptors (Daaka et al., 1998), activation of PKA appears to be independent of the endocytosis of PrP^C, whereas ERK1/2 appears to be highly dependent on PrP^C internalization. ERK1/2 activation mediated by PrP^C–STI1 interaction is known to promote neuronal differentiation (Lopes et al., 2005) and synaptic plasticity (Lopes et al., 2005; Coitinho et al., 2007). Further details on the mechanism of activation of the ERK pathway by STI1 should help clarify this biologically relevant neurotrophic role of PrP^C.

Our data revealed that extracellular STI1 is also internalized by endocytosis. The site that STI1 binds for its entry in cells has not been identified, but the experiments with the mutant $STI1_{\Delta 230-245}$ and with *Prnp*$^{0/0}$ neurons conclusively discarded the need of PrP^C for STI1 entry in cells. Colocalization experiments implicate lipid raft-derived organelles in the intracellular trafficking of STI1. Although we found that a small fraction of fluorescent STI1 colocalizes with clathrin-coated vesicles, STI1 was not found in classical early endosomes in living cells. In contrast, a significant portion of the protein was found in flotillin-derived vesicles. Flotillin1-positive vesicles were proposed to differ from caveolae-derived vesicles (Glebov et al., 2006), but both likely originate from lipid raft-derived regions of the membrane (Harder and Simons, 1997). In agreement with these results, fluorescent STI1 also accumulates in acidic organelles that recruit GFP-Rab7, a marker of late endosomes/lysosomes. In this aspect, internalized STI1 presents a remarkable similarity to fluorescent PrP^{res}, which was recently shown to be sequestered in SN56 cells in Rab7-positive acidic organelles (Magalhães et al., 2005).

Intracellular trafficking of GPI-anchored proteins is complex, and these proteins can follow distinct pathways depending on the cell type (Fivaz et al., 2002). Despite reports suggesting internalization of PrP^C via caveolae (Peters et al., 2003), overwhelming evidence favors a model of endocytosis of PrP^C via clathrin-coated vesicles (Shyng et al., 1994; Sunyach et al., 2003; Taylor et al., 2005). Recently, an essential role in the endocytosis of PrP^C has been ascribed to the low-density lipoprotein receptor-like protein (LRP1) (Morris et al., 2006; Taylor and Hooper, 2006; Parkyn et al., 2008), by allowing PrP^C to enter clathrin-coated vesicles. In addition, LRP1 appears to have a role in the surface trafficking of PrP^C (Parkyn et al., 2008). Dynamin I dominant-negative mutant K44A blocks both clathrin-mediated endocytosis and caveolae-mediated endocytosis (Henley et al., 1998; Nichols and Lippincott Schwartz, 2001; Conner and Schmid, 2003). We found that dynamin I K44A suppressed the endocytosis of both STI1 and PrP^C. Furthermore, the use of dynamin I K44A revealed that interaction of STI1 and PrP^C at the cell surface has a transient nature, but inhibition of endocytosis allowed the identification of an intermediate step in which the two proteins appear to remain together.

A likely scenario to explain these results is that STI1 binds to PrP^C at the cell surface and this triggers the interaction of the complex with unknown plasma membrane components that may mediate signaling by PKA. Simultaneously, PrP^C endocytosis is triggered, and that may lead to a new set of interactions, perhaps involving LRP1 or other proteins that can help PrP^C to piggyback to clathrin-coated vesicles, which may be important to cause ERK1/2 activation. Indeed, LRP1 has been shown to link cellular activation to ERK signaling (Orr et al., 2003) and is therefore a likely candidate to participate in this process for STI1–PrP^C. Thereafter, STI1 and PrP^C appear to follow parallel pathways downstream into the cells.

The physiological roles for STI1–PrP^C signaling *in vivo* remain to be established (see (Linden et al., 2008). However, it is of remarkable interest that expression of truncated forms of PrP^C in a PrP-null background has been consistently shown to cause neurodegeneration in transgenic mice (Shmerling et al., 1998; Baumann et al., 2007; Li et al., 2007). This intriguing phenotype resembles some of the alterations in prion disorders and can be mitigated by expression of wild-type PrP^C in transgenic mice (Shmerling et al., 1998; Baumann et al., 2007; Li et al., 2007). The binding site of STI1 onto PrP^C (amino acids 113–128) (Zanata et al., 2002) is lacking in all truncated proteins that produce this phenotype (Shmerling et al., 1998; Baumann et al., 2007), including a recently described mouse line with a deletion in amino acids 105–125 of PrP^C (Li et al., 2007). Future experiments should unravel whether the mechanisms described here for STI1-mediated PrP^C signaling contribute to such phenotypes.

References

Americo TA, Chiarini LB, Linden R (2007) Signaling induced by hop/STI-1 depends on endocytosis. Biochem Biophys Res Commun 358:620–625.

Barbosa Jr J, Ferreira LT, Martins-Silva C, Santos MS, Torres GE, Caron MG, Gomez MV, Ferguson SS, Prado MA, Prado VF (2002) Trafficking of the vesicular acetylcholine transporter in SN56 cells: a dynamin-sensitive step and interaction with the AP-2 adaptor complex. J Neurochem 82:1221–1228.

Baron GS, Magalhães AC, Prado MAM, Caughey B (2006) Mouse-adapted scrapie infection of SN56 cells: greater efficiency with microsome-associated versus purified PrP-res. J Virol 80:2106–2117.

Baumann F, Tolnay M, Brabeck C, Pahnke J, Kloz U, Niemann HH, Heikenwalder M, Rulicke T, Burkle A, Aguzzi A (2007) Lethal recessive myelin toxicity of prion protein lacking its central domain. EMBO J 26:538–547.

Bucci C, Thomsen P, Nicoziani P, McCarthy J, van Deurs B (2000) Rab7: a key to lysosome biogenesis. Mol Biol Cell 11:467–480.

Bueler H, Fischer M, Lang Y, Bluethmann H, Lipp HP, DeArmond SJ, Prusiner SB, Aguet M, Weissmann C (1992) Normal development and behaviour of mice lacking the neuronal cell-surface PrP protein. Nature 356:577–582.

Caughey B, Baron GS (2006) Prions and their partners in crime. Nature 443:803–810.

Caughey B, Raymond GJ (1991) The Scrapie-associated form of Prp is made from a cell-surface precursor that is both protease-sensitive and phospholipase-sensitive. J Biol Chem 266:18217–18223.

Chiarini LB, Freitas AR, Zanata SM, Brentani RR, Martins VR, Linden R (2002) Cellular prion protein transduces neuroprotective signals. EMBO J 21:3317–3326.

Coitinho AS, Lopes MH, Hajj GN, Rossato JI, Freitas AR, Castro CC, Cammarota M, Brentani RR, Izquierdo I, Martins VR (2007) Short-term memory formation and long-term memory consolidation are enhanced by cellular prion association to stress-inducible protein 1. Neurobiol Dis 26:282–290.

Conner SD, Schmid SL (2003) Regulated portals of entry into the cell. Nature 422:37–44.

Daaka Y, Luttrell LM, Ahn S, la Rocca GJ, Ferguson SS, Caron MG, Lefkowitz RJ (1998) Essential role for G protein-coupled receptor endocytosis in the activation of mitogen-activated protein kinase. J Biol Chem 273:685–688.

Drake MT, Shenoy SK, Lefkowitz RJ (2006) Trafficking of G protein-coupled receptors. Circ Res 99:570–582.

Erlich RB, Kahn SA, Lima FR, Muras AG, Martins RA, Linden R, Chiarini LB, Martins VR, Moura Neto V (2007) STI1 promotes glioma proliferation through MAPK and PI3K pathways. Glia 55:1690–1698.

Eustace BK, Jay DG (2004) Extracellular roles for the molecular chaperone, hsp90. Cell Cycle 3:1098–1100.

Evdonin AL, Martynova MG, Bystrova OA, Guzhova IV, Margulis BA, Medvedeva ND (2006) The release of Hsp70 from A431 carcinoma cells is mediated by secretory-like granules. Eur J Cell Biol 85:443–455.

Fivaz M, Vilbois F, Thurnheer S, Pasquali C, Abrami L, Bickel PE, Parton RG, van der Goot FG (2002) Differential sorting and fate of endocytosed GPI-anchored proteins. EMBO J 21:3989–4000.

Gaidarov I, Santini F, Warren RA, Keen JH (1999) Spatial control of coated-pit dynamics in living cells. Nat Cell Biol 1:1–7.

Glebov OO, Bright NA, Nichols BJ (2006) Flotillin-1 defines a clathrin-independent endocytic pathway in mammalian cells. Nat Cell Biol 8:46–54.

Gonzalez-Gaitan M (2003) Signal dispersal and transduction through the endocytic pathway. Nat Rev Mol Cell Biol 4:213–224.

Guzhova I, Kislyakova K, Moskaliova O, Fridlanskaya I, Tytell M, Cheetham M, Margulis B (2001) In vitro studies show that Hsp70 can be released by glia and that exogenous Hsp70 can enhance neuronal stress tolerance. Brain Res 914:66–73.

Hammond DN, Lee HJ, Tonsgard JH, Wainer BH (1990) Development and characterization of clonal cell lines derived from septal cholinergic neurons. Brain Res 512:190–200.

Harder T, Simons K (1997) Caveolae, DIGs, and the dynamics of sphingolipid-cholesterol microdomains. Curr Opin Cell Biol 9:534–542.
Henley JR, Krueger EW, Oswald BJ, McNiven MA (1998) Dynamin-mediated internalization of caveolae. J Cell Biol 141:85–99.
Hernandez MP, Sullivan WP, Toft DO (2002) The assembly and intermolecular properties of the hsp70-Hop-hsp90 molecular chaperone complex. J Biol Chem 277:38294–38304.
Honore B, Leffers H, Madsen P, Rasmussen HH, Vandekerckhove J, Celis JE (1992) Molecular cloning and expression of a transformation-sensitive human protein containing the TPR motif and sharing identity to the stress-inducible yeast protein STI1. J Biol Chem 267:8485–8491.
Houenou LJ, Li L, Lei M, Kent CR, Tytell M (1996) Exogenous heat shock cognate protein Hsc 70 prevents axotomy-induced death of spinal sensory neurons. Cell Stress Chaperones 1:161–166.
Keller M, Ruegg A, Werner S, Beer HD (2008) Active caspase-1 is a regulator of unconventional protein secretion. Cell 132:818–831.
Lassle M, Blatch GL, Kundra V, Takatori T, Zetter BR (1997) Stress-inducible, murine protein mSTI1. Characterization of binding domains for heat shock proteins and in vitro phosphorylation by different kinases. J Biol Chem 272:1876–1884.
Lee KS, Magalhães AC, Zanata SM, Brentani RR, Martins VR, Prado MAM (2001) Internalization of mammalian fluorescent cellular prion protein and N-terminal deletion mutants in living cells. J Neurochem 79:79–87.
Lee KS, Raymond LD, Schoen B, Raymond GJ, Kett L, Moore RA, Johnson LM, Taubner L, Speare JO, Onwubiko HA, Baron GS, Caughey WS, Caughey B (2007) Hemin interactions and alterations of the subcellular localization of prion protein. J Biol Chem 282:36525–36533.
Lefkowitz RJ, Whalen EJ (2004) beta-arrestins: traffic cops of cell signaling. Curr Opin Cell Biol 16:162–168.
Li A, Christensen HM, Stewart LR, Roth KA, Chiesa R, Harris DA (2007) Neonatal lethality in transgenic mice expressing prion protein with a deletion of residues 105–125. EMBO J 26:548–558.
Lima FR, Arantes CP, Muras AG, Nomizo R, Brentani RR, Martins VR (2007) Cellular prion protein expression in astrocytes modulates neuronal survival and differentiation. J Neurochem 103:2164–2176.
Linden R, Martins VR, Prado MA, Cammarota M, Izquierdo I, Brentani RR (2008) Physiology of the prion protein. Physiol Rev 88:673–728.
Lopes MH, Hajj GN, Muras AG, Mancini GL, Castro RM, Ribeiro KC, Brentani RR, Linden R, Martins VR (2005) Interaction of cellular prion and stress-inducible protein 1 promotes neuritogenesis and neuroprotection by distinct signaling pathways. J Neurosci 25:11330–11339.
Luttrell LM, Ferguson SS, Daaka Y, Miller WE, Maudsley S, Della Rocca GJ, Lin F, Kawakatsu H, Owada K, Luttrell DK, Caron MG, Lefkowitz RJ (1999) Beta-arrestin-dependent formation of beta2 adrenergic receptor-Src protein kinase complexes. Science 283:655–661.
Magalhães AC, Silva JA, Lee KS, Martins VR, Prado VF, Ferguson SSG, Gomez MV, Brentani RR, Prado MAM (2002) Endocytic intermediates involved with the intracellular trafficking of a fluorescent cellular prion protein. J Biol Chem 277:33311–33318.
Magalhães AC, Baron GS, Lee KS, Steele-Mortimer O, Dorward D, Prado MA, Caughey B (2005) Uptake and neuritic transport of scrapie prion protein coincident with infection of neuronal cells. J Neurosci 25:5207–5216.
Manson JC, Clarke AR, Hooper ML, Aitchison L, McConnell I, Hope J (1994) 129/Ola mice carrying a null mutation in PrP that abolishes mRNA production are developmentally normal. Mol Neurobiol 8:121–127.
Martins VR, Linden R, Prado MAM, Walz R, Sakamoto AC, Izquierdo I, Brentani RR (2002) Cellular prion protein: on the road for functions. FEBS Lett 512:25–28.
Morris RJ, Parkyn CJ, Jen A (2006) Traffic of prion protein between different compartments on the neuronal surface, and the propagation of prion disease. FEBS Lett 580:5565–5571.
Mouillet-Richard S, Ermonval M, Chebassier C, Laplanche JL, Lehmann S, Launay JM, Kellermann O (2000) Signal transduction through prion protein. Science 289:1925–1928.
Nichols BJ, Lippincott-Schwartz J (2001) Endocytosis without clathrin coats. Trends Cell Biol 11:406–412.
Orr AW, Pedraza CE, Pallero MA, Elzie CA, Goicoechea S, Strickland DK, Murphy-Ullrich JE (2003) Low density lipoprotein receptor-related protein is a calreticulin coreceptor that signals focal adhesion disassembly. J Cell Biol 161:1179–1189.
Parkyn CJ, Vermeulen EG, Mootoosamy RC, Sunyach C, Jacobsen C, Oxvig C, Moestrup S, Liu Q, Bu G, Jen A, Morris RJ (2008) LRP1 controls biosynthetic and endocytic trafficking of neuronal prion protein. J Cell Sci 121:773–783.
Parsell DA, Lindquist S (1993) The function of heat-shock proteins in stress tolerance: degradation and reactivation of damaged proteins. Annu Rev Genet 27:437–496.
Peters PJ, Mironov Jr A, Peretz D, van Donselaar E, Leclerc E, Erpel S, DeArmond SJ, Burton DR, Williamson RA, Vey M, Prusiner SB (2003) Trafficking of prion proteins through a caveolae-mediated endosomal pathway. J Cell Biol 162:703–717.
Pimpinelli F, Lehmann S, Maridonneau-Parini I (2005) The scrapie prion protein is present in flotillin-1-positive vesicles in central- but not peripheral-derived neuronal cell lines. Eur J Neurosci 21:2063–2072.
Prusiner SB (1998) Prions. Proc Natl Acad Sci U S A 95:13363–13383.
Ribeiro FM, Black SA, Cregan SP, Prado VF, Prado MA, Rylett RJ, Ferguson SS (2005) Constitutive high-affinity choline transporter endocytosis is determined by a carboxyl-terminal tail dileucine motif. J Neurochem 94:86–96.
Robinson MB, Tidwell JL, Gould T, Taylor AR, Newbern JM, Graves J, Tytell M, Milligan CE (2005) Extracellular heat shock protein 70: a critical component for motoneuron survival. J Neurosci 25:9735–9745.
Samaia HB, Brentani RR (1998) Can loss-of-function prion-related diseases exist? Mol Psychiatry 3:196–197.
Santos MS, Barbosa Jr J, Veloso GS, Ribeiro F, Kushmerick C, Gomez MV, Ferguson SS, Prado VF, Prado MA (2001) Trafficking of green fluorescent protein-tagged vesicular acetylcholine transporter to varicosities in a cholinergic cell line. J Neurochem 78:1104–1113.
Santuccione A, Sytnyk V, Leshchyns'ka I, Schachner M (2005) Prion protein recruits its neuronal receptor NCAM to lipid rafts to activate p59fyn and to enhance neurite outgrowth. J Cell Biol 169:341–354.
Shmerling D, Hegyi I, Fischer M, Blattler T, Brandner S, Gotz J, Rulicke T, Flechsig E, Cozzio A, von Mering C, Hangartner C, Aguzzi A, Weissmann C (1998) Expression of amino-terminally truncated PrP in the mouse leading to ataxia and specific cerebellar lesions. Cell 93:203–214.
Shyng SL, Heuser JE, Harris DA (1994) A glycolipid-anchored prion protein is endocytosed via clathrin-coated pits. J Cell Biol 125:1239–1250.
Shyng SL, Moulder KL, Lesko A, Harris DA (1995) The N-terminal domain of a glycolipid-anchored prion protein is essential for its endocytosis via clathrin-coated pits. J Biol Chem 270:14793–14800.
Stuermer CA, Langhorst MF, Wiechers MF, Legler DF, Von Hanwehr SH, Guse AH, Plattner H (2004) PrPc capping in T cells promotes its association with the lipid raft proteins reggie-1 and reggie-2 and leads to signal transduction. FASEB J 18:1731–1733.
Sunyach C, Checler F (2005) Combined pharmacological, mutational and cell biology approaches indicate that p53-dependent caspase 3 activation triggered by cellular prion is dependent on its endocytosis. J Neurochem 92:1399–1407.
Sunyach C, Jen A, Deng J, Fitzgerald KT, Frobert Y, Grassi J, McCaffrey MW, Morris R (2003) The mechanism of internalization of glycosylphosphatidylinositol-anchored prion protein. EMBO J 22:3591–3601.
Taylor DR, Hooper NM (2006) The low-density lipoprotein receptor-related protein 1 (LRP1) mediates the endocytosis of the cellular prion protein. Biochem J 402:17–23.
Taylor DR, Watt NT, Perera WS, Hooper NM (2005) Assigning functions to distinct regions of the N-terminus of the prion protein that are involved in its copper-stimulated, clathrin-dependent endocytosis. J Cell Sci 118:5141–5153.
Tidwell JL, Houenou LJ, Tytell M (2004) Administration of Hsp70 in vivo inhibits motor and sensory neuron degeneration. Cell Stress Chaperones 9:88–98.
Vieira AV, Lamaze C, Schmid SL (1996) Control of EGF receptor signaling by clathrin-mediated endocytosis. Science 274:2086–2089.
Weissmann C (1999) Molecular genetics of transmissible spongiform encephalopathies. J Biol Chem 274:3–6.
Westergard L, Christensen HM, Harris DA (2007) The cellular prion protein (PrP(C)): its physiological function and role in disease. Biochim Biophys Acta 1772:629–644.
Yu Q, Kent CR, Tytell M (2001) Retinal uptake of intravitreally injected Hsc/Hsp70 and its effect on susceptibility to light damage. Mol Vis 7:48–56.
Zanata SM, Lopes MH, Mercadante AF, Hajj GN, Chiarini LB, Nomizo R, Freitas AR, Cabral AL, Lee KS, Juliano MA, de Oliveira E, Jachieri SG, Burlingame A, Huang L, Linden R, Brentani RR, Martins VR (2002) Stress-inducible protein 1 is a cell surface ligand for cellular prion that triggers neuroprotection. EMBO J 21:3307–3316.

The Journal of Neuroscience, March 1992, 12(3): 793–799

SN56 cells

Acetylcholine Synthesis and Release Is Enhanced by Dibutyryl Cyclic AMP in a Neuronal Cell Line Derived from Mouse Septum

Jan Krzysztof Blusztajn,[1,2] Amy Venturini,[1] Darrell A. Jackson,[1,3] Henry J. Lee,[4] and Bruce H. Wainer[4,5]

Departments of [1]Pathology and [2]Psychiatry, Boston University School of Medicine, Boston, Massachusetts 02118, [3]Department of Brain and Cognitive Sciences, Massachusetts Institute of Technology, Cambridge, Massachusetts 02139, and Departments of [4]Pharmacological and Physiological Sciences and [5]Pathology, The University of Chicago, Chicago, Illinois 60637

Cholinergic properties of the SN56.B5.G4 cell line derived from the fusion of neurons of the mouse postnatal day 21 septum and the murine neuroblastoma cell line N18TG2 were investigated and correlated with morphological differentiation. In basal serum-containing growth medium, few cells developed neurites. Neurite extension occurred in cells grown for 2 d with forskolin or dibutyryl cAMP (dbcAMP) but not with butyrate. In cells treated with these compounds, the activity of ChAT and ACh content were two- to threefold higher relative to controls. The cells synthesized ACh from choline taken up by the sodium-dependent high-affinity transport. Forskolin-, dbcAMP-, and butyrate-treated cells (but not the controls) were capable of spontaneous and depolarization-evoked ACh release. The results indicate that the morphological and the neurochemical aspects of SN56.B5.G4 cell differentiation are independently regulated.

The process of synthesis, storage, and release of ACh requires the expression of several specialized enzymatic systems. In the initial step of ACh synthesis, choline is taken up from the extracellular space by a sodium-dependent high-affinity uptake system (SDHACU). SDHACU is present predominantly in the nerve terminals of cholinergic cells (Suszkiw and Pilar, 1976). Since a large proportion of choline taken up by this process is converted to ACh, it has been postulated that SDHACU may be coupled to ChAT, which catalyzes ACh synthesis utilizing acetylCoA as the acetate donor. AcetylCoA generation and turnover may be regulated in a specific fashion in cholinergic cells (Szutowicz et al., 1983). The ACh may then be taken up into the secretory vesicles by a specific carrier (Parsons et al., 1987). The synthesis and assembly of the vesicular membrane are likely to require enzymes specific for cholinergic neurons. The molecular mechanisms that mediate ACh release into the synapse are poorly understood. In order to investigate the regulation of these and other properties of brain cholinergic neurons, we have developed cell lines derived from fusion of the murine neuroblastoma cells, N18TG2, which lack cholinergic markers, with postnatal day 21 mouse brain septal neurons. At this age, the septal cells do not divide and their ACh synthesis is similar to that of the adult (Shelton et al., 1979). We also expect that these hybrid cell lines should prove useful in studying the mechanisms of action of a variety of growth factors that enhance the cholinergic phenotype. The list of such molecules includes NGF (Hefti et al., 1985), basic fibroblast growth factor (Vaca et al., 1989), ciliary neurotrophic factor (Saadat et al., 1989), ChAT development factor (McManaman et al., 1988), cholinergic differentiation factor (Fukada, 1985) recently shown to be identical to leukemia inhibitory factor (Yamamori et al., 1989), membrane-derived factor (Adler et al., 1989), target-derived neuronal cholinergic differentiation factor (Rao and Landis, 1990), interleukin 3 (IL-3) (Kamegai et al., 1990b), and granulocyte–macrophage colony-stimulating factor (GM-CSF) (Kamegai et al., 1990a). Cholinergic differentiation may also be enhanced by pharmacologic agents. Among them, the analogs of the second messenger cAMP have been shown to increase the activity of ChAT in neuron-like cell lines including the murine neuroblastoma lines (Prasad and Kumar, 1974), rat pheochromocytoma, PC12 cells (Green and Tischler, 1976), and the neuroblastoma × glioma hybrid NG108-15 cells (Daniels and Hamprecht, 1974). In this report, we describe some attributes of a murine septal cell line, SN56.B5.G4, and show that these properties are similar to those characteristic of septal neurons. The cholinergic features of SN56.B5.G4 cells are enhanced by treatment with a cAMP analog, N^6,$O^{2'}$-dibutyryl-adenosine 3′,5′-cyclic monophosphate (dbcAMP). In addition, our data indicate that the enhancement of the cholinergic phenotype is regulated independently from the neuron-like morphological differentiation of these cells.

Materials and Methods

Materials

Cell culture plastic was from Costar Corp. (Cambridge, MA) or Becton Dickinson Labware (Lincoln Park, NJ). Media and sera were from GIBCO Laboratories Inc. (Grand Island, NY). Chemicals were from Sigma Chemical Co. (St. Louis, MO). ^{14}C-Methyl-choline chloride (55 Ci/mol) and ^{3}H-acetyl-CoA (15 Ci/mmol) were from ICN Biomedicals, Inc. (Irvine, CA).

Cell culture

The SN56.B5.G4 cells were created by fusing N18TG2 neuroblastoma cells with murine (strain C57BL/6) neurons from postnatal day 21 septa (Hammond et al., 1990; Lee et al., 1990). The SN56.B5.G4 and the parent neuroblastoma N18TG2 cells were maintained at 37°C in an atmosphere of 95% air, 5% CO_2 in Dulbecco's Modified Eagle's Medium (DMEM) containing 10% fetal bovine serum (FBS), and 50 μg/ml gentamicin. Media in stock flasks were changed every 2–3 d. The cells were subcultured by mechanically removing them from the substratum with squirts of fresh media. Cells of up to passage 25 were used. When cells

Received May 3, 1991; revised Oct. 8, 1991; accepted Oct. 10, 1991.

This study was supported by NSF BNS8808942, MH46095, and NS25787, and the Center for Alternatives to Animal Testing grants.

Correspondence should be addressed to Jan Krzysztof Blusztajn, Room M1009, Boston University School of Medicine, 85 East Newton Street, Boston, MA 02118.

were grown in the presence of various pharmacologic agents, the media were changed daily.

ACh content

In order to measure the cellular ACh content, the cells were incubated for 1 hr in their growth media containing various pharmacologic agents (see figure captions and table notes) and 15 μM neostigmine. The cells were then washed twice with ice-cold Hank's balanced salt solution containing 15 μM neostigmine and extracted with methanol, and their ACh was determined as described below.

^{14}C-ACh accumulation

To measure ^{14}C-ACh accumulation, the cells were incubated at 37°C in a physiological salt solution (containing, in mM: NaCl, 135; KCl, 5; $CaCl_2$, 1; $MgCl_2$, 0.75; glucose, 5; eserine, 0.015; HEPES, 10; pH, 7.4) in the presence of ^{14}C-choline. The time periods of incubations and ^{14}C-choline concentrations are given in figure captions. The ^{14}C-ACh accumulated by the cells was extracted and purified by HPLC, and its radioactivity was determined.

^{14}C-ACh release

To measure ^{14}C-ACh release, the cells were incubated for 180 min at 37°C in L-15 medium containing 10 μM ^{14}C-choline and 15 μM eserine. The cells were washed with L-15 medium (as above) and then incubated for an additional 30 min in a physiological salt solution (containing, in mM: NaCl, 135; $CaCl_2$, 1; $MgCl_2$, 0.75; glucose, 5; eserine, 0.015; HEPES, 10; pH, 7.4) and either 5 mM (control) or 40 mM potassium chloride (the concentration of sodium chloride was reduced to 100 mM). The media were collected, and ^{14}C-ACh released from the cells was purified by HPLC and its radioactivity determined.

Analytical methods

Extraction of cells. After the desired treatment, the media were removed from the culture dishes and methanol was added (1 ml and 1.4 ml per 35 mm and 60 mm diameter dish, respectively). The cells were scraped off the dishes and the methanolic suspensions transferred to polypropylene tubes. Two volumes of chloroform were then added, and the tubes were vortexed. The extracts were then washed with a volume of water equal to the initial amount of methanol, and centrifuged to separate the two phases. The water-soluble metabolites of choline (choline, ACh, phosphocholine, glycerophosphocholine, cytidinediphosphocholine) were in the aqueous (upper) phase, and the lipids were in the organic (lower) phase. Proteins collected at the interface and could be used for protein assay. The phases were collected and dried under a vacuum.

Purification of water-soluble choline metabolites. The water-soluble choline metabolites were purified by a modification of our HPLC method (Liscovitch et al., 1985) on a normal phase column 10 cm long, 4.6 mm internal diameter containing 3 μm silica particles (Dynamax, Rainin Instruments Co., Woburn, MA), using a linear gradient elution based on increasing polarity and ionic strength, with two mobile phases: A, containing acetonitrile/water/ethanol/acetic acid/1.0 M ammonium acetate/0.1 M sodium phosphate monobasic (800:127:68:2:3:10, v/v), and B (same components, 400:400:68:53:79:10, v/v). The mobile phase was varied from 0 to 100% of B with a slope of 5%/min, starting 6 min after sample injection. At a flow rate of 1.5 ml/min, typical retention times for the following compounds were (in min) ACh, 8; choline, 9; glycerophosphocholine, 12; cytidinediphosphocholine, 14; and phosphocholine, 17. In experiments utilizing ^{14}C-choline, the radioactivities associated with these peaks were quantitated by an on-line monitor using a solid-phase scintillation flow cell (Berthold, model LB 507 A).

ACh measurements. ACh was determined by HPLC with an enzymatic reactor containing acetylcholinesterase and choline oxidase and an electrochemical detector using a commercial kit (Bioanalytical Systems Inc., West Lafayette, IN) based on the method of Potter et al. (1983).

Quantitative analyses

Choline acetyltransferase activity was determined in cell homogenates by the method of Fonnum (1975). Protein was determined using bicinchoninic acid by the method of Smith et al. (1985) and DNA by the method of Labarca and Paigen (1980).

Statistics

Significance of difference between means was determined by *t* test or analysis of variance and Tukey test as appropriate. Hyperbolic regression was performed with the aid of SYSTAT version 5 software (Systat Inc., Evanston, IL) on a Macintosh IIci personal computer.

Results

Morphological differentiation of SN56.B5.G4 cells

When maintained in basal growth medium (DMEM/10% FBS), SN56.B5.G4 cells were polygonal and extended few neurites (Fig. 1*A*). Addition of 1 mM dbcAMP (Fig. 1*B*), a cell-permeant analog of cAMP, or of 10 μM forskolin, an activator of adenylate cyclase, to the medium slowed down cell division and caused neurite outgrowth. Because the dbcAMP molecule can be hydrolyzed to liberate free butyric acid, the effect of butyrate (2 mM) on the morphology of SN56.B5.G4 cells was also investigated. Under those conditions, the cells were rounder than controls and no neurite extension was observed (Fig. 1*C*).

Stimulation of ACh synthesis and neurite extension are regulated independently in SN56.B5.G4 cells

In order to investigate whether there was a correlation between neurite extension and ACh synthesis and content, the cells were grown for 2 d in the basal medium or in the presence of 1 mM dbcAMP, 10 μM forskolin, or 2 mM butyrate. ChAT activity as well as the ACh content were determined. The specific activity of ChAT was elevated approximately 2.7–3-fold by each of the treatments (Fig. 2). The cells grown in the basal medium contained 0.88 ± 0.19 nmol/mg protein (mean ± SD) of ACh. The ACh content was elevated by approximately 70–85% by each of the treatments (Fig. 2). However, cells treated with butyrate did not extend neurites, indicating that morphological differentiation did not correlate with elevations in ChAT activity and/or ACh levels. Because elevated ChAT activity and ACh levels were observed both in neurite-bearing (i.e., dbcAMP- and forskolin-treated) as well as in neurite-free (i.e., butyrate-treated) cells, it is concluded that the enhancement of the cholinergic phenotype is regulated independently from neurite extension.

ACh synthesis in SN56.B5.G4 cells is enhanced by dbcAMP in a time- and dose-dependent manner

The dbcAMP-treated cells accumulated more ^{14}C-ACh when incubated with ^{14}C-choline than did the controls. The effect of dbcAMP was both time and dose dependent. The maximal enhancement (275% of control) of ^{14}C-ACh accumulation was observed after 2 d of exposure to 1 mM dbcAMP (Fig. 3). The ^{14}C-ACh accumulation was enhanced by dbcAMP in a saturable manner, reaching a maximum of 3.4-fold at 5 mM dbcAMP after a 2 d treatment (Fig. 4). The concentration of dbcAMP that caused half-maximal stimulation of ^{14}C-ACh accumulation was 1.3 mM (Fig. 4). No ^{14}C-ACh was observed in the N18TG2 parent neuroblastoma cells grown in the basal medium or treated with 1 mM dbcAMP for 48 hr (data not shown).

SN56.B5.G4 septal cells release ACh upon depolarization

We investigated whether ACh could be released upon depolarization by elevating extracellular potassium concentrations. The cells were prelabeled with 10 μM ^{14}C-choline and then incubated for an additional 30 min in a physiological salt solution containing either 5 or 40 mM K^+, and ^{14}C-ACh released from the cells was purified by HPLC and its radioactivity determined. The results, expressed as dpm/μg of DNA, are shown in Figure

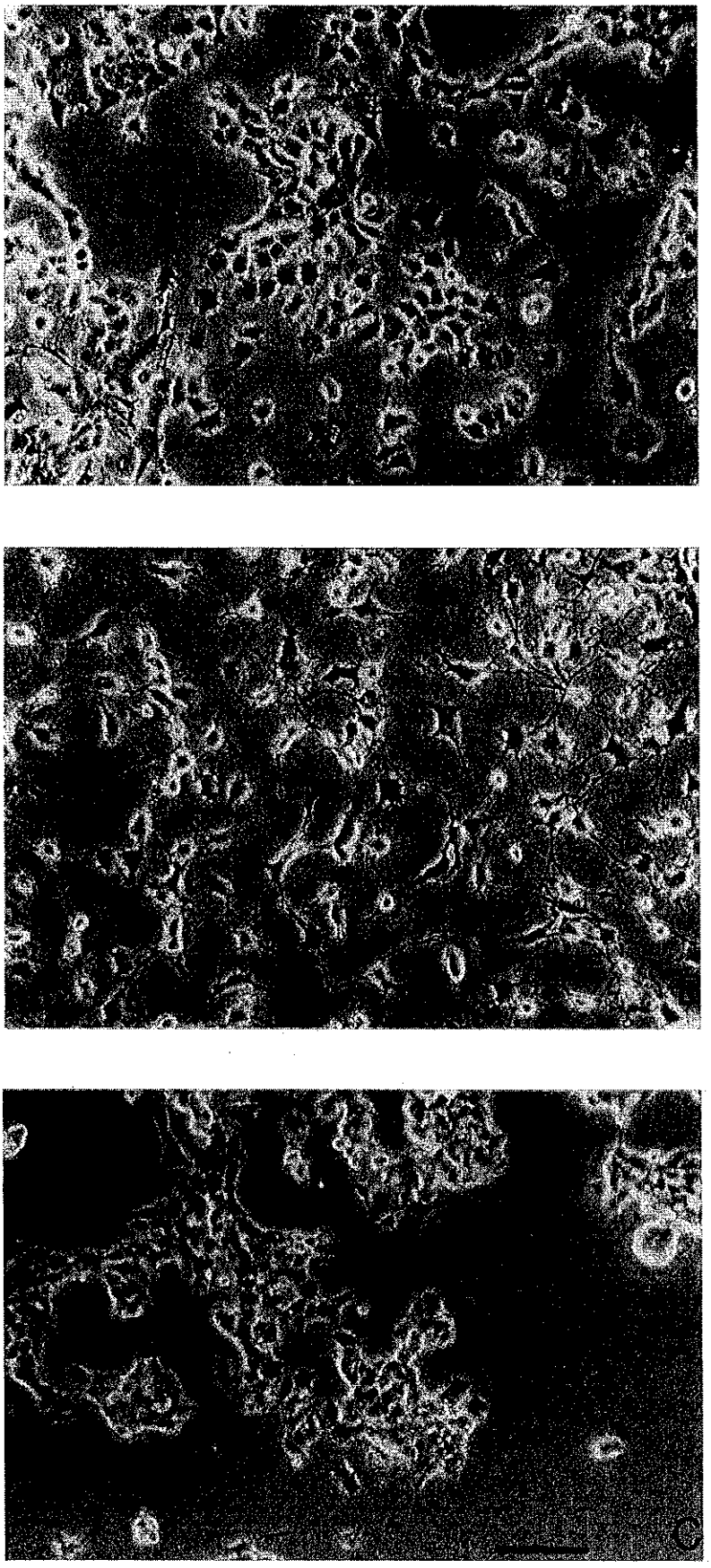

Figure 1. Morphological differentiation of SN56.B5.G4 cells. Phase-contrast photomicrographs of SN56.B5.G4 cells grown as described in Materials and Methods in 35 mm diameter culture dishes containing 2 ml of the basal medium (DMEM/10% FBS) (*A*) supplemented with 1 mM dbcAMP (*B*) or 2 mM butyrate (*C*). The medium was changed daily, and the cells were photographed after 2 d of treatment. Scale bar, 100 μm for *A–C*.

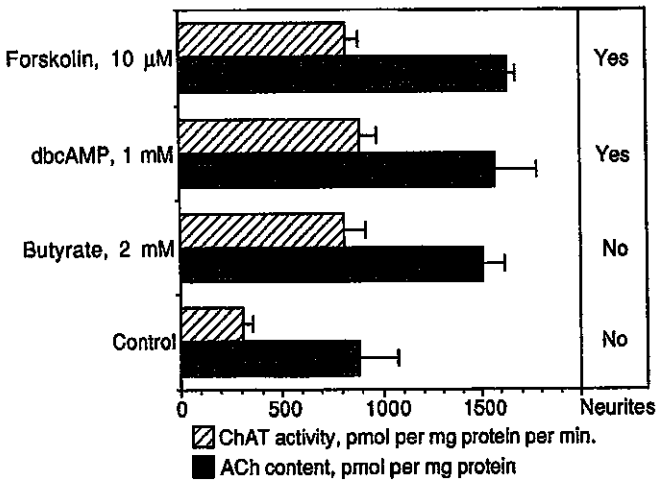

Figure 2. The morphological and neurochemical differentiation of SN56.B5.G4 cells are independently regulated. The cells were grown for 2 d in the presence of the agents indicated. Neurite formation was assessed by an observer who was not aware of the nature of the treatments. The growth media were removed and the cells were incubated at 37°C for an additional 1 hr period in fresh growth media containing the agents indicated and 15 μM neostigmine. The media were removed, and the cells were washed twice with Hank's balanced salt solution containing 15 μM neostigmine prior to the extraction of ACh. ACh was determined by HPLC. ChAT activity was measured in cell homogenates. The results are reported as means ± SD. One-way ANOVA followed by a Tukey test was used to determine the statistical significance of differences between groups. ChAT activity and ACh content was significantly different ($p < 0.005$) in control cells relative to each of the treatment groups. No other statistically significant differences were found.

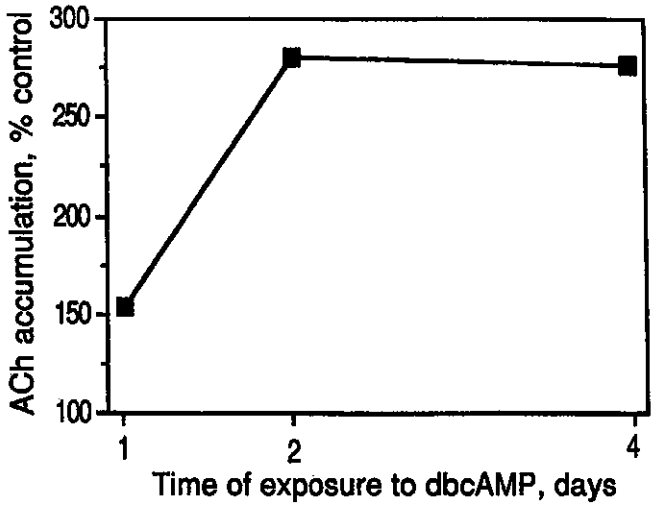

Figure 3. Time course of stimulation of ^{14}C-ACh accumulation by dbcAMP in SN56.B5.G4 cells. The cells were grown for various periods of time in the presence of 1 mM dbcAMP with daily medium change. ^{14}C-ACh accumulation was determined in cells incubated for 10 min at 37°C in the presence of 2.5 μM ^{14}C-choline. ^{14}C-ACh was extracted and purified by HPLC, and its radioactivity was determined.

5 and are taken from an experiment in which ACh could be detected in cells grown in the basal medium. In the majority of experiments, ACh release was undetectable, indicating that the SN56.B5.G4 cells were incapable of ACh release when grown in their basal medium. Therefore, we tested the hypothesis that the differentiated cells would release ACh. When the SN56.B5.G4 cells were grown in the presence of 1 mM dbcAMP, 10 μM forskolin, or 2 mM butyrate for 48 hr, ACh release was reliably observed and depolarization led to elevation of ACh release (Fig. 5). The spontaneous and the depolarization-evoked ACh release occurred both in neurite-free (butyrate-treated) and neurite-bearing (dbcAMP- or forskolin-treated) cells.

SN56.B5.G4 cells synthesize ACh from choline taken up by a sodium-dependent high-affinity transport

In order to determine whether SN56.B5.G4 cells express SDHACU, the apparent affinity for choline of the choline uptake and of the ACh synthetic process was studied by incubating the cells for 10 min in a medium of varying ^{14}C-choline concentration. The radioactivity of the total intracellular ^{14}C-choline was measured, and ^{14}C-ACh was purified and its radioactivity determined. The total uptake of choline could be resolved into a saturable process exhibiting an apparent K_m of 5.3 μM and a linear component, perhaps reflecting diffusion (data not shown). The process of ^{14}C-ACh accumulation was saturable with choline and could be best described by a rectangular hyperbola (Fig. 6). The apparent affinity for choline of ^{14}C-ACh accumulation was determined by least-squares hyperbolic regression. The apparent K_m was 4.6 μM and the apparent V_{max} was 16.5 pmol per dish per 10 min. The K_m value is thus in the range characteristic of SDHACU. No ^{14}C-ACh was observed in similar experiments performed on the N18TG2 parent neuroblastoma cells (data not shown). When the cells were incubated in medium in which sodium was replaced by lithium, accumulation of ^{14}C-ACh from 1 μM ^{14}C-choline was diminished to 29% of control (Table 1). This inhibition was less pronounced when ^{14}C-ACh accumulation was measured in the presence of 5 μM extracellular ^{14}C-choline. These data show that when extracellular choline concentration is low (1 μM), most (70%) of the ACh in SN56.B5.G4 cells is synthesized from choline taken up by an SDHACU. At higher choline concentrations, the low-affinity process (or diffusion) also provides choline for ACh synthesis. Similar results have been obtained by others using primary cultures of rat septum [i.e., 50–70% of ACh was derived from choline taken up by the high-affinity transport (Keller et al., 1987; Bostwick et al., 1989)]. These data suggest that SN56.B5.G4 cells express high-affinity sodium-dependent uptake for choline and that their ACh is synthesized from choline taken up by this system.

Discussion

The phenotypic properties of any hybrid cell line will depend on the contribution of each of the parents. The SN56.B5.G4 cells exhibit several features of the cholinergic phenotype that presumably were contributed by the septal neuronal parent. This assertion is supported by our inability to detect ChAT activity or ^{14}C-ACh accumulation in the N18TG2 parent neuroblastoma cells grown either in basal or in dbcAMP-supplemented medium (data not shown). Thus, it is likely that the cholinergic properties as well as their enhancement by the differentiating protocols reported here are due to the expression of septal neuronal genes (although the possibility that activation of the N18TG2 genes occurred cannot be excluded).

The SN56.B5.G4 cells have been selected from other septal lines based on ChAT activity. However, in order to serve as a useful model of brain cholinergic neurons, it was important to establish whether these cells exhibit other features of the cholinergic phenotype. The ACh content of these cells is similar to NS20 neuroblastoma cells (2 nmol/mg protein) (Kato et al.,

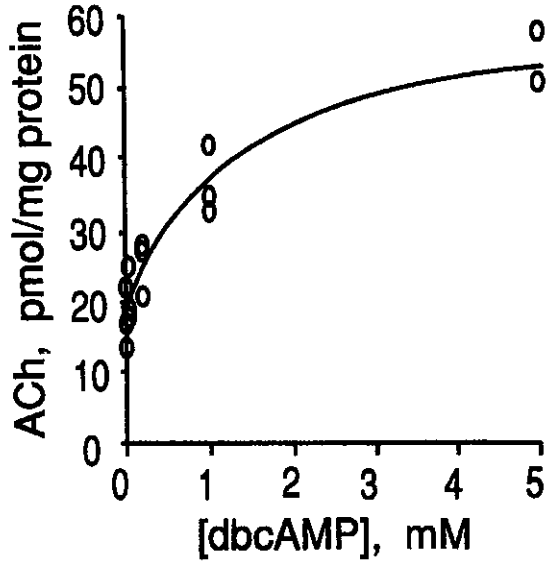

Figure 4. ^{14}C-ACh accumulation in SN56.B5.G4 cells is enhanced by dbcAMP in a dose-dependent manner. The cells were grown for 2 d in the presence of dbcAMP at various concentrations. ^{14}C-ACh accumulation was determined in cells incubated for 10 min at 37°C in the presence of 2.5 μM ^{14}C-choline. ^{14}C-ACh was extracted and purified by HPLC, and its radioactivity was determined. The results were calculated using the specific radioactivity of the ^{14}C-choline precursor. The data are results from triplicate determinations. A rectangular hyperbola was fit to the data according to the Michaelis equation plus a constant reflecting the fact that untreated cells contained ACh. EC_{50} = 1.3 mM. Correlation coefficient of this regression was r^2 = 0.991.

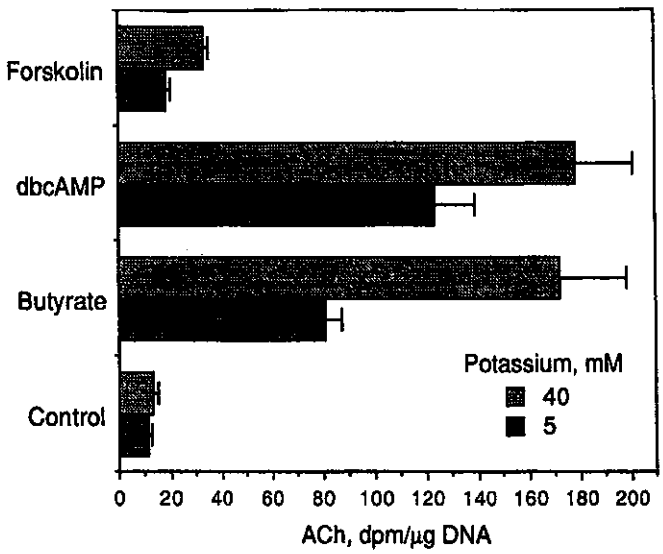

Figure 5. ^{14}C-ACh release from SN56.B5.G4 cells. The cells were grown as described in Materials and Methods in DMEM containing 10% FBS and 1 mM dbcAMP, 2 mM butyrate, or 10 μM forskolin for 48 hr. They were washed with 2 ml of L-15 medium containing 15 μM eserine and incubated for 180 min at 37°C in 1 ml of the same medium containing 10 μM ^{14}C-choline. The cells were then washed with 2 ml of L-15 medium and incubated for an additional 30 min in 0.7 ml of physiological salt solution containing (in mM) NaCl, 135; KCl, 5; $CaCl_2$, 1; $MgCl_2$, 0.75; glucose, 5; eserine, 0.015; and HEPES, 10; pH 7.4 (control) or elevated (40 mM) potassium concentrations (in the high-potassium medium sodium concentration was reduced to 100 mM). ^{14}C-ACh released from the cells was purified by HPLC and its radioactivity determined. The data are means ± SEM of four determinations. The data were analyzed by a two-way ANOVA. The effect of treatment and the effect of depolarization were statistically significant at $p < 0.001$.

1977) but lower than that of the human neuroblastoma LA-N-2 cells grown in a similar medium (approximately 10 nmol/mg protein) (Richardson et al., 1989). By comparison, ACh content of rat striatum is 0.3 nmol/mg protein (Cohen and Wurtman, 1976) and that of purely cholinergic synaptosomes from *Torpedo* electric organ is 130 nmol/mg protein (Morel et al., 1977).

SDHACU has been used extensively in the studies of cholinergic function as a marker of cholinergic nerve terminals (Blusztajn and Wurtman, 1983, for a review). The observation that ACh synthesized by SN56.B5.G4 cells is produced from choline taken up by SDHACU (Fig. 6) set these cells apart from a variety of ChAT-expressing cell lines including NS20 neuroblastoma (Lanks et al., 1974), NG108-15 neuroblastoma × glioma (McGee, 1980), PC12 pheochromocytoma (Melega and Howard, 1981), and LA-N-2 neuroblastoma (Richardson et al., 1989), all of which synthesize ACh from choline taken up by the ubiquitous low-affinity carrier. Thus, the SN56.B5.G4 cells resemble septal neurons, which maintain their ability to express SDHACU in organotypic cultures (Keller et al., 1987).

Another feature of cholinergic neurons is the release of ACh upon depolarization. SN56.B5.G4 cells grown in basal medium (DMEM/10% FBS) failed to release ACh reliably. Therefore, we hypothesized that a differentiating treatment might be found that would allow these cells to release the neurotransmitter. We used initially a cAMP analog, dbcAMP, because of extensive literature showing that a variety of neuronal cell lines both undergo morphological differentiation and, in some cases, respond by elevations in ChAT activity when treated with dbcAMP (Daniels and Hamprecht, 1974; Prasad and Kumar, 1974; Green and Tischler, 1976). Indeed, the dbcAMP-treated (1 mM, 2 d) SN56.B5.G4 cells released ACh, and this release more than doubled in cells depolarized by high extracellular concentrations of potassium (Fig. 3). ACh release was also observed in cells treated with butyrate or forskolin. The permissive effects of these agents on ACh release in SN56.B5.G4 cells may be due to either differentiation of the excitable properties of cell membranes, including expression of specific ion channels, or differentiation of ACh release mechanisms such as vesicular storage of ACh or proteins involved in vesicular release.

The ability to release ACh in dbcAMP-treated cells accompanied neurite outgrowth (Fig. 1) and stimulation of ChAT activity and ACh synthesis (Fig. 2). The latter effect of dbcAMP was maximal after 2 d of treatment, suggesting that it was mediated by changes in ChAT gene expression, translation, or ChAT

Table 1. Effect of sodium on the accumulation of ^{14}C-ACh in SN56.B5.G4 cells

	ACh	
Conditions	1 μM Choline	5 μM Choline
Control (pmol/dish)	4.1 ± 0.6	20.4 ± 1.1
No sodium (pmol/dish)	1.2 ± 0.3	12.0 ± 0.6
No sodium (% control)	29	60
Significance	$p < 0.011$	$p < 0.003$

The cells were treated as described in Figure 6. The physiological salt solution contained 135 mM NaCl (Control) or 135 mM LiCl (No sodium). The results are means ± SEM of three determinations. Statistical significance of differences between means was determined by *t* test.

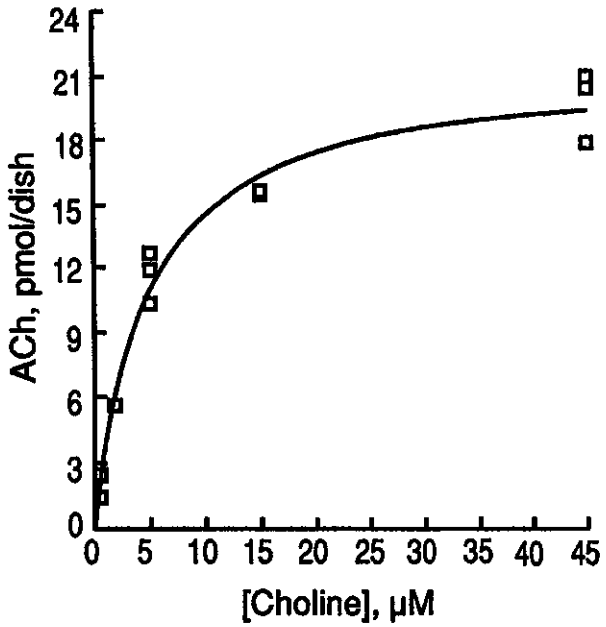

Figure 6. ^{14}C-ACh accumulation in SN56.B5.G4 cells. SN56.B5.G4 cells were grown as described in Materials and Methods in 35 mm diameter culture dishes until approximately 50% confluent. The cells were washed with 1 ml of physiological salt solution, and then 1 ml of the same solution containing ^{14}C-choline at various concentrations was added. The cells were incubated for 10 min at 37°C and then washed with 1 ml of the same medium devoid of label. Choline metabolites were extracted and purified by HPLC, and their radioactivities were determined as described in Materials and Methods. The results were calculated using the specific radioactivity of the ^{14}C-choline precursor. The data are results from triplicate determinations. A rectangular hyperbola was fit to the data according to the Michaelis equation. Correlation coefficient of this regression was $r^2 = 0.994$.

protein turnover rather than by a direct enzyme activation. However, it is also possible that ChAT was activated by a factor (perhaps an enzyme that modifies ChAT) whose expression required 2 d to develop fully. If these effects of dbcAMP were due to the cAMP moiety of this molecule, then in cells treated with forskolin, which should activate the cellular adenylate cyclase and thus increase the intracellular cAMP concentration, similar results should be observed. Consistent with this prediction, the forskolin-treated (10 μM, 2 d) cells developed neurites and had ChAT activity and ACh content similar to that of dbcAMP-treated cells, and higher than the controls (Fig. 2). The molecule of dbcAMP permeates into cells due to its butyrate moieties. Hydrolysis of dbcAMP yields free butyrate, which has been shown to stimulate ChAT activity in neuroblastoma cells (Prasad and Kumar, 1974; Szutowicz et al., 1983; Casper and Davies, 1989). A similar effect of butyrate (2 mM, 2 d) was observed here (Fig. 2). In addition, butyrate increased ACh content of SN56.B5.G4 cells (Fig. 2), but no neurite extension was seen in such cells (Fig. 1*C*).

Each of the three treatments used (dbcAMP, forskolin, butyrate) had a characteristic effect on SN56.B5.G4 cells. Forskolin and dbcAMP caused neurite outgrowth, suggesting that elevated intracellular cAMP concentration was involved in the morphological differentiation of these cells. Forskolin- and dbcAMP-treated cells exhibited high ChAT activity and contained 70–80% more ACh than did the controls. However, the ^{14}C-ACh release in the forskolin-treated cells was only 15–18% of that observed in cells grown in the presence of dbcAMP (Fig. 5). In butyrate-treated cells, ChAT activity was stimulated, ACh content was increased, and ACh release was high, but no neurite extension occurred, indicating that morphological differentiation was not necessarily associated with the enhancement of the cholinergic phenotype.

Taken together, the data presented above show that SN56.B5.G4 cells are characterized by (1) ACh synthesis and storage, (2) SDHACU, and (3) depolarization-evoked ACh release. These properties satisfy the criteria indicative of the cholinergic phenotype. Treatment with dbcAMP causes both morphological and neurochemical differentiation, stimulates ACh synthesis, and allows the cells to release ACh upon depolarization. It will be important to determine whether physiologically relevant agents alter the cholinergic phenotype. In this regard, it is worth noting that IL-3 (Kamegai et al., 1990b) and GM-CSF (Kamegai et al., 1990a) have been reported to stimulate ChAT activity in septal neurons as well as in one of our cell lines (SN6.10.2.2) derived from embryonic septum, indicating that these cells will be useful as models to study the molecular mechanisms of action of these and other growth and differentiating factors on the cholinergic phenotype.

References

Adler JE, Schleifer LS, Black IB (1989) Partial purification and characterization of a membrane-derived factor regulating neurotransmitter phenotypic expression. Proc Natl Acad Sci USA 86:1080–1083.

Blusztajn JK, Wurtman RJ (1983) Choline and cholinergic neurons. Science 221:614–620.

Bostwick JR, Landers DW, Crawford G, Lau K, Appel SH (1989) Purification and characterization of a central cholinergic enhancing factor from rat brain: its identity as phosphoethanolamine. J Neurochem 53:448–458.

Casper D, Davies P (1989) Stimulation of choline acetyltransferase activity by retinoic acid and sodium butyrate in a cultured human neuroblastoma. Brain Res 478:74–84.

Cohen EL, Wurtman RJ (1976) Brain acetylcholine: control by dietary choline. Science 191:561–562.

Daniels MP, Hamprecht B (1974) The ultrastructure of neuroblastoma glioma somatic cell hybrids. Expression of neuronal characteristics stimulated by dibutyryl adenosine 3',5' cyclic monophosphate. J Cell Biol 63:691–699.

Fonnum F (1975) A rapid radiochemical method for the determination of choline acetyltransferase. J Neurochem 24:407–409.

Fukada K (1985) Purification and partial characterization of a cholinergic neuronal differentiation factor. Proc Natl Acad Sci USA 82: 8795–8799.

Green LA, Tischler AS (1976) Establishment of noradrenergic clonal line of rat adrenal pheochromocytoma cells which respond to NGF. Proc Natl Acad Sci USA 73:2424–2428.

Hammond DN, Lee HJ, Tonsgard JH, Wainer BH (1990) Development and characterization of clonal cell lines derived from septal cholinergic neurons. Brain Res 512:190–200.

Hefti F, Hartikka J, Eckenstein F, Gnahn H, Heumann R, Schwab ME (1985) Nerve growth factor increases choline acetyltransferase but not survival or fiber outgrowth of cultured fetal septal cholinergic neurons. Neuroscience 14:55–68.

Kamegai M, Konishi Y, Tabira T (1990a) Trophic effect of granulocyte-macrophage colony-stimulating factor on central cholinergic neurons *in vitro*. Brain Res 532:323–325.

Kamegai M, Niijima K, Kunishita T, Nishizawa M, Ogawa M, Araki M, Ueki A, Konishi Y, Tabira T (1990b) Interleukin 3 as a trophic factor for central cholinergic neurons *in vitro* and *in vivo*. Neuron 4: 429–436.

Kato AC, Lefresne P, Berwald-Netter Y, Bojouan JC, Glowinski J, Gross F (1977) Choline stimulates the synthesis of acetylcholine from acetate and the accumulation of acetate in a cholinergic neuroblastoma clone. Biochem Biophys Res Commun 78:350–356.

Keller F, Rimvall K, Waser PG (1987) Choline and acetylcholine

metabolism in slice cultures of the newborn rat septum. Brain Res 405:305–312.
Labarca C, Paigen K (1980) A simple, rapid, and sensitive DNA assay procedure. Anal Biochem 102:344–352.
Lanks K, Somers L, Papirmeister B, Yamamura H (1974) Choline transport by neuroblastoma cells in tissue culture. Nature 252:476–478.
Lee HJ, Hammond DN, Large TH, Wainer BH (1990) Immortalized young adult neurons from the septal region: generation and characterization. Dev Brain Res 52:219–228.
Liscovitch M, Freese A, Blusztajn JK, Wurtman RJ (1985) High-performance liquid chromatography of water-soluble choline metabolites. Anal Biochem 151:182–187.
McGee R Jr (1980) Choline uptake by the neuroblastoma × glioma hybrid, NG 108-15. J Neurochem 35:829–837.
McManaman JL, Crawford FG, Stewart SS, Appel SH (1988) Purification of a skeletal muscle polypeptide which stimulates choline acetyltransferase activity in cultured spinal cord neurons. J Biol Chem 263:5890–5897.
Melega WP, Howard BD (1981) Choline and acetylcholine metabolism in PC12 secretory cells. Biochemistry 20:4477–4483.
Morel N, Israel M, Manaranche R, Mastour-Frachon P (1977) Isolation of pure cholinergic nerve endings from *Torpedo* electric organ. J Cell Biol 75:43–55.
Parsons SM, Bahr BA, Gracz LM, Kaufman R, Kornreich WD, Nilsson L, Rogers GA (1987) Acetylcholine transport: fundamental properties and effects of pharmacologic agents. Ann NY Acad Sci 493: 220–233.
Potter PE, Meek JL, Neff NH (1983) Acetylcholine and choline in neuronal tissue measured by HPLC with electrochemical detection. J Neurochem 41:188–194.
Prasad KN, Kumar S (1974) Cyclic AMP and the differentiation of neuroblastoma cells in culture. In: Control of proliferation in animal cells (Clarkson B, Baserga R, eds), pp 581–594. Cold Spring Harbor, NY: Cold Spring Harbor Laboratory.
Rao MS, Landis SC (1990) Characterization of a target-derived neuronal cholinergic differentiation factor. Neuron 5:899–910.
Richardson UI, Liscovitch M, Blusztajn JK (1989) Acetylcholine synthesis and secretion by LA-N-2 human neuroblastoma cells. Brain Res 476:323–331.
Saadat S, Sendtner M, Rohrer H (1989) Ciliary neurotrophic factor induces cholinergic differentiation of rat sympathetic neurons in culture. J Cell Biol 108:1807–1816.
Shelton DL, Nadler JV, Cotman CW (1979) Development of high affinity choline uptake and associated acetylcholine synthesis in the rat fascia dentata. Brain Res 163:263–275.
Smith PK, Krohn RI, Hermanson GT, Mallia AK, Gartner FH, Provenzano MD, Fujimoto EK, Goeke NM, Olson BJ, Klenk DC (1985) Measurement of protein using bicinchoninic acid. Anal Biochem 150: 76–85 [published erratum appears in Anal Biochem 163:279].
Suszkiw JB, Pilar G (1976) Selective localization of a high affinity choline uptake system and its role in ACh formation in cholinergic nerve terminals. J Neurochem 26:1133–1138.
Szutowicz A, Morrison MR, Srere PA (1983) The enzymes of acetyl-CoA metabolism in differentiating cholinergic (S-20) and noncholinergic (NIE-115) neuroblastoma cells. J Neurochem 40:1664–1670.
Vaca K, Stewart SS, Appel SH (1989) Identification of basic fibroblast growth factor as a cholinergic growth factor from human muscle. J Neurosci Res 23:55–63.
Yamamori T, Fukada K, Aebersold R, Korsching S, Fann M-J, Patterson PH (1989) The cholinergic neuronal differentiation factor from heart cells is identical to leukemia inhibitory factor. Science 246: 1412–1416.

Construction Name (GENE)	Vector	Comments
GGA1 VHS-pGAD10	pGAD10	
GGA2 VHS-pGAD424	pGAD424	
GGA3S-pcDNA3 HAN	pcDNA3	
146 (Pancortina)	pBluesc	
146 (Pancortina)	pACT2	
3F4 HYGRO+ 1.15ug/ul march2009	pcDNA3	???
3F4 NGAG 1.63µg/µl	pcDNA3	???
3F4 WT G418 resis. 2.82ug/ul june2007	pcDNA3	???
57Cx (α-tubulina)	pBluesc	
57Cx (α-tubulina)	pACT2	
α-7 FLAG 0.72ug/ul april 2010	pcDNA3	??? J Ryllet
α-adaptina	pGAD	
AP180 1.45µg/µl	pcDNA3	???
AP180-MYC	pCMV-MYC	
β- adaptina	pGAD	
B-20-64 (Toxina)	pBluesc	
$\beta_2$adaptin	pcDNA	
$\beta_2$adaptin-FLAG	PcDNA	
β-arrestina	pACT-2	
Caveolin1-A61-100	pcB7	
Caveolin1-pcB7	pcB7	
Caveollin1-GFP original DNA	pEGFP	???
CED –RFP (Col 1)	pRFPC1	
CED6-127AX	pACT2	
CED6-pGEX	pGEX	
CED6-pMAL	pMAL	
CED-GFP	pEGFP	
CED-pBKCMV	pBKCMV	
CED-pBS	pBluesc	
CED-pEBG	pEBG	
CED-pPROEX	pPROEX	
CHT1	pEGFP-N3	
CHT1-CTerminal	pMAL	
CHT1-GFPC1	pEGFP-C1	
CHT1-HA-pBKCMV	pBKCMV	
CHT1-Loop	pMAL	
CHT1-pBKCMV	pBKCMV	
CHT1-pSPORT	pSPORT	
Clatrin-GFP2.84µg/µl	pEGFP	???
CT-VAChT-SerAla	pAS2-1	
CT-VAChT-SerGlu	pAS2-1	
DYNAMIN WT 0.65ug/ul	pcDNA3	???
Dynamin-K44A	pcDNA3	???

EPS15-GFP	pEGFP	???
EPSIN-FLAG	pcDNA3	???
Flotillin1-GFP original DNA	pEGFP	???
GAPDH	pcDNA3	???
GGA1 VHS-pET32a	pET32a	
GGA1-pcDNA3 HAN	pcDNA3	
GGA1S VHS-pET32a	pET32a	
GGA2 VHS-pET32a	pET32a	
GGA2-pcDNA3 HAN	pcDNA3	
GGA3S VHS-pET32a	pET32a	
GGA3S VHS-pET32a	pET32a	
GGA3S VHS-pGAD424	pGAD424	
GPI-GFP(PRP)	pEGFP	
GRLP-CFP 3.31µg/µl	pCFP	???
GRLT-CFP original DNA	pCFP	???
Hind 2.4 (VAChT)	PMECA	
HIPK2- pCMV-Flag 1.6µg/µl (max) (L SCHMITZ)	pCMV-flag	
LAMP1-CFP original DNA	pCFP	???
LAMP1-mRFP original DNA	pRFP	???
µ- adaptina	pGAD	
mChery	pmChery	
mRFP-Rab7 0.72µg/µl (Pasternak Lab)	pRFP	???
NGAG-Hygro 1.22µg/µl (Fabi)	pcDNA3	???
PC2-FLAG (D Wotton) 0.831ug/ul	pcDNA3	???
pC2-GST-PGEX 1.69µg/µl (L SCHMITZ)	pGEX	???
pC2-Myc 0.217µg/µl (L SCHMITZ)	pCMV-Myc	???
Pc2-pCMV5T7 1.28µg/µl (max) (D WOTTON)	pCMV5T7	
pCDN3.1 HYGRO+ 0.909ug/ul INVITROGEN	pCDNA3.1	
pCMV-Flag 2B10γ (max) (S SODDU)	pCMV	
pCMV-MYC 1.226ug/ul	pCMV-Myc	
pD3Red-C1	pD3Red-C1	
pEGFP C3 1.241ug/ul	pEGFP-C3	
Pepsig GFP-PrPc (Prion)	pEGFP	
PIAS1-MYC 0.789ug/ul	pCMV-Myc	???
PIAS-HA 1-651 1.37 µg/µl	pCMV-HA	???
PIASY-MYC 1.042µg/µl (L SCHMITZ)	pCMV-Myc	???
PIASy-MYC 0.7ug/ul nov2007	pCMV-MYC	???
pIX-CD8 original from J MacDonald's lab	pcDNA3	???
PKC βII- GFP	pEGFP	???
PML-pCMX-YFP original from M Tini's Lab	pYFP	???
PML-YFP 1.068ug/ul april2010 Marc Tini	pYFP	???
PrP Δ144-173-GFP	pEGFP	???
PrP Δ173-180-GFP	pEGFP	???
PrP Δ51-90/105-128/144-173-GFP	pEGFP	???
PrPc -GFP	pEGFP	

Prpc(del 51-90) Cu^{++}	pEGFP	???
PrPc-CFP original from Vilma's Lab	pCFP	???
PrPC-GFP 0.78ug/ul april 2010 Vilma	pEGFP	???
Prpc-RFP	pRFP	
PrPc-YFP original from Vilma's Lab	pYFP	???
PrP-ΔE-GFP	pEGFP	
PrP-ΔF-GFP-	pEGFP	
PRP-WT-GFP	pEGFP	
pVAT3(VAChT)	pBluesc	???
pVAT4(VAChT)	pBluesc	???
pVAT5(VAChT)	pBluesc	???
pYFP 1.281 ug/ul	pYFP	
Rab11 Q70L-GFP	pEGFPC2	???
Rab11 Q70L-HA	pcDNA3	
Rab11 S25N-HA	pcDNA3	
Rab11-GFP	pEGFPC2	
Rab11-GFPC3	pEGFPC3	
Rab11-HA	pcDNA3	
Rab11-Q70L-GFP-	pEGFPC2	
Rab15 N121I-HA	pcDNA3	
Rab15 Q67L-GFP	pEGFPC2	
Rab15 Q67L-HA	pcDNA3	
Rab15-GFP	pEGFPC2	
Rab15-HA	pcDNA3	
Rab4	pcDNAamp	
Rab4 N121I	pcDNAamp	
Rab4 N121I-GFP	pEGFPC2	???
Rab4-GFP	pEGFPC2	
Rab4-N121I-GFP	pEGFPC2	
Rab5 – pcDNA	pcDNA	
Rab5 – Q79L	pEGFP	???
Rab5 – S34N	pEGFP	???
Rab5-GFP C2 original from S Ferguson's Lab	pEGFP	???
Rab5-L79Q (1A)	pEGFP	???
Rab5-mRFP- 0.88µg/µl (Pasternak Lab)	pRFP	???
Rab5-N34 (2A)	pEGFP	???
Rab7-HA-	pcDNA3	
Rab7-mRFP- 0.471µg/µl april2010 (Pasternak Lab)	pRFP	???
Rab7-N125I-GFP-	pEGFPC1	
Rab7-Q67L-GFP-	pEGFPC1	
Rab7-T22N-GFP-	pEGFPC1	
RIC3-HA 0.841ug/ul april 2010 J Ryllet	pcDNA3	???
σ- adaptina	pGAD	
SNAP 25-HA	pcDNA3	???
STI1-HA 1.066ug/ul Cristiane	pCMV-HA	

STI1-MUT10-HA (K50,136R)	pCMV-HA	
STI1-MUT11-HA (K50,210,272R)	pCMV-HA	
STI1-MUT12-HA (K51,238,513R)	pCMV-HA	
STI1-MUT13-HA (K373R)	pCMV-HA	
STI1-MUT14-HA (K207R)	pCMV-HA	
STI1-MUT15-HA (K207,210,373R)	pCMV-HA	
STI1-MUT1-GFP (K32R)	pEGFP	???
STI1-MUT2-GFP (K68R)	pEGFP	???
STI1-MUT3-GFP (K100R)	pEGFP	???
STI1-MUT4-HA (K32,68,100R)	pCMV-HA	
STI1-MUT5-HA (K109,312R)	pCMV-HA	
STI1-MUT6-HA (K32,68,100,109,312R)	pCMV-HA	
STI1-MUT7-HA (K50,210R)	pCMV-HA	
STI1-MUT8-HA (K50,210,239R)	pCMV-HA	
STI1-MUT9-HA (K50,206R)	pCMV-HA	
STI1-pTRC 1.4ng/ul	pTRC	???
STI1-YFP 0.89µg/µl	pYFP	???
SUMO1-CFP 1.365ug/ul	pCFP	???
SUMO1-HA(max) 0.2µg/µl (L SCHMITZ)	pCMV-HA	???
SUMO3-Flag 0.86µg/µl (D WOTTON)	pcDNA3	???
SUMO3-FLAG 1.44ug/ul	pcDNA3	???
Syntaxin 1A	pSP73	
SYNTAXIN-EBFP	pBKCMV	
SYNTAXIN-EGFP	pBKCMV	
TRPV1_pCDNA3	pCDNA	
Tx3.1 proex 06/02/	pPROEX	
Tx3.1pMal13/09/06	pMAL	
Tx3.4pBAD	pBAD	
Tx3.4pESUMO MP 20/05/09	pESUMO	
Tx3.4pET 1st elution	pET	
Tx3.6 - pBADmycHis	pBAD-myc-his	
Tx3.6pp - pBAD HisB	pBAD	
Tx3.6pPICZ 622 ng/µg	pPICZ	
Tx3-1 (tese)	pMAL	
Tx3-1 ENT	pMAL	
Tx3-1(BS131)	pBluesc	
Tx3-2	pBluesc	
Tx3-6proex	pPROEX	
UBC9-Flag- pCMV5 1.126µg/µl (max) (D WOTTON)	pCMV5	
UBC9-YFP (max) 1.89 µg/µl (D WOTTON)	pYFP	???
VAChT (1.6F-0.8R)	pUC18	
VAChT (Inicio-0.8R)	pUC18	
VAChT -EGFPC2	pEGFPC2	
VAChT pEGFPC2	pEGFPC2	
VAChT-12TM	pEGFPC2	
VAChT-COL5	pBluesc	

VAChT-COL7	pBluesc	
VAChT-CT-LeuAla	PAS2-1	
VAChT-CT-PAS2-1	PAS2-1	
VAChT-CT-pMAL	pMAL	
VAChT-HA480E	pcDNA	
VAChT-HA-LLAA	pcDNA	
VAChT-LeuAla-RFP	pRFP	
VAChT-RFP	pRFP	
VAChT-Ser480/478-RFP	pRFP	
VAChT-SerAla-RFP	pRFP	
VAChT-Trans-pMAL	pMAL	
VAMP2-Myc	pCMV-Myc	???
VAMP-RFP Myc	pRFP	???
VAT HA-480A	pcDNA	
VAT-20INI	pEGFPC2	
VAT-5A	pEGFPC2	
VAT-5B	pEGFPC2	
VAT-5C	pEGFPC2	
VAT-5D	pEGFPC2	
VAT-DEL11	pGFPC1	
VAT-EGFPC2	pEGFPC2	
VAT-HA-WT	pcDNA	
VaT-LeuAla	PEGFPC1	
VAT-LeuAla	pEGFPC1	
VAT-S480A-LLAA	pEGFPC2	
VAT-S480E-LLAA	pEGFPC2	
VATSEM20	pEGFPC2	
VAT-Ser480-A	pEGFPC1	
VAT-SerGlu	pEGFPC1	
VSVG Syntaxim	pCDNA3	???
VSVG-Syntaxin1A-RFP	pRFP	
Xho 3.0 (VAChT)	pMECA	
Xho 5.8(VAChT)	pBluesc	???
Xho Hind 5.0 (VAChT)	pMECA	
	pCCALL2-IRES-EGFP	
	pLD53.5CA-E-B	

i2eg

CLONE RECORD

Clone Name: pCCALL2-IRES-EGFP/anton **Date:** 22. Jan. 03.

Vector: _____ **Vector Supplier:** Dr. Connne Lobe

Insert size: _____ **Total Size:** 10985 bp

Sites cloned into: _____

Originally Obtained from: _____

Bacteria: DH5α **Antibiotic resistance:** Amp

Read sense from (orientation): _____

Sequence confirmation: yes no (please circle)

Sequence disk attached: yes no (please circle)

Map attached: (yes) no (please circle)

Promoters: Chicken beta-actin

Glycerol stocks location: Lab stocks box

DNA location: _____

Aliquot in lab stock box: (yes) no (please circle)

Person who made clone: Glycerol stocks + plasmid (Artee)

Comments: _____

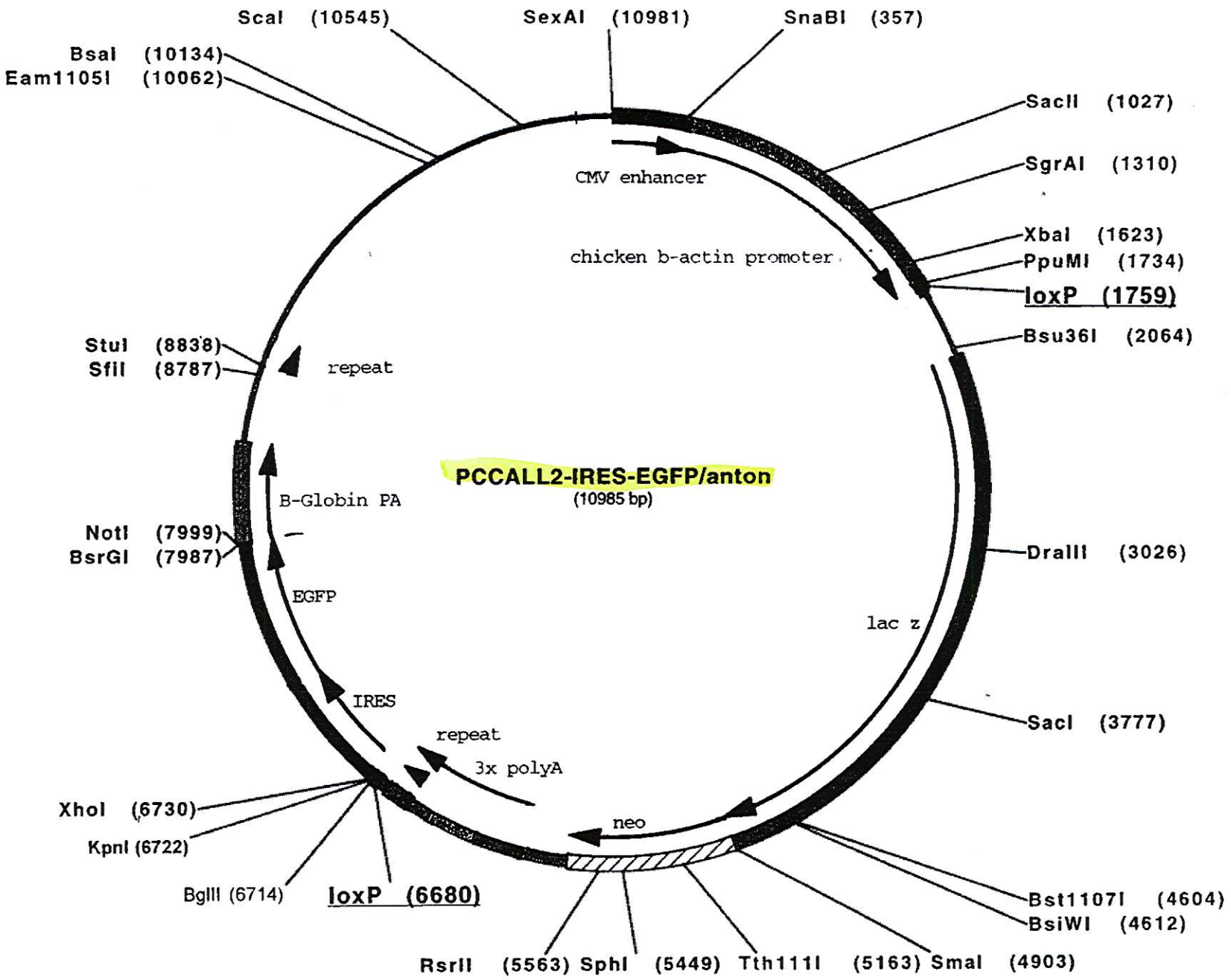
ScaI (10545)
SexAI (10981)
SnaBI (357)
BsaI (10134)
Eam1105I (10062)
SacII (1027)
SgrAI (1310)
CMV enhancer
chicken b-actin promoter
XbaI (1623)
PpuMI (1734)
loxP (1759)
Bsu36I (2064)
StuI (8838)
SfiI (8787)
repeat
PCCALL2-IRES-EGFP/anton
(10985 bp)
B-Globin PA
NotI (7999)
BsrGI (7987)
DraIII (3026)
EGFP
lac z
IRES
SacI (3777)
repeat
3x polyA
XhoI (6730)
neo
KpnI (6722)
BglII (6714)
loxP (6680)
Bst1107I (4604)
BsiWI (4612)
RsrII (5563)
SphI (5449)
Tth111I (5163)
SmaI (4903)

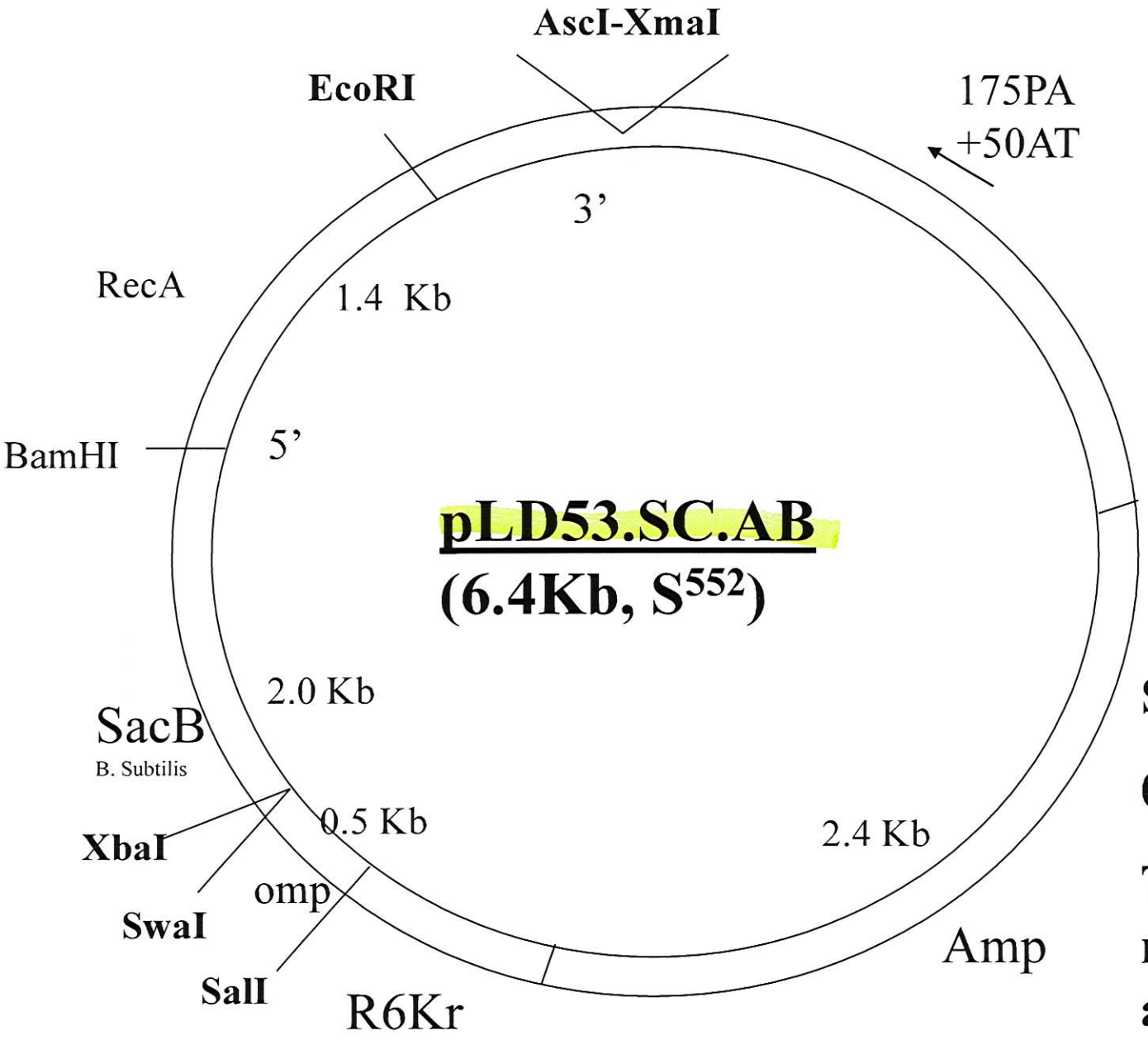

Shiaoching Gong

03/27/08

The unique restriction sites are in bold

Western

TOXIN USE RISK ASSESSMENT

Name of Toxin:	Spider venom toxin (Phoneutria nigriventer)
Proposed Use Dose:	200 µg
Proposed Storage Dose:	**2000** µg
LD $_{50}$ (species):	137 µg

Calculation:

137 µg/kg x 50 kg/person

Dose per person based on LD $_{50}$ in µg = 6850

LD_{50} per person with safety factor of 10 based on LD_{50} in µg = ***685***

Comments/Recommendations: